

THE MECHANISM OF TYPE I COLLAGEN
CROSSLINKING WITH CATECHOL
DERIVATIVES

by

Jay N. Gade

A Dissertation
Presented to the Department of Biochemistry and Molecular Biology
School of Medicine
and the Graduate Division of the
Oregon Health Sciences University
in Partial fulfillment of
the requirements for the degree of
Doctor of Philosophy

September 1989

APPROVED:



(Professor in charge of thesis)



(Chairman, Graduate Council)

TABLE OF CONTENTS

LIST OF FIGURES	iii
ABBREVIATIONS	vii
I. ACKNOWLEDGEMENTS.	viii
II. ABSTRACT.	x
III. INTRODUCTION.	1
A. Historical Background - Protein Tanning.	1
1. Protein Crosslinking; Natural and Unnatural.	1
a. Natural Collagen Crosslinking.	2
b. Physiological Correlates of Collagen Crosslinking. ..	7
c. Mechanisms of Protein Tanning.	9
d. Insect Cuticle Tanning.	21
e. Catecholamines and Collagen.	22
2. Melanogenesis	25
B. Rationale.	32
IV. EXPERIMENTAL.	34
A. PART I. The Chemical, Thermal, and Physical Stability of DOPA-Collagen Matrices.	35
1. Introduction.	35
2. Pepsin collagen gel stabilization with DOPA.	36
3. The solubility of DOPA-collagen gels.	43
4. The thermal stability of DOPA-collagen matrices.	51
5. Tensile strength of collagen felts prepared in the presence of DOPA.	60
6. Transmission electron microscopy of DOPA stabilized reconstituted collagen fibrils.	70
7. The DOPA induced stabilization of preformed Type I collagen fibrils.	75
8. Summary.	79
B. Part II. The Mode of Interaction of Catechol Derivatives and Collagen Reactive Groups.	81
1. Introduction.	81
2. Quantitative binding of DOPA to collagen.	82
3. Binding of DOPA to soluble type I collagen.	86
4. Is DOPA covalently bound to collagen?	93

5. The involvement of the lysine side chains of collagen in DOPA binding.	99
6. Peptide mapping of type I collagen DOPA reactive lysine residues.	108
7. Summary.	119
B. PART III. Studies on the Mechanism of Crosslinking of DOPA Derivatized Type I Collagen Alpha Chains.	121
1. Introduction.	121
2. The concentration dependency of DOPA.	124
3. The reactions of DOPA during collagen gel stabilization. . .	129
4. The Role of oxygen in DOPA stabilization of collagen gels. .	139
5. Identification of the precursors of melanin in DOPA-collagen solutions.	146
6. Inhibition of catechol polymerization and the effect on collagen gel stability.	151
7. Summary.	170
V. CONCLUSIONS AND SIGNIFICANCE OF RESULTS.	172
VI. REFERENCES.	180
VII. APPENDIX: GENERAL EXPERIMENTAL METHODS.	192
A. Type I collagen extraction and purification.	192
B. The preparation of buffered type I collagen solutions.	195
C. Collagen gel stability assay	195
D. Hydroxyproline analysis	195
E. Interrupted SDS-Polyacrylamide Gel Electrophoresis	197
F. Radioassay by liquid scintillation counting.	198
G. Collagen gel solubility assay.	198
H. The preparation of collagen felts.	199
I. Shrinkage temperature measurements.	199
J. Gel filtration HPLC elution of labeled DOPA-collagen adducts.	201

LIST OF FIGURES

Figure 1.	The four sequence specific crosslinking residues of type I collagen.	3
Figure 2.	The three "aldimine" crosslinks that are isolated following reduction with borohydride.	5
Figure 3.	A proposed "mature" collagen crosslink produced by oxidation of hydroxylysino-leucine to form an amide linkage.	6
Figure 4.	Protein tanning with chromium.	13
Figure 5.	Molecular crosslinking models of glutaraldehyde fixation.	14
Figure 6.	Two proposed "mechanisms" of protein crosslinking with formaldehyde.	16
Figure 7.	The hydrogen bonding model of vegetable (quinone) tanning.	18
Figure 8.	The covalent crosslinking model of vegetable (quinone) tanning.	19
Figure 9.	The Raper-Mason pathway of melanogenesis.	26
Figure 10.	Lewis base attack of <i>ortho</i> -quinones.	29
Figure 11.	The proposed mechanism of melanochrome and higher melanin polymer formation.	30
Figure 12.	Tropocollagen gel stabilization at 37°C, and destabilization at 0°C.	37
Figure 13.	DOPA treated collagen gel stabilization.	39
Figure 14.	DOPA-collagen and pepsin control-collagen gels following 24 hours at 37°C and 1 hour at 0°C, and a pepsin control gel prior to cooling.	40
Figure 15.	The solubility of DOPA-collagen and control-collagen gels.	46
Figure 16.	SDS page of cyanogen bromide digested DOPA-collagen gels.	48

Figure 17.	Scanning electron micrographs of a pepsin collagen felt.	53
Figure 18.	Shrinkage temperatures of DOPA-collagen felts following varying incubation periods at 37°C.	56
Figure 19.	Breakage temperatures of collagen felts prepared at lowered DOPA concentrations, following varying periods of incubation at 37°C.	57
Figure 20.	Instron Series IV Automated Materials Testing System V4.01C, used for testing collagen felts for tensile properties.	62
Figure 21.	The stress-strain curve of a 1×10^{-3} M DOPA-collagen felt incubated for 4 days at 37°C.	64
Figure 22.	The wet tensile strengths of DOPA-collagen felts and after varying periods of incubation at 37°C.	65
Figure 23.	The extensibility of DOPA-collagen felts following varying periods of incubation at 37°C.	67
Figure 24.	Transmission electron micrograph of an acetic acid soluble collagen gel and a pepsin treated collagen gel.	73
Figure 25.	Transmission electron micrograph of DOPA-collagen gels following a 2 day and a 70 day period of incubation at 37°C.	74
Figure 26.	The solubility of DOPA exposed and control-collagen felts.	77
Figure 27.	The stability of collagen gels exposed to DOPA at 4°C for 24 hours and 72 hours, followed by exhaustive dialysis.	88
Figure 28.	The solubility of collagen gels exposed to DOPA at 4°C for 24 hour, and for 72 hours followed by exhaustive dialysis.	90
Figure 29.	Gel filtration HPLC elution of $3\text{-}^{14}\text{C}$ -DOPA labelled collagen and unbound DOPA under denaturing conditions.	96
Figure 30.	Gel filtration HPLC elution of collagen exposed to $3\text{-}^{14}\text{C}$ -DOPA for 24 hours at 4°C followed by exhaustive dialysis. Elution was performed under denaturing conditions.	97
Figure 31.	Gel filtration HPLC elution of $3\text{-}^{14}\text{C}$ -DOPA exposed poly-L-lysine and N-acetylated poly-L-glutamic acid under denaturing conditions.	103

Figure 32.	Chromatogram showing the PITC amino acid composition of a DOPA-collagen gel incubated at 37°C for 10 days.	104
Figure 33.	Cyanogen bromide peptide maps of the $\alpha 1$ and $\alpha 2$ chains of type I collagen.	109
Figure 34.	SDS-Page gel and autoradiograph of cyanogen bromide peptides of $3\text{-}^{14}\text{C}$ -DOPA labelled collagen.	113
Figure 35.	Gel filtration HPLC elution of $3\text{-}^{14}\text{C}$ -DOPA labelled type I collagen cyanogen bromide peptides under denaturing conditions	114
Figure 36.	Collagen gel stability and solubility at varying concentrations of DOPA.	126
Figure 37.	Proposed interaction of collagen bound melanin polymers.	130
Figure 38.	The reactions of DOPA which lead to the formation of melanin like polymers in DOPA-collagen gels.	132
Figure 39.	$3\text{-}^{14}\text{C}$ -DOPA labelled collagen isolated by gel filtration HPLC under denaturing conditions.	134
Figure 40.	DOPA-collagen gel stability after 3 hours at 37°C under varying conditions of aeration.	142
Figure 41.	The effect of mushroom tyrosinase on DOPA-collagen gel solutions incubated at 37°C.	143
Figure 42.	The visible spectrum of a $1 \times 10^{-3}\text{M}$ DOPA-collagen solution after 5 hours of incubation at 37°C.	149
Figure 43.	Comparison of the molecular structures of the <i>ortho</i> -quinones of (a) DOPA, (b) 4- <i>tert</i> -butyl catechol, and (c) 3,5-ditert-butylcatechol.	152
Figure 44.	Ultraviolet-visible spectrum of 4- <i>tert</i> -butyl catechol bound collagen	156
Figure 45.	The stability of $1 \times 10^{-3}\text{M}$ TBC-collagen gels.	157
Figure 46.	The stability of collagen gels exposed to various catechol derivatives	159

Figure 47.	The solubility of 1×10^{-3} M TBC-collagen gels following 24 hours of incubation at 37°C.	160
Figure 48.	The solubility of collagen gels exposed to various catechol derivatives.	161
Figure 49.	A comparison of the wet tensile strengths of 4-tert-butyl catechol-collagen DOPA-collagen felts over 10 days of incubation at 37°C.	162
Figure 50.	A comparison of the wet tensile strengths of collagen felts exposed to 3,5-ditert-butyl catechol and DOPA at a concentration of 5×10^{-5} M.	163
Figure 51.	The proposed structure of the simplest (dimer) DOPA crosslink between collagen molecules.	178
Figure 52.	Interrupted SDS-PAGE separation of α -chains of type I and type III collagen.	194
Figure 53.	The collagen gel stability assay.	196
Figure 54.	Schematic of the apparatus used to measure the shrinkage temperature of collagen felts.	200
Figure 55.	Gel filtration HPLC separation of DOPA-collagen adducts.	202

ABBREVIATIONS

BAPN	β -aminopropionitrile
B.M.E.	β -mercaptoethanol
CB peptides	cyanogen bromide peptides
DHI	5,6-dihydroxyindole
DHIC	5,6-dihydroxyindole-4- carboxylic acid
DHLNL	dihydroxylysino-leucine
diTBC	3,5-ditert-butylcatechol
DOPA	L-3,4-dihydroxyphenylalanine
E.M.	electron microscopy
Gu-HCl	guanidine-hydrochloride
HLNL	hydroxylysino-leucine
HPLC	High Performance Liquid Chromatography
LNL	lysino-leucine
PBS	phosphate buffered saline
PITC	phenyl-isothiocyanate
pO ₂	partial pressure of oxygen
SDS-PAGE	sodium dodecyl sulfate- poly-acrylamide gel electrophoresis
TEM	transmission electron micrograph
TBC	tert-butylcatechol
TS	tensile strength
T _s ^o	shrinkage temperature
U.V.	ultraviolet

I. ACKNOWLEDGEMENTS.

This thesis would not be complete without acknowledging the many individuals who have contributed their assistance and expertise not only towards the completion of this document, but also to my training over the past five years. I would like to pay special thanks my advisor Dr. J. Peter Bentley. His constant demand for excellence in all my scientific pursuits as well as his willingness to allow me a high level of independence in the projects I pursued has been responsible for my development as a scientist. I consider myself fortunate to have trained under him.

Thanks are also given to the members of my advisory committee, Drs. Jones, Glanville, Hollister, and Fellman. I am especially grateful to Dr. Fellman for showing me the exciting side of Organic Chemistry. His contribution to this project has been invaluable.

I thank all the members of the laboratory in which I have completed this thesis. Bert Hanson has shared his technical expertise, and in many case his hands. Gordon Davies tested many of my samples for bacterial contamination, helped with the photography within this thesis, and was always willing to offer advice at those times when I hit roadblocks. David Buck provided much of the purified collagen used in these studies, and Winnie Chau was the closest thing to a Research Assistant a graduate student could have. She assisted in the shrinkage temperature studies as well as many additional experiments described in this thesis. Thanks are also

given to Diane Steele and Myca Morgan for their contributions in the preparation of this manuscript. All have been good friends, and for that I thank them most.

Finally, I would like to acknowledge Dr Kent Thornburg for his kind help with the electron microscopy, Dr. Jim Hare for helping with the autoradiography, and Charlotte Head for running the amino acid analyses described in this thesis.

This thesis is dedicated to my parents, Les and Norma Gade for their loving support.

II. ABSTRACT.

The effect of DOPA exposure on reconstituted collagen fibrils was determined. Collagen fibrils reconstituted in the presence of DOPA at a concentration of $1 \times 10^{-3}M$ were completely stabilized with respect to fibril dispersion after 24 hours of incubation at $37^{\circ}C$. Gels were nearly insoluble in dilute acid under denaturing condition ($100^{\circ}C$), and could not be extracted with cyanogen bromide. The thermal stability was also dramatically increased after 24 hours and the wet tensile strength increased to four times that of control collagen felts after three days of incubation at $37^{\circ}C$. Matrix extensibility initially increased to 1.5 times that of control felts after four days of incubation at $37^{\circ}C$, but decreased to below control values following six additional days of incubation. Increased fibrillar stability was not associated with an alteration in fibrillar structure at the E.M. level. Intact collagen fibrils exposed to DOPA at a concentration of $1 \times 10^{-3}M$ had decreased solubilities and increased thermal stabilities.

The manner in which DOPA mediates these changes was investigated. DOPA was retained by collagen gels and soluble collagen following suitable incubation periods and exhaustive dialysis. DOPA-collagen covalent adducts were formed following one hour of incubation at $37^{\circ}C$, or 24 hours of incubation at $4^{\circ}C$. Poly-L-lysine also interacted covalently with DOPA, whereas N-acetylated poly-L-glutamic acid did not. There was a 2-3 residue decrease in lysine content in DOPA-collagen hydrolysates following 30 days of incubation, suggesting that lysine interacted covalently with DOPA, and had precipitated with polymerized DOPA

following hydrolysis. Cyanogen bromide peptide mapping of $3\text{-}^{14}\text{C}$ DOPA labelled type I collagen peptides demonstrated a substantial binding to the $\alpha 1(\text{I})\text{CB}6$, $\alpha 1(\text{I})\text{CB}7$, and $\alpha 1(\text{I})\text{CB}8$ peptides, but little if any to the $\alpha(\text{I})\text{CB}3$ peptide. These cumulative results suggested that DOPA binds covalently to a specific population of lysine residues. Excess DOPA may polymerize with bound DOPA to produce covalently bound melanin-like polymers.

A polymerization model of collagen fibril crosslinking was supported. The gel stabilization and insolubilization effect of DOPA was shown to be concentration dependent. The DOPA effect was greatly decreased when less than one mole of DOPA was bound per collagen α chain suggesting a DOPA-dimer and higher polymer model of crosslinking. Covalently bound DOPA was incorporated into melanin like polymers formed in large part from DOPA not directly bound to collagen. The stabilizing effect of DOPA was inhibited in the absence of oxygen, and was accelerated in the presence of tyrosinase. Precursors of melanin-like polymers were detectable by various chemical means. Decarboxylation of DOPA-collagen gels indicated that indole-5,6-quinone, one of the diverse subunits of melanin, was produced. Dopachrome and the melanochrome dimer were spectrophotometrically detectable within 5 hours of incubation at 37°C . 4-tert-butyl catechol (TBC), a DOPA analogue, also stabilized collagen gels, and decreased the gel solubility in dilute acetic acid under non-denaturing conditions. The gels were, unlike DOPA-collagen, almost completely soluble in dilute acid under denaturing conditions (100°C). The wet tensile strength of TBC-collagen gels reached a maximum after one day of incubation at 37°C . This apparent enhanced rate of stabilization was likely due to a lower oxygen requirement for TBC-polymer

formation. 3,5-ditert-butylcatechol, a DOPA analogue with only one unblocked polymerization/protein binding site, increased collagen gel stability, decreased gel solubility, and increased the wet tensile to a level greater than control felts but less than DOPA-collagen felts following 10 days of incubation at 37°C. These results suggested that diTBC monomers binds to collagen and stabilizes the matrix through a dehydration mechanism. Due to the inability to form covalent crossbridges, tensile strength were unaffected.

DOPA and other catechol derivatives stabilize collagen fibrillar matrices by an initial covalent modification of collagen which dehydrates the matrix followed by polymeric crosslink formation resulting in a dramatic increases in thermal stability and tensile strength, and decreases in solubility.

III. INTRODUCTION.

The structural and functional physiology of the fibrous collagen matrix depends, in large part, on the integrity of the natural crosslinking system which has been well defined. For years investigators have attempted to introduce additional artificial crosslinks into the connective tissue matrix so as to produce a highly stable material which can further be studied microscopically in a form as close to the native state as possible, or can be used to create suitable biological prostheses. This thesis will describe a group of novel crosslinking agents, 3,4-dihydroxyphenylalanine (DOPA) and other catechol derivatives, which crosslink type I collagen fibrils in a biphasic process. Initially, following oxidation, *ortho*-quinones bind to lysine epsilon amino groups of the collagen α helix. The bound *ortho*-quinones then react to form melanin like crosslinks. The result is a highly stable collagen fibrillar matrix with increased tensile properties, thermal stability, and insolubility in acidic solutions.

A. Historical Background - Protein Tanning.

1. Protein Crosslinking; Natural and Unnatural.

The introduction of covalent bonds, other than peptide bonds, into proteins, serves a variety of functions, including the insurance of the correct three dimensional structure required for post-translational processing as is the role of disulfide bonds in insulin processing, and the proper alignment of polypeptide chains in a multimeric

protein. The proteins of the extracellular matrix, which perform a structural function, are examples of proteins which feature intermolecular covalent bonds, or crosslinks. Here, many protein molecules are aggregated into a firmly crosslinked fiber or lattice structure. The development of these crosslinks is, of course, responsible for the mechanical properties of connective tissues which are enhanced as the tissue and the animal matures. Keratin is an extracellular matrix protein crosslinked by a transglutaminase which catalyzes the reaction between the side chain of lysine and the gamma amino group of glutamine ¹. The result is a fibrous protein system which is highly insoluble. Lysine derived covalent bonds are used to crosslink collagen and elastin molecules into large fibrous structures. The nature of these crosslinks has been well defined, and will be reviewed below.

a. Natural Collagen Crosslinking.

The early phases of natural collagen crosslinking are well understood. The crosslinks formed are derived from lysine and hydroxylysine side chains and their derivatives. The four specific lysines involved in crosslinking have been identified (Figure 1). The two lysine residues located within the "telopeptides", which are the short non-helical regions at both the amino and carboxyl terminal of the collagen α chain ², are oxidized via an oxidative deamination mechanism to the corresponding aldehyde, and these derivatives are given the trivial names allysine and hydroxyallysine and have been reviewed by Bentley ³. This reaction is catalyzed by the copper requiring enzyme, lysyl oxidase ⁴, and can be inhibited ² by β -amino-propionitrile (BAPN) resulting in prevention of normal crosslinking ⁵. Two aldehyde

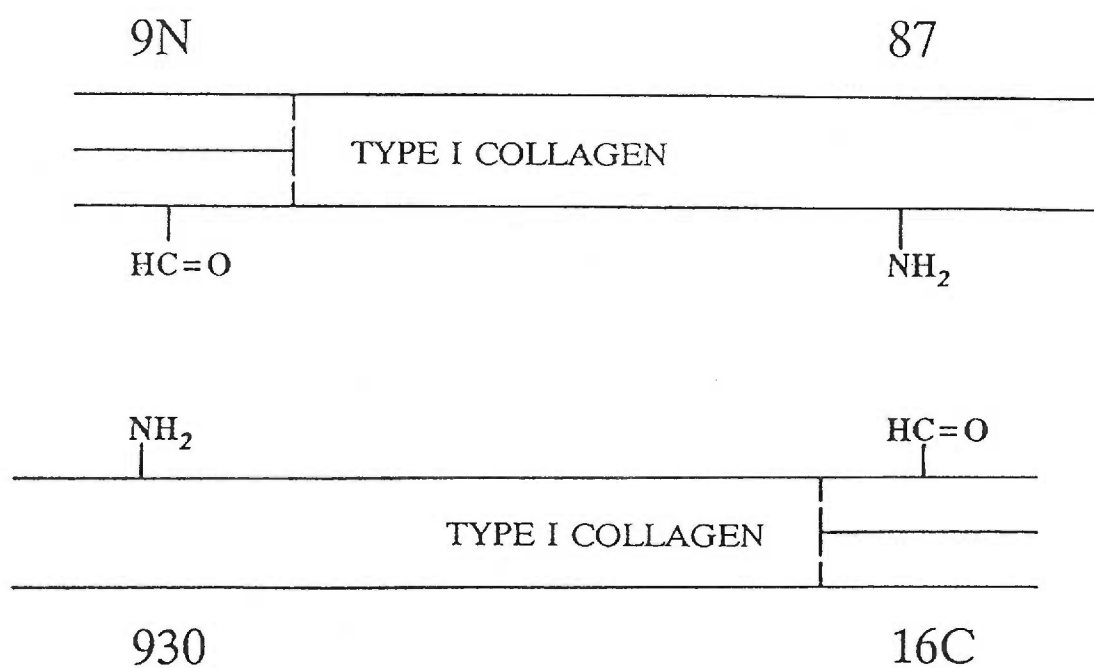


Figure 1. The four sequence specific crosslinking residues of type I collagen. N and C designations represent the amino and carboxyl terminal telopeptides². The residues located within the telopeptide regions are shown in their oxidized form.

functional groups can condense to form an intramolecular aldol crosslink ^{6,7}, which has been identified between amino terminal telopeptides. Intermolecular crosslinks, on the other hand are derived from the reaction of aldehyde and amino functional groups to give Schiff bases ³. These crosslinks are identifiable following reduction with tritiated borohydride ⁸, and are shown in Figure 2. As with many Schiff bases, conversion to the more stable keto form via an Amadori rearrangement can occur ^{9,10}. The proportion of aldol to keto form varies from tissue to tissue, as does the relative proportion of the three major reducible crosslinks ^{3,11}.

The level of these reducible crosslinks, measurable by borohydride reduction, decreases as a tissue ages, while the mechanical stability of the tissue increases ¹²⁻¹⁵. This obvious paradox can most likely be explained by a molecular rearrangement of the crosslink which results in increased stabilization. Several molecular models have been proposed as possible structural rearrangement products. Bailey, *et al* ¹⁶, proposed that HLNL, the predominant reducible crosslink in skin is oxidized as shown in Figure 3, to form a peptide bond. By hydrolyzing the *in vivo* labeled tissue, they were able to isolate amino adipic acid derived from the labeled lysine, providing indirect support of its significance. However, there is not as yet any direct evidence of its existence.

The trivalent hydroxypyridinium crosslink reported originally by Fujimoto, *et al* ¹⁷⁻¹⁹ is well accepted as a mature crosslink of the fibrous collagens ²⁰. It appears to form via the reaction of two ketamine crosslinks with the elimination of a single hydroxylysine residue. The mechanism of the reaction is nucleophilic substitution. In an alternative hypothesis, a keto form of HLNL reacts with a single residue of

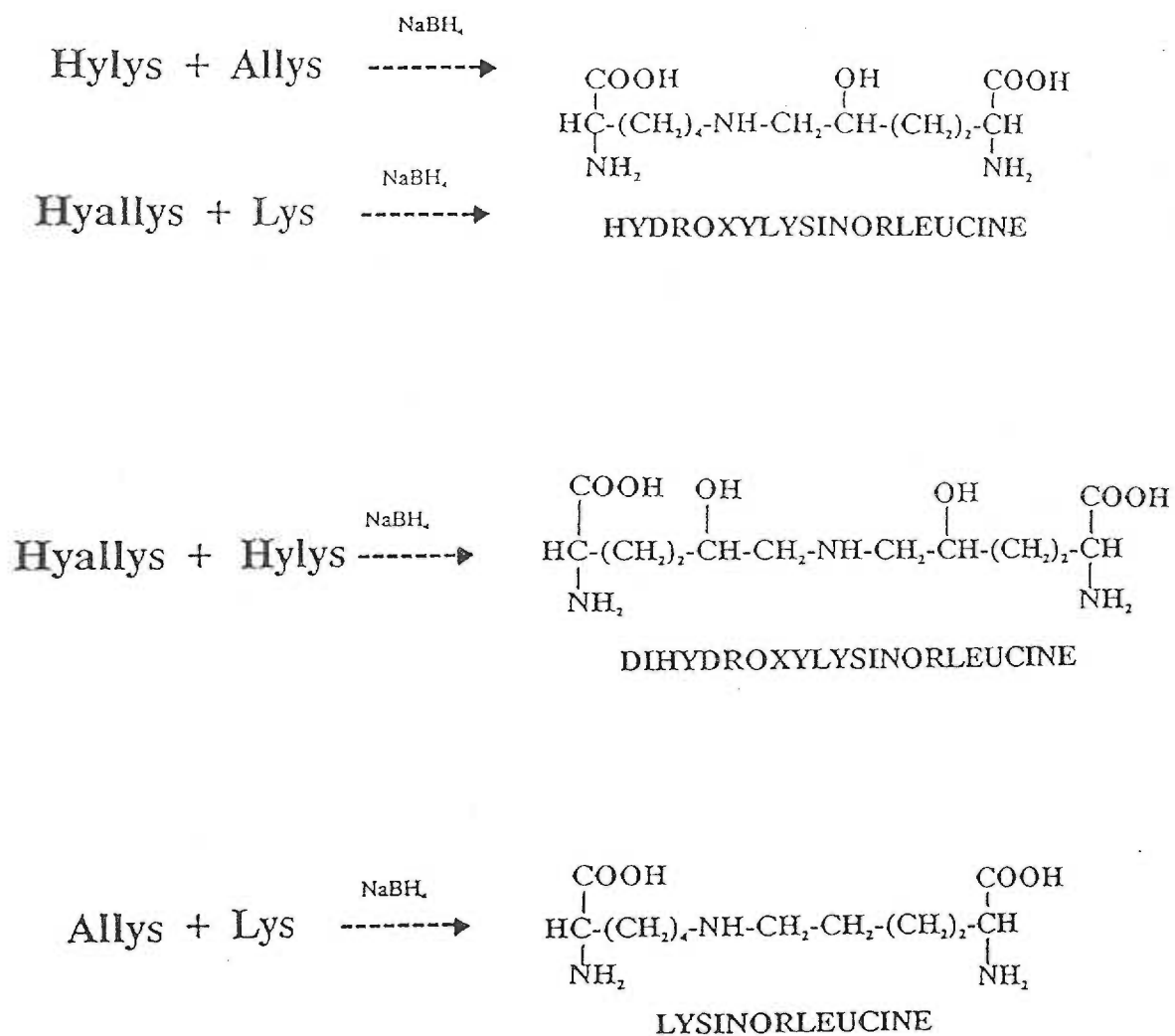


Figure 2. The three "aldimine" crosslinks that are isolated following reduction with borohydride³.

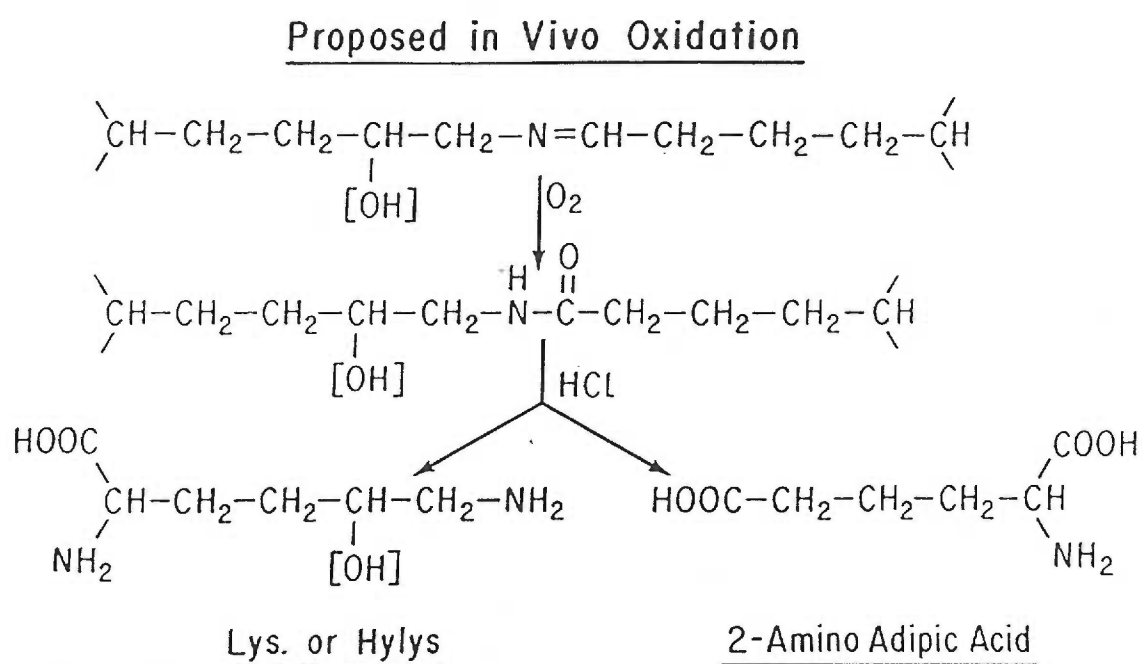


Figure 3. A proposed "mature" collagen crosslink produced by oxidation of hydroxylysine to form an amide linkage¹⁶. Reproduced from Bentley³.

hydroxyallysine ²¹. The crosslink is highly fluorescent, is UV radiation labile ^{22,23}, and is not identifiable in skin collagen ²⁴.

Two additional mature collagen crosslinks have been proposed, though their significance is controversial. Histidinohydroxymerodesmosine which is formed from an allysine aldol, a histidine residue, and a hydroxylysine residue has been called an artefact of borohydride reduction ²⁵. However, Bernstein and Mechanic ²⁶ have strong evidence that the crosslink is a naturally occurring one. If so, four collagen chains could be linked together. Hydroxyaldolhistidine, a trifunctional crosslink, has been isolated from bovine skin without borohydride treatment ²⁷. Finally, a trifunctional crosslink with identical properties has been recently isolated from adult bovine skin ²⁸. It is formed from histidine, lysine and hydroxylysine. The latter two residues appear to initially form an HLNL immature crosslink which then reacts through its norleucine C-2 position with the C-6 imidazole position on histidine. It has been given the appropriate trivial name, histidinohydroxylysinorleucine.

b. Physiological Correlates of Collagen Crosslinking.

The inhibition of normal collagen crosslinking, *in vivo*, both inherited and acquired, compromises the structural integrity of the connective tissue matrix. Defective crosslinking is often a feature of the pathology of the many identified inborn connective tissue diseases which have been described, including Ehlers Danlos Syndrome types VI ^{29,30}, VII ^{31,32}, and IX ³³, and forms of cutis laxa ³⁴. The molecular defect in abnormal type I collagen crosslinking can be due to absent or mutated lysyl oxidase ³⁵ or aminopropeptidase ³⁶ enzymes, or mutations which affect

the substrate structure at or near the four specific lysine and hydroxylysine residues involved in crosslink formation ².

Acquired defects in collagen crosslinking generally occur as a result of a nutritional copper deficiency ³⁷. The result is a less active lysyl oxidase enzyme, and a decrease in the number of aldehyde functional groups formed. The gross pathology of this disorder, which includes skeletal deformities and vascular aneurysms ³⁵, can be reversed by supplementing the diet with trace amounts of copper. Another less common crosslinking defect, or lathyrism, results from eating the peas of the *Lathyrus odoratus*, or sweet pea plant, which contains the toxic agent, β -amino propionitrile (BAPN). BAPN inhibits the activity of lysyl oxidase ³⁸. As was the case above, a decrease in the activity of lysyl oxidase results in a crosslinking deficiency. In several studies, BAPN has been shown to affect the tensile properties of tissues. In an experiment that might not be undertaken in today's "kinder and gentler" society, Levine and Gross ³⁹ incubated chick embryos in the presence of BAPN and then tested the whole embryo for overall tensile properties by measuring the time necessary to separate the head from the neck under a constant breaking load. The increase in embryo "fragility" increased with respect to the BAPN dose. Wirtschafter and Bentley ⁴⁰ found that the aortas of lathyritic rats had a greater level of extractable collagen, and were more likely to develop aneurysms, due to a drop in tensile strength. Also, BAPN has been shown to inhibit the increase in tensile strength of healing wounds ⁴¹. Once BAPN treatment ceases, the tensile strength of the wounds increase.

c. Mechanisms of Protein Tanning.

Even though connective tissues, *in vivo*, exist in a crosslinked state, they are still susceptible to postmortem degradation. It is for this reason that for thousands of years, man has found it necessary to introduce additional crosslinks into connective tissues in order to make useful products ranging from bow strings to leather. The preparation of tissues for histological examination also requires that crosslinks be introduced prior to tissue processing. Much more recently, many medical prosthetic devices have been manufactured from reconstituted connective tissue proteins, such as collagen, and these products, in turn need to be stabilized by introduction of some form of artificial crosslink.

As leather making has become a unique chemical science, three major classifications of connective tissue protein crosslinking agents, the inorganic, aldehyde, and vegetable tannins, have been described in great detail. The information that has resulted from these studies, has benefited the fields of histology and medical prosthesis development. In all classifications, the ability of the tanning agent to interact with the reactive side groups of the protein is essential. This can occur through various molecular forces from weak hydrogen and hydrophobic interactions to extremely strong coordinate and covalent interactions. The following review will describe the numerous chemical modifiers of proteins with respect to the mechanisms of interaction.

1). Protein Ligands.

Chemical modifications of proteins with various ligands provide numerous tools for not only studying structure and function, but also developing new and useful materials. The catalytic sites of enzymes can be modified to provide information on the molecular mechanism of catalysis ^{42,43}, and proteins have been modified to reveal information on the binding sites of protein-nucleic acid complexes ⁴⁴. Chemotherapeutic agents have been modified to improve their effectiveness ⁴⁵. Ligand receptors can be blocked to provide information on the role of specific drugs on these receptors ⁴⁶, and nutritionists have experimented with modification of food proteins to increase the nutritional value of the food ⁴⁷.

The development of systems for chemical modification of proteins has used strategies to attack the available reactive functional groups of the N and C-terminal alpha carbons, and the individual amino acid side chains, by reactive ligands. The list of reactive functional groups available include the amino groups of the N-terminal alpha carbon and the epsilon amino carbon of lysine and hydroxylysine side chains, the sulfhydryls of cysteine side chains, the disulfides of cystine, the thioether group of methionine, the phenols of tyrosine, the imidazole group of histidine, the hydroxyl group of serine and threonine, the indole of proline and hydroxyproline, the guanidinyll group of arginine, and the carboxyl groups of the C-terminal alpha carbon and of the side chains of aspartic acid and glutamic acid. Protein modification protocols have been reviewed by Glazer ⁴⁸. The majority of the functional groups listed above have limited reactivity, and therefore, only a few methods of modification have been described. The ϵ -amino group of lysine and

hydroxylysine residues and the sulfhydryl group of cysteine are very reactive, and therefore many methods of modification have been described for these. Notable examples of modifications include acetylations, and Schiff base formation between the ϵ -amino group of lysine and aldehyde groups. Hemoglobin⁴⁹, as well as collagen⁵⁰ is naturally glycosylated via Schiff base formation with the aldehyde functional group of glucose.

Protein ligands can alter the structure and function of the protein to which it binds. Those which create molecular bonding forces which stabilize a protein system are termed tanning agents. Several such ligands have been described, and can be grouped into general categories. In the following pages, three categories of tanning agents will be described with respect to the amino acid side chain target, and the type of molecular bonding force of crosslink which are formed.

2). Protein Crosslinking With Inorganic Salts.

Crosslinking of proteins with inorganic elements such as chromium, zirconium, aluminum, iron, and titanium is unique to the leather industry. The metals are generally introduced as salts, and the crosslinks formed are diverse. In general, however, the bond type is coordinate which indicates a sharing of d orbitals of the metal with specific reactive groups on the protein⁵¹. Chromium (Cr^{3+}) complexes form coordinate bonds with carboxyl side chains of proteins⁵¹, for if the carboxyl groups are acetylated, the overall stability of the crosslink is greatly reduced. Chvapil, *et al*,⁵² showed that the intact crosslink can be formed either by two carboxyl groups entering into the same chromium complex, or via an olation

reaction. In this reaction, two chromium complexes, each coordinately bound to a carboxyl group, condense through the elimination of one molecule of water (Fig. 4). The crosslink is then stabilized through an oxolation reaction.

3). Protein Crosslinking With Aldehyde Compounds (Fixation).

The second class of tanning agents are the aldehyde tannins. Glyceraldehyde, glyoxal, acetaldehyde, acrolein, dialdehyde starch, glutaraldehyde, and formaldehyde are examples of aldehyde tannins which react to covalently modify proteins. The latter two have proved most significant as protein crosslinkers and thus shall be described in some detail.

Glutaraldehyde forms various covalent crosslinks with proteins by reacting through its two functional carbonyls primarily with available amino groups⁵³⁻⁵⁷ and specifically epsilon amino groups of lysine residues⁵⁸ as shown in Figure 5. A 265 nm absorbing compound results from the reaction of glutaraldehyde and amine compounds. Hardy, et al⁵⁹ isolated a pyridinium type compound which absorbs at 265nm, and have proposed it to be the structure of the covalent crosslink. On the other hand, Michael addition products of Schiff bases formed between glutaraldehyde and amines have been proposed^{60,61}. Finally, long chain polymers of glutaraldehyde are thought to form through some unknown mechanism⁵³.

Glutaraldehyde has served as an important crosslinking agent in many protein systems. It has been widely used as a fixative in high resolution scanning electron microscopy of chromatin⁶², cytoskeletal elements⁶³, and many other proteins. Glutaraldehyde has also been used to modify antigens for use in treatment of

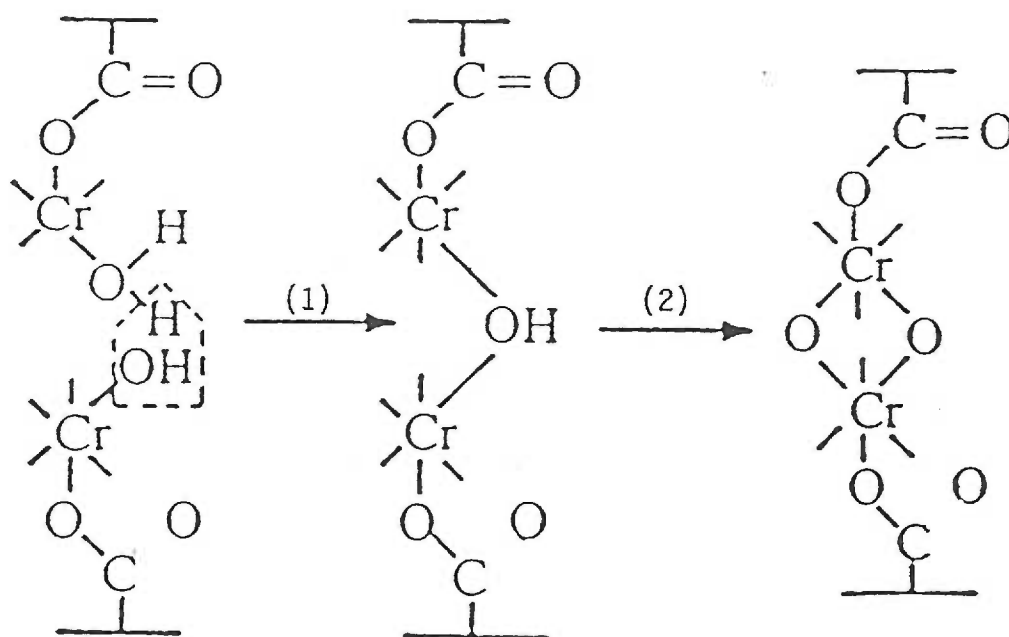


Figure 4. Protein tanning with chromium. Chromium complexes bond coordinately to protein carboxyl groups, followed by oxidation 1) and oxidation 2) reactions to form a stable crosslink⁵². Reproduced from Bienkiwicz⁵¹.

┊ = Protein backbone

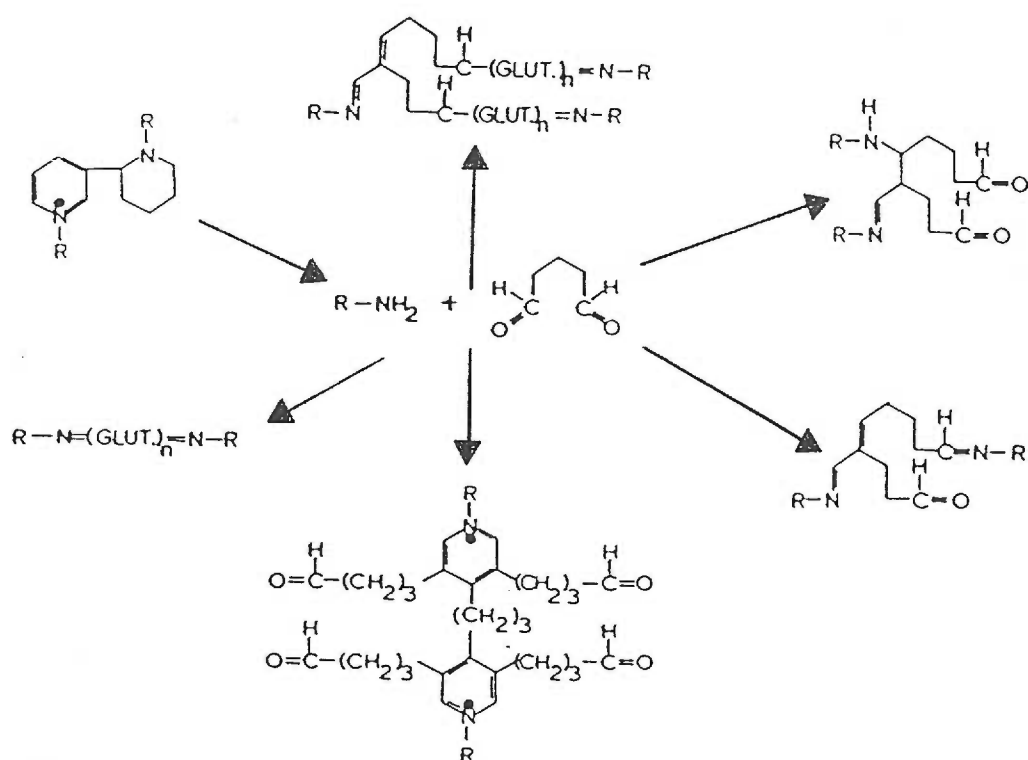


Figure 5. Molecular crosslinking models of glutaraldehyde (Glut.) fixation⁵³⁻⁵⁸.

$R-NH_2$ = Protein with free amine group.

allergic disease ⁶⁵, and to modify hemoglobin so as to alter its oxygen affinity ^{66,67}. The most important role of glutaraldehyde in the biomedical field, however, is as a crosslinking agent used in the production of biological prostheses, such as glutaraldehyde crosslinked porcine heart valves ⁶⁸.

Glutaraldehyde crosslinking of proteins was introduced in part to overcome the shortcomings of formaldehyde. The chemically related formaldehyde failed to produce crosslinks which were chemically or thermally stable enough for use in the bioprosthesis field. Unlike glutaraldehyde, formaldehyde has only one carbonyl group, and therefore the mechanism of crosslinking is not as apparent. Frankel, Conrat and Olcott ⁶⁹ have described the reactions of formaldehyde with proteins. Formaldehyde initially reacts through its aldehyde functional group with a lysyl ϵ amino group to form an alkanolamine. This adduct can then either react with an amide group, or a tyrosine residue through a Mannich reaction to form the respective acid labile and non-acid labile crosslink structures shown in Figure 6.

A drawback common to both glutaraldehyde and formaldehyde is their well accepted cytotoxicity, since both have been shown to leach out from the interstices of collagen fibrils of bioprostheses ⁷⁰.

4). Protein Crosslinking With Vegetable Tannins.

The final category is that of the vegetable tannins. These became popular during World War II due to the shortage of chrome, but have since fallen out of favor due to the expense of preparation. This fact probably explains the sparse ⁶⁹ literature in this field of chemistry in recent years. The term vegetable tanning

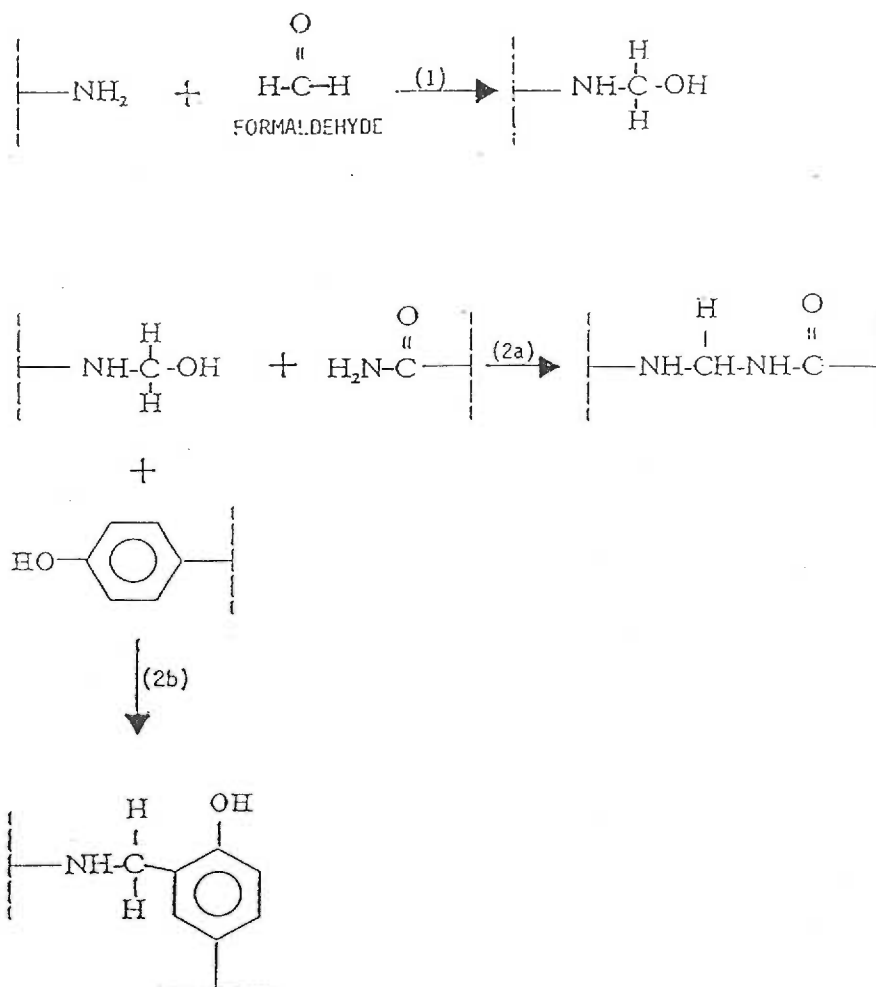


Figure 6. Two proposed "mechanisms" of protein crosslinking with formaldehyde⁶⁴. Both mechanisms initially pass through a common reaction step 1). The first mechanism 2a) produces an alkanolamine crosslink. The second mechanism 2b) adds tyrosine via a Mannich reaction.

|—NH₂ = Protein with free amine group.

comes from the fact that many of these tannins can be derived from metabolites of the shikimic acid pathway in plants. However, in general all vegetable tannins possess a carboxyl group and are polyphenols which can be oxidized to quinones.

Whether or not vegetable tannins introduce covalent crosslinks has not always been agreed upon. Figure 7 shows that one model de-emphasized the role of covalent crosslinks⁵¹. Instead the tanning effect was the result of hydrogen bonding of phenol groups to collagen peptide bond carbonyls, and the noted increased thermal stability or shrinkage temperature was the result of a bridging effect. Gustavson⁷¹, however, rejected this model stating that interactions between collagen and phenolic vegetable tannins were too strong to be of a hydrogen bonding nature. He proposed a covalent model of crosslinking between basic groups on collagen and the oxidized form of the tannins.

The following mechanism⁵¹ of covalent crosslinking of collagens with hydroquinones has been proposed (Fig. 8). In step one of the mechanism, a free amine group of a amino acid is added to the quinone ring resulting in a hydroquinone collagen adduct. This can be oxidized back to the quinone form through the participation of an additional quinone. Mason⁷² recognized the necessity of excess *ortho*-quinone in oxidizing catechol-lysyl epsilon amino derivatives to the corresponding *ortho*-quinone derivative. A second side chain amine can be added to form a complete hydroquinone crosslink which can itself be oxidized to the quinone.

In the same study, it was shown that quinone tanning is a two step process. In the key experiment, a hide was incubated in a tanning medium containing three

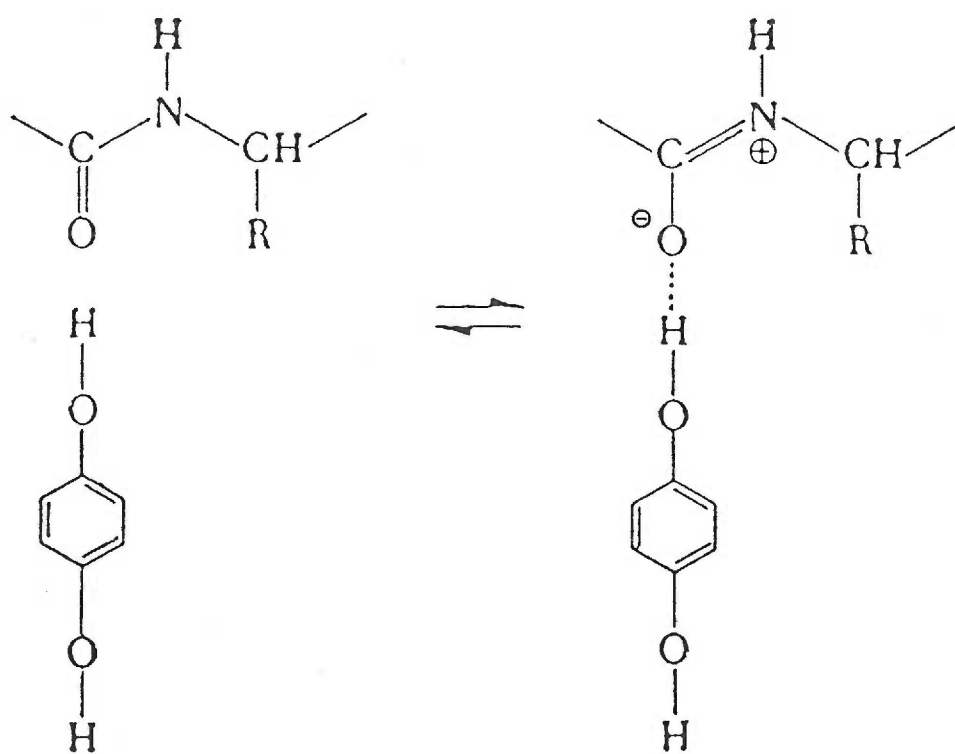


Figure 7. The hydrogen bonding model of vegetable (quinone) tanning ⁵¹.

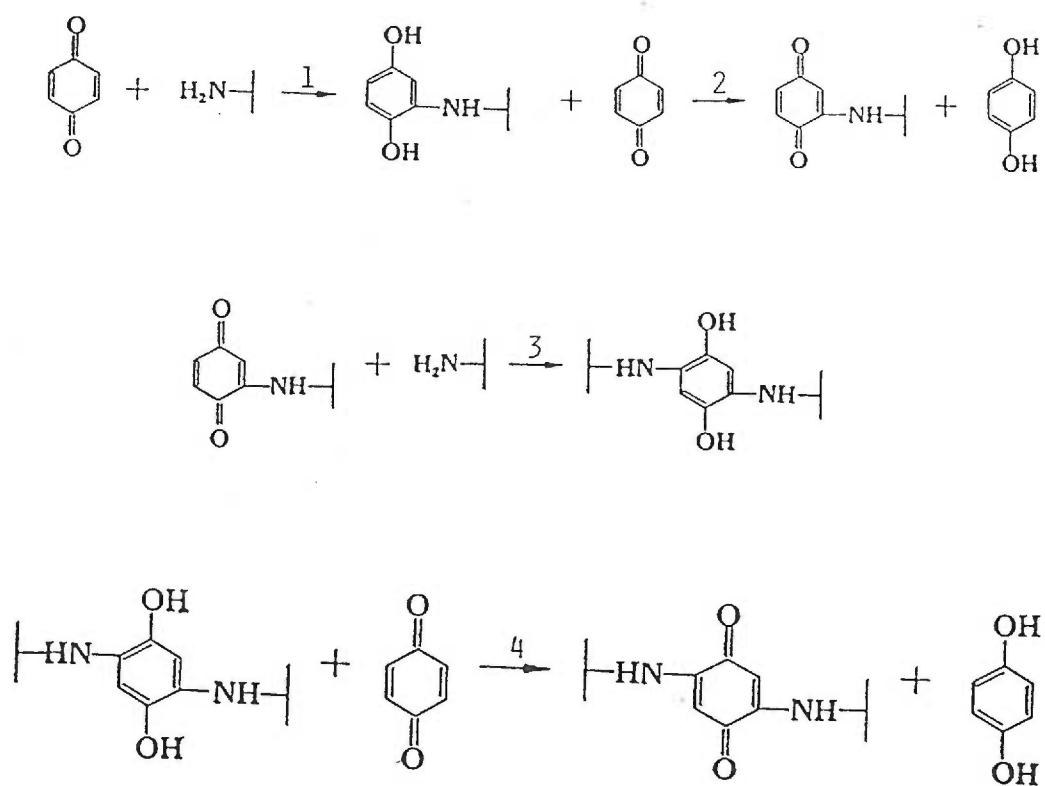


Figure 8. The covalent crosslinking model of vegetable (quinone) tanning ⁵¹.

—NH₂ = Protein with free amine group.

quinone tannins free of oxygen at pH 5.6 for 24 hours. An initial rapid increase in the thermal stability of the tissue was noted. This increase could be solely attributed to the introduction of phenolic hydrogen bonds since under these conditions the hydroxyl groups were neither dissociated nor oxidized to the quinone. At 24 hours the oxidant, potassium ferro cyanate was added, and the pH adjusted to 8.0. At this pH, phenolic hydroxyls are totally dissociated and can not take part in hydrogen bonding. The thermal stability under these conditions was greatly increased, though at a slower rate. This slow increase was likely due to the covalent addition of collagen chains to the quinones. In the final step of the experiment, the pH was adjusted to 4.5. At this pH, the phenolic hydroxyls are completely associated and can hydrogen bond. The result is an additional substantial increase in the thermal stability. Through monitoring of the electronic spectra of the tanning medium, Endres⁵¹ found that tanning occurred through a two step mechanism of covalent interaction of protein amines and quinones, followed by hydrogen bonding of the hydroxyl group of the hydroquinone crosslink with the carbonyl of the peptide bonds of the protein.

The derivatives of catechol fit into the loose definition of the vegetable tannins due to their polyhydroxyl nature, and their ability to be oxidized to the *ortho*-quinone form. Important members of this class of compounds are the tyrosine metabolites, DOPA, dopamine, epinephrine, and norepinephrine. As the following sections shall demonstrate, *ortho*-quinones appear to play an important role in at least two models of *in vivo* protein tanning, and can bind to and effect the properties of connective tissue protein systems.

c. Insect Cuticle Tanning.

The hardening of the insect cuticle has provided a useful model for investigating the mechanism by which *ortho*-quinones crosslink proteins in a biological system. Pryor⁸⁰, proposed that the cockroach cuticle, and in fact all insect cuticles, are hardened by a protein tanning mechanism similar to the well established process of leather tanning by benzoquinone⁷¹. Quinones were thought to introduce crosslinks between protein chains, thus stabilizing the newly synthesized matrix. Support for this mechanism has recently been provided by Sugamaran, et al⁷³⁻⁷⁶. By using radioactive tracer techniques, they demonstrated the incorporation of tyrosine metabolites into the sarcophage pupal cuticle. By hydrolyzing the cuticle and then separating the components of the hydrolysate on a Dowex 50 Column, highly basic tyrosyl derivatives were isolated which were different from the parent amino acids. In addition, a 68kD polypeptide released by either chymotrypsin cleavage, or by trifluoromethane sulfonic acid had a dipeptide sequence of tyrosyl metabolites within its primary sequence.

In direct contrast with the covalent cuticle tanning mechanism is the non-covalent hydrophobic interaction model proposed by Vincent and Hillerton⁷⁷. The premise of this model is that covalent crosslinking can not alone account for the great physical strength of the cuticle and in fact would only be of secondary importance. Rather, they proposed that the quinones secreted into the developing matrix are converted to 5,6-dihydroxyindole which is in turn polymerized to form melanin^{78,79}. The melanin like polymer, once formed would interact with the cuticle

proteins through both hydrophobic and hydrogen bonding molecular forces. The result is an occupation of the important hydrating groups of the protein and a concomitant dehydration of the matrix. There is, in fact, some support for this mechanism. Pryor ⁸⁰ demonstrated that a cube of gelatin, when soaked in concentrated benzoquinone, shrank to nearly 50% its original size in two months and "became as hard as wood". Fraenkel and Rudall ⁸¹ demonstrated a loss of water content from 70% to 12% in the blowfly purpurin which coincided with the increased stiffness of the cuticle. In addition, Vincent and Hillerton ⁷⁷ showed that by simply drying the cuticle protein, in the absence of tanning agents, the material had similar physical properties to the tanned cuticle.

It seems likely that both matrix dehydration as well as covalent modification and crosslink formation contribute to the hardening processes of the insect cuticle. Quinone compounds may covalently bind to the cuticle protein and polymerize with other quinones to form large polymers which could then expel water from around the protein.

e. Catecholamines and Collagen.

Prior to our current knowledge of the primary role of lysine in forming covalent crosslinks between collagen chains, tyrosine was itself thought to be a likely candidate as a key player in collagen crosslinking and ageing. Though the helical region of the type I ($\alpha 1$) collagen molecule has a very low tyrosine composition (2 residues/collagen helix), there are 2 residues in the 30 residue telopeptide crosslinking region of the $\alpha 1$ chain of type I collagen ⁸². Grant and Alburn ⁸³, utilized

the *in vitro* collagen gelling model of Gross¹⁰² where soluble collagen when warmed to 37°C at neutral pH precipitates forming a fibril system which appears identical at the E.M. level to *in vivo* fibrils, to determine the effect of tyrosine derivatives on the expected redispersion of the fibril system when cooled to 4°C. Micromolar concentrations of catecholamines and polyhydric phenols including epinephrine, DOPA, dopamine and catechol inhibited dispersion of the collagen gel. On the other hand, tyrosine and other mono-hydroxylated compounds did not affect the dispersion rate of the gel. Those compounds which inhibited dispersion of the gels also slightly decreased the extractability of the collagen with bacterial collagenase as well as trypsin, with respect to control. Also epinephrine treated gels had a slightly higher thermal stability than control gels, which suggests an increase in gel stabilization. Finally, using a spectrophotometric technique, they showed that the catecholamines were in fact bound to the protein, though the mode of interaction was uncertain.

In a related study⁸⁴, purified acid soluble and pepsin soluble collagen solutions, were treated with mushroom tyrosinase and placed under conditions at which *in vitro* fibril formation occurs. The acid soluble collagen solutions developed a yellow brown color and demonstrated a dramatic increase in fluorescence with respect to the control. Also, physical properties of the tyrosinase treated collagen solution were indicative of stabilization of the matrix. Pepsin treatment, which removes the non-helical telopeptides, caused a significant decrease in the tyrosinase induced properties, though not a total loss. Obviously, removal of the telopeptides removes the two tyrosine residues mentioned previously. Tyrosinase, therefore,

oxidizes the tyrosine residues to DOPA and its corresponding quinone which the authors asserted, can introduce intra and intermolecular crosslinks.

Catecholamines have been shown fluorometrically to bind to both collagenous and elastic tissues. Powis¹³³ estimated the quantitative binding of noradrenaline to blood vessel collagen with Scatchard analyses. He demonstrated both a high and low affinity site for catecholamine binding, and proposed that collagen is a catecholamine sink which can terminate adrenergic nerve stimulation by rapidly clearing catecholamines from the blood stream.

The bioadhesive of *mytilus byssus* (the sea mussel) is the only naturally occurring protein known to contain L-DOPA within its primary sequence⁸⁵. Interestingly, its amino acid composition is also similar to that of collagen. The adhesive precursor polypeptide has 48 DOPA residues per 1000. The adhesive has a high bonding strength which allows the sea mussel to attach itself firmly to the sea bottom. The authors hypothesized that the DOPA residues condense with nucleophilic groups on the collagen like protein following oxidation by the enzyme phenyloxidase, resulting in quinone crosslinking of the protein.

The crosslinking of proteins with DOPA oxidative metabolites has, thus, been proposed to occur through a dopaquinone monomer structure. However, DOPA metabolites are relatively unstable and are readily oxidized to form the large polymer, melanin. Melanin, found throughout the animal kingdom, provides a protective shield against the harmful ultraviolet rays of the sun. Melanin production is generally restricted, *in vivo*, to the specialized epithelial cells, melanocytes⁸⁶, but can be duplicated *in vitro* in a well oxygenated, neutrally buffered environment. The importance of DOPA polymer formation in the previously discussed crosslinking

processes can, therefore, not be overlooked and is indeed a key proposal of this thesis. For this reason, the following section will review the proposed mechanisms of DOPA metabolite polymerization to form melanin.

2. Melanogenesis.

Melanin formation, *in vivo*, occurs via a series of enzymatic and spontaneous oxidation reactions. Raper⁸⁷ and Mason⁸⁸ originally described the reactions and proposed a defined sequence of events which resulted in the formation of a melanin homopolymer of the terminal precursor. The reactions of the so-called Raper-Mason pathway of melanogenesis are shown in Figure 9, and are briefly described below. The first step, the *ortho*-hydroxylation of tyrosine to form 3,4-dihydroxyphenylalanine (DOPA) is catalyzed by tyrosinase. This enzyme occurs in both eukaryotic and prokaryotic organisms, and has been well studied in both. Along with this cresolase activity, tyrosinase also catalyzes the second step of melanogenesis. Through this so-called catecholase activity, tyrosinase oxidizes DOPA to dopaquinone a highly reactive molecule which is capable of undergoing a number of spontaneous chemical reactions. Dopaquinone, in a fast reaction is cyclized to leucodopachrome, or cyclodopa, which is, in an equally fast reaction oxidized to the corresponding quinone, dopachrome through a dehydrogenation reaction. The oxidizing power is supplied by an additional dopaquinone. Dopachrome absorbs in the visible and ultraviolet range with wavelength maxima of 305 and 475 nm⁸⁸. According to the Raper-Mason pathway, this compound is then

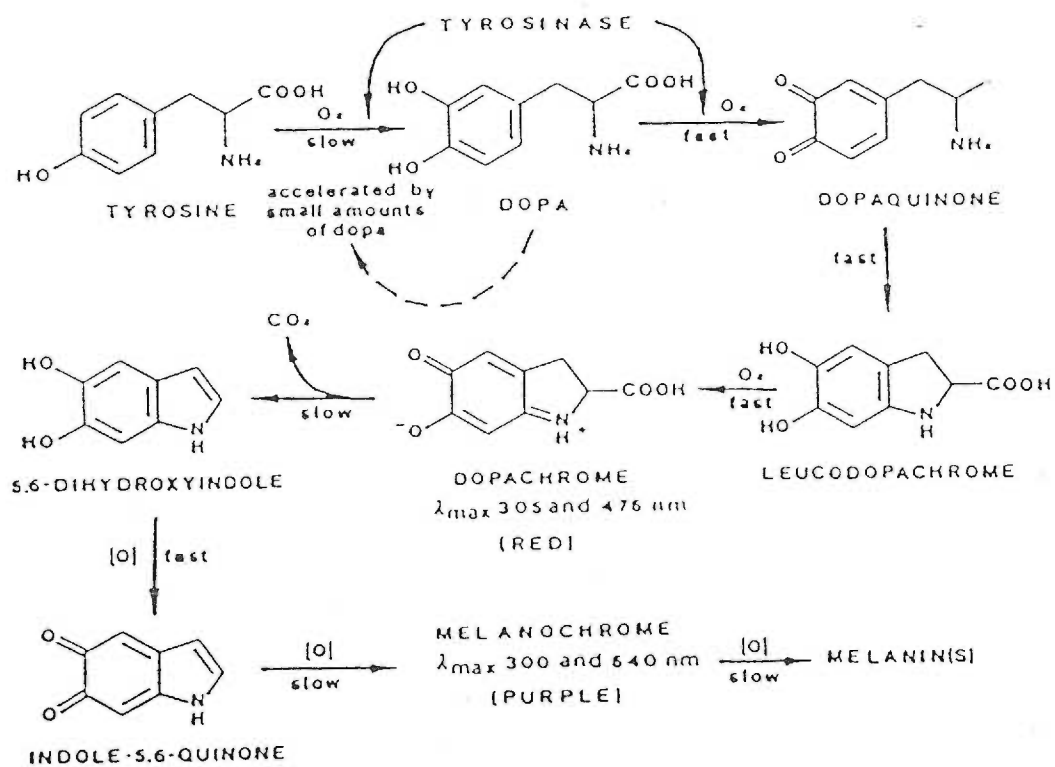


Figure 9. The Raper-Mason pathway of melanogenesis^{87,88}. Reproduced from Prota⁸⁹.

rearranged and decarboxylated to form 5,6-dihydroxyindole (DHI) which is in turn oxidized to the corresponding quinone, indole-5,6-quinone. It is a basic premise of this pathway that melanin is a homopolymer of this *ortho*-quinone. Mason⁸⁸ identified a melanochrome with spectrophotometric characteristics (absorbance maxima of 300 and 540 nm) which corresponded to a dimer of indole-5,6-quinone.

More recent evidence⁸⁹⁻⁹¹ supports the contention that melanin is a highly heterologous polymer formed from at least three *ortho*-quinones derived from DOPA. Gruhn, *et al*⁹², have identified DOPA oligomers from the urine of melanoma patients containing cyclodopa which are formed through alternative additive reactions, and are considered as one possible melanin precursor. Palumbo, *et al*⁹³ used acid decarboxylation and permanganate degradation to show that melanin formed in the presence of various divalent cations (Cu^{2+} , Co^{2+} , and Zn^{2+}) contained a high concentration of the 5,6-dihydroxyindole-2-carboxylic acid, and Palumbo, *et al*⁹³, showed that in the presence of divalent cations, decarboxylation of dopachrome was less favorable than when divalent cations were absent. The heteropolymer theory of melanin polymerization is based upon basic principles of organic chemistry. The quinoidal groups of an *ortho*-quinone withdraw electrons from the aromatic ring creating a partial positive electrophilic site at ring carbons 2, 5, and 6 (Fig. 10). These potential Lewis acids can be attacked by Lewis bases. The alpha amino group of dopaquinone is a Lewis base which attacks at ring carbon 6, resulting in cyclization to form cyclodopa and the indole structures which follow. This ability to form an indole ring gives rise to the diversity of the melanin subunits and the complexity of the polymer formed.

The *ortho*-quinones of DOPA can react with other Lewis bases. Proteins provide a number of potential nucleophiles such as the hydroxyls of serine and threonine, the sulfhydryls of cysteine and the amines of lysine and hydroxylysine sidechains of proteins (Fig. 10). One such reaction which itself is important in melanogenesis is the addition of sulfhydryl groups to the quinone ring. Cysteinyl sulfhydryl side chains are capable of reacting with quinones^{94,95}. The cysteinyl-DOPA adducts formed from free cysteine are the basic monomers of the sulfur containing phenylamines, and can be further cyclized to give a 1,4-benzothiazine derivative which can be fed into the eumelanin pathway to give mixed melanins. Several groups have demonstrated the binding of glutathione to dopaquinone in a similar mechanism giving glutathione-DOPA derivatives. These adducts are converted via the activity of glutamyl transferase and peptidase to cysteinyl-DOPA and finally pheomelanin. Rorsman⁹⁶ proposed that this reaction mechanism serves to protect human melanocytes against the oxidative potential of tyrosine metabolites. *Ortho*-quinones also react readily with amines. Aniline reacts with the *ortho*-quinone, catechol, via a 1,4-Michael addition⁹⁷. Amino acids can also react through their alpha-amino acids with *ortho*-quinones⁹⁷. Proline, with its secondary amino group, reacts to form an intense purple compound⁸⁸. *Ortho*-quinones also appear to react with free ϵ -amino groups along the length of a protein chain⁷², and it is through this process that *ortho*-quinones are believed to crosslink proteins.

Attempts to understand the structure of melanin through a procedure which would dismantle the polymer have met with little success. Only soluble dimers and oligomers have been isolated and identified. Bu'Lock and Harley-Mason⁹⁸ used extensive model studies in demonstrating that melanochrome is formed by

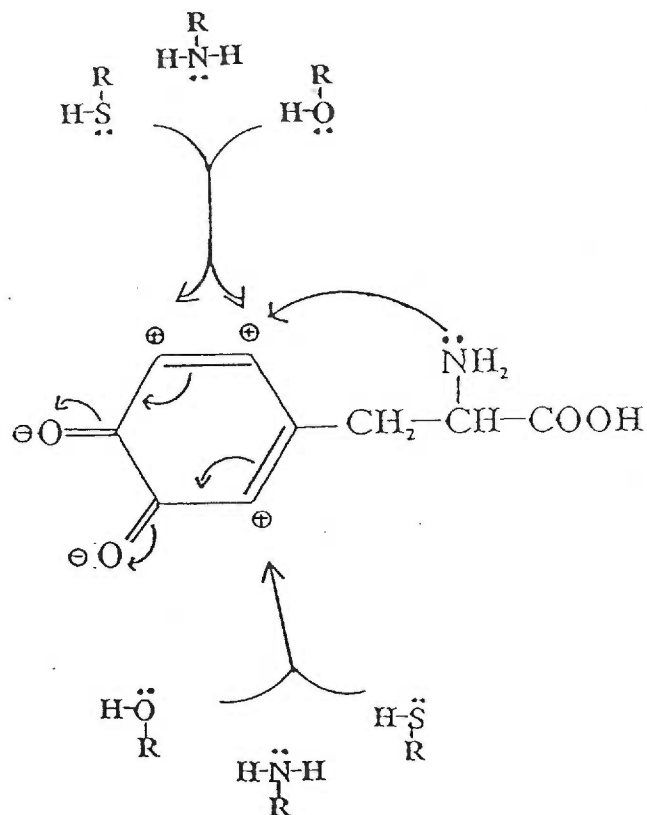


Figure 10. Lewis base attack of orthoquinones. The quinoidal groups of orthoquinones withdraw electrons from the quinone ring creating partial positive charges or electrophiles (Lewis acids) which can react with available Lewis bases. The alpha amino group of dopaquinone reacts at the adjacent ring carbon to form an indole. This reaction is highly favored due to the neighboring group effect. Lewis bases of proteins, as shown, can react at three electrophilic ring positions. Though not shown, the nitrogen of the newly formed indole ring, also a Lewis base, can react with with electrophiles of other orthoquinones to form dimers and other melanin like polymers.

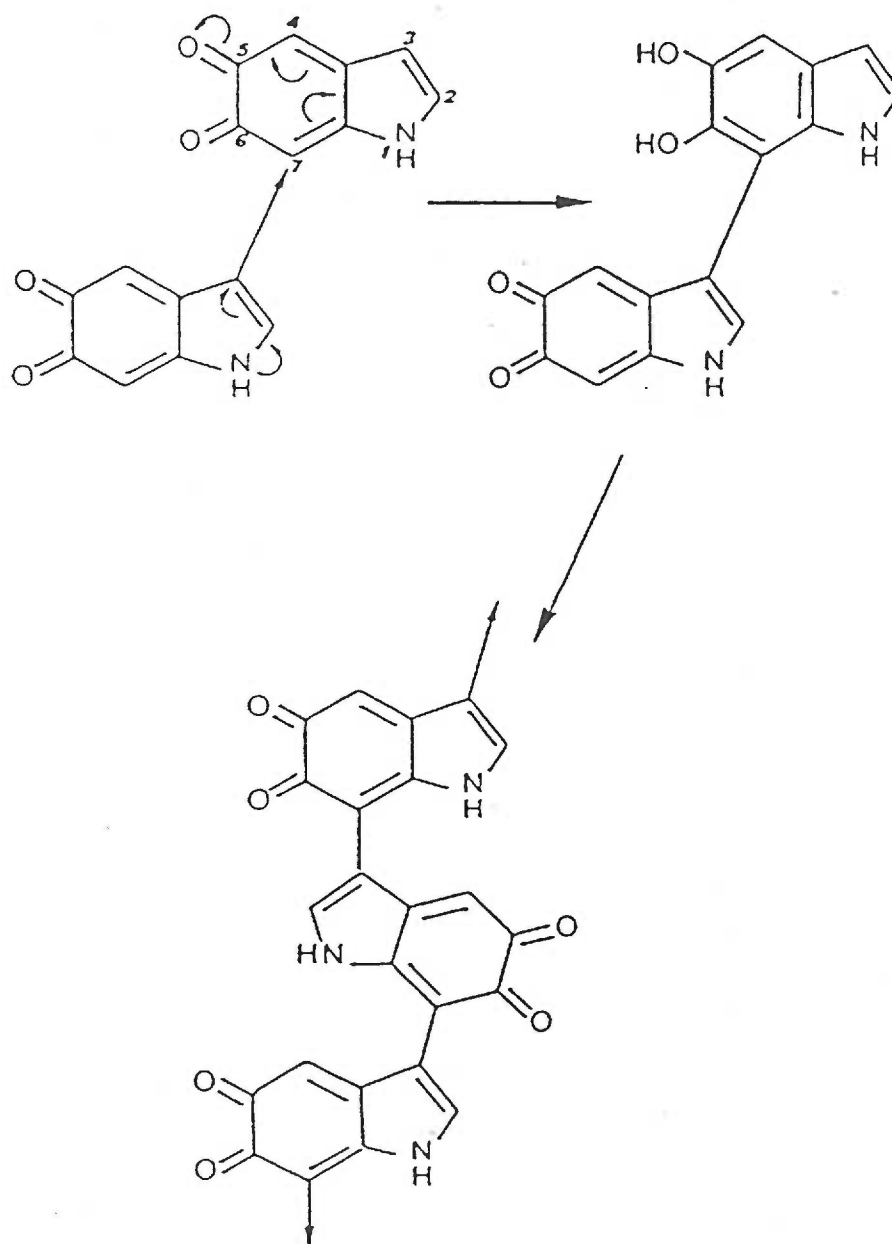


Figure 11. A proposed mechanism of melanochrome and higher melanin polymer formation by reaction at the 3 and 7 ring positions of dihydroxyindole¹¹. This dimer of indole-5,6-quinone represents the simplest orthoquinone condensate.

condensation at ring positions 3 and 7 of DHI as shown in Figure 11. Prota⁸⁹ has recently isolated a reduced and acetylated leucomelanochrome formed via the interaction of DHI monomers at the unique 2 and 4 positions on the ring. The reaction is catalyzed by divalent cations, and the mechanism appears to involve the coupling of phenoxyl radicals. A melanochrome dimer of DHIC has also been described which forms by a similar mechanism as that described above, with interaction of the 4 and 7 positions⁸⁹. In contrast, Fattorusso and Cimmino⁹⁰ have proposed a mechanism similar to that proposed for the non-carboxylated indole quinone in which condensation of indole-5,6-quinone-carboxylate subunits occurs at the 3 and 7 ring positions.

In summary, the alanine group of DOPA allows the production of a unique group of *ortho*-quinones. Melanin is a heteropolymer of at least three of these, and it is this complexity which results in the noted black pigmentation. In addition, these orthoquinones can react with Lewis bases of proteins and it is proposed, form covalent crosslinks between the derivatized proteins.

B. Rationale.

The present work will test the hypothesis that DOPA and other catechol derivatives can stabilize reconstituted collagen through a two step mechanism. In step 1, oxidized catechol monomers (*ortho*-quinones) derivatize collagen by reacting with lysine ϵ -amino groups through 1,4-Michael additions. Binding at these hydrophilic sites results in a partial dehydration, collapse and compaction of the matrix. The end result is a stabilization of the matrix. These bound monomers can then, in step 2, polymerize to form melanin like covalent crosslinks between adjacent collagen fibrils, following a series of oxidation reactions. A dimer crosslink would be the simplest structure, though much larger polymers could occur. The result is a collagen matrix with normal fibrillar banding at the E.M. level, and enhanced chemical and physical properties.

The Experimental section of this thesis will be divided into three parts. Part I will describe the nature of the fibrous collagen matrix formed when collagen fibrils were reconstituted in the presence of DOPA. Chemical, physical, and structural data will be presented. Part II will address the mode of interaction of collagen with oxidized catechols (*ortho*-quinones) with reactive groups on collagen. Included within this section will be data that supports covalent interaction of DOPA and collagen, identification of the reactive residue which binds DOPA, and mapping of these residues to specific collagen peptides. Finally, Part III will address the mechanism by which the prebound *ortho*-quinones form covalent crosslinks between collagen molecules. A polymerization model of crosslinking will be proposed and

supported. The thesis will then conclude with a general discussion which will tie together the three parts and discuss the significance and implications of the findings herein.

IV. EXPERIMENTAL.

In the experiments that follow, the effect of catechol derivatives on type I collagen fibril stabilization will be considered. Throughout the thesis, the term "collagen" will be taken to mean **only type I collagen**. Extensive purification of bovine collagen extracts have been undertaken to eliminate type III collagen contaminants, and this has been described in the appendix. Type I collagen contains no cysteine residues within its primary sequence, whereas type III collagen has one cysteine at the C-terminal end. *Ortho*-quinones, as is discussed in the introduction, can interact covalently with both sulfhydryl and amino groups. Through the elimination of cysteine containing proteins, this thesis will be able to focus solely on lysine mediated interactions (other lewis bases such as serine and threonine are less likely to react with *ortho*-quinones, and therefore, are also not considered).

In determining the effect of catechol derivatives on collagen fibrils, and the mechanism of this effect, 3,4-dihydroxyphenylalanine (DOPA) was employed as the model compound of this classification of compounds. In the latter stages of the thesis, three analogues of DOPA were used to further clarify the mechanism of action of DOPA and other derivatives of catechol. Preliminary data from this lab suggested that at a concentration of $1 \times 10^{-3}M$, the gel stabilizing effect of DOPA was at a maximum. For this reason, this concentration was used in determining the effect of DOPA in the majority of the experiments which follow.

In the appendix which follows this thesis, detailed descriptions of the general methods used repeatedly throughout the experimental section are provided.

A. PART I. The Chemical, Thermal, and Physical Stability of DOPA-Collagen Matrices.

1. Introduction.

The binding of ligands to proteins can alter the structural and functional properties of the protein system. Several ligands bind to hemoglobin and alter the oxygen affinity of the tetramer¹⁰⁰. The physical properties of collagen fibril systems are enhanced by the binding of glutaraldehyde and other tanning agents¹⁰¹. Unpublished data from this lab has shown that pyridoxal-6-phosphate can enhance the dry tensile properties of reconstituted collagen fibrils following binding through the formation of a Schiff base with the epsilon amino group of lysine residues. In a section of this thesis to follow, DOPA and other catechol derivatives will be shown to bind covalently to collagen and other proteins at lysine epsilon amino groups, through what is apparently a 1,4-Michael addition. How does this binding affect the structural and functional properties of reconstituted collagen fibrils? In very limited studies, Grant and Alburn⁸³ showed that several catecholamines, including DOPA, could inhibit the cold dispersion of reconstituted collagen fibrils, and that the fibrils were slightly stabilized with respect to chemical and enzymatic solubility. The effect of DOPA will be addressed in detail in this section through both chemical and

physical studies. Reconstituted type I collagen fibrils will be used as a model system in measuring the effect of DOPA on these properties.

2. Pepsin collagen gel stabilization with DOPA.

Introduction.

Collagen fibrils can be reconstituted from soluble collagen in a neutral buffer at 37°C, and these fibrils can in turn be dispersed when cooled to temperatures near 0°C ¹⁰². The fibrils formed appear identical at the electron microscope level to native fibrils ¹⁰³. At the gross level, the fibrillar matrix appears gelatinous, and has been given the trivial name, collagen gel. Acetic acid soluble collagen, or tropocollagen, has at the N and C terminal end of the collagen helix, non-helical telopeptides which are known to provide lysine residues necessary for the formation of aldimine crosslinks ². If reconstituted and incubated at 37°C for extended periods of time, the fibrils gradually become resistant to dispersion when cooled due to the reformation of aldimine crosslinks between fibrils (Fig. 12). The result is a "stabilization" of the collagen gel.

The proteolytic enzyme, pepsin, cleaves the non-helical telopeptides from tropocollagen ¹⁰⁴. When reconstituted, pepsin treated collagen gels are completely dispersed upon cooling, no matter how long the gels have been incubated at 37°C. The loss of the telopeptides results in the loss of two of the four critical crosslinking residues, and thus the ability to form aldimine crosslinks. Collagen gel stabilization

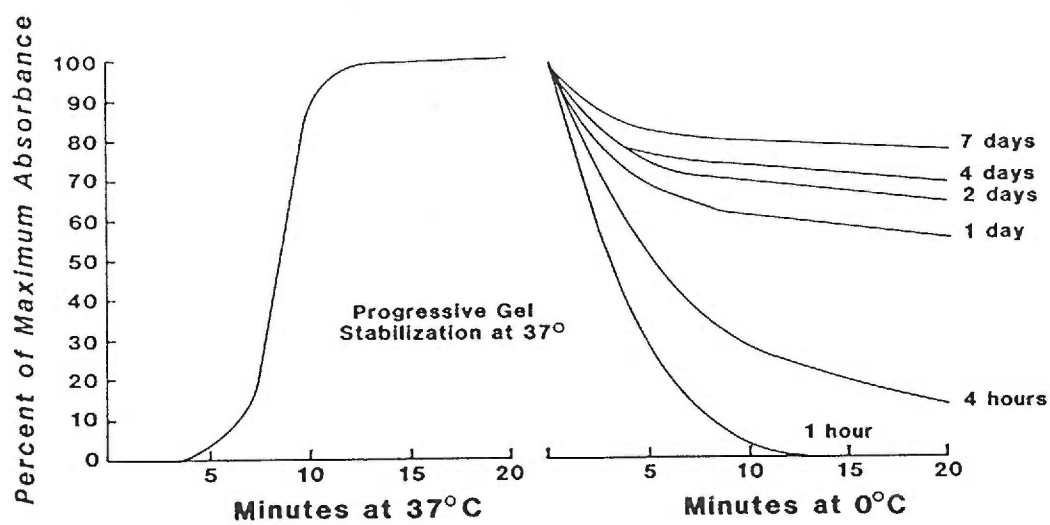


Figure 12. Tropocollagen gel stabilization at 37°C, and destabilization at 0°C. Acetic acid soluble collagen gels are progressively stabilized with increasing periods of time at 37°C due to the formation of aldimine crosslinks. Reproduced from Bentley and Fellman¹⁵⁶.

is not possible. Therefore, the pepsin collagen gel system provides a useful system for testing the effectiveness of putative collagen crosslinking agents. The introduction of artificial crosslinks into the reconstituted fibril system should take the place of the aldimine crosslinks, and gel stabilization should follow. The following experiment made use of this model system, testing the effectiveness of DOPA as a collagen gel stabilizer.

Materials and Methods.

Two buffered type I collagen solutions, pretreated with pepsin, were prepared as described in the general methods section. DOPA (Aldrich Chemical Co.) at a concentration of 1×10^{-3} was added to the first solution. The second solution served as the control. 4 ml aliquots from each solution were transferred to 10 ml Bausch and Lomb spectrophotometric tubes. The tubes were placed in a 37°C water incubator and removed at 1, 1.5, 2, 2.5, 3, and 24 hour time points. At each time point the tubes were placed in an ice bath and the absorbance at 535nm read at 0, 5, 10, 15, 30, 45, and 60 minute time points using Bausch and Lomb Spectronic 20. Following the 60 minute time point, the samples were refrigerated for an additional 23 hours and the absorbance read.

Results.

The results of this experiment are shown in Figure 13. Only the fibril dispersion, or "degelling" phase is given. Figure 14 shows a 24 hour DOPA-collagen

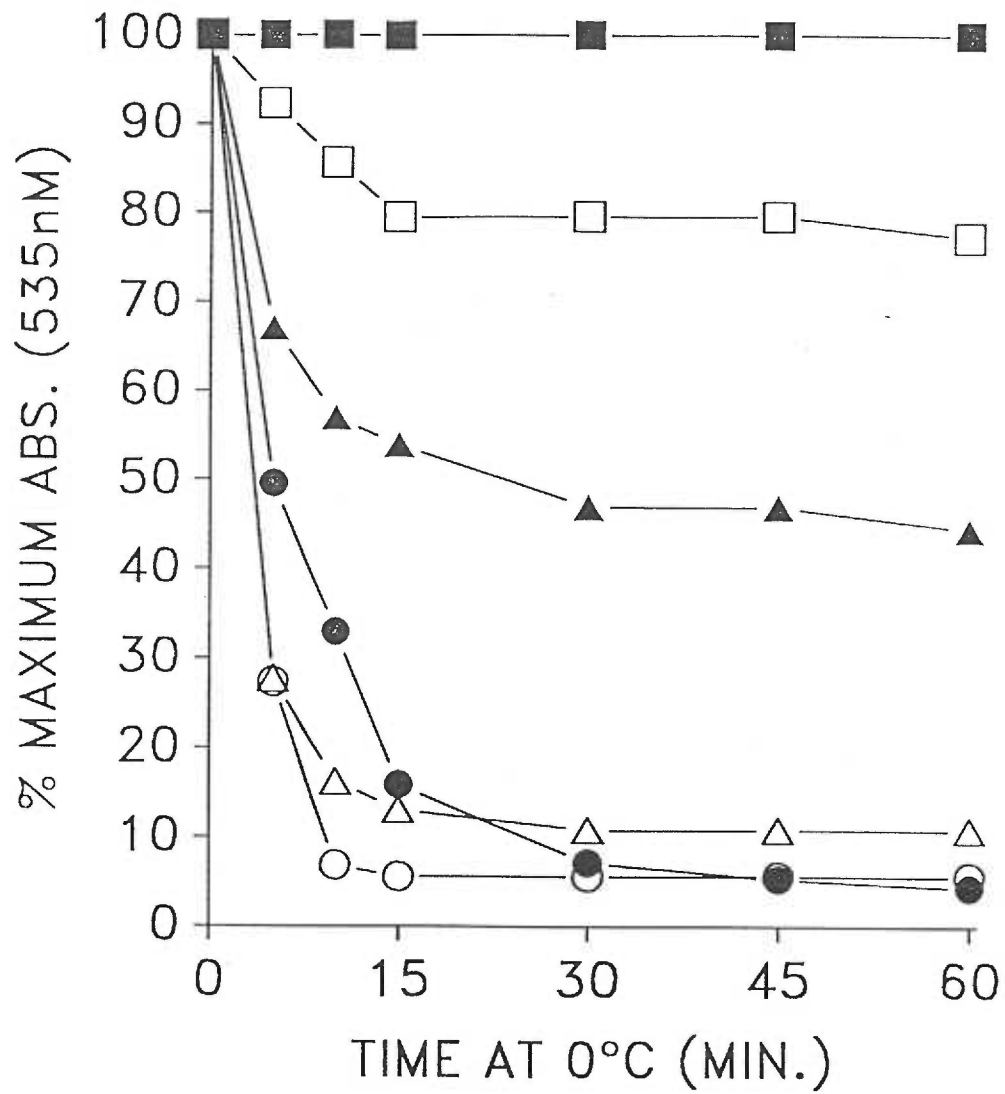
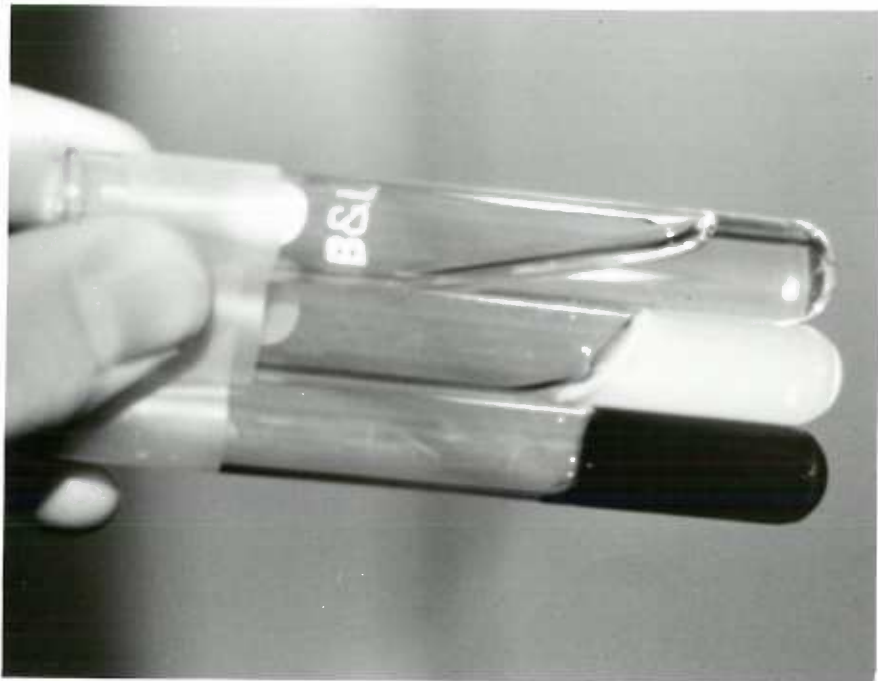


Figure 13. DOPA treated collagen gel stabilization. DOPA stabilization of collagen gels is time dependent.

- 1 hour control
- △ 24 hour control
- 1 hour DOPA
- ▲ 1.5 hour DOPA
- 3 hour DOPA
- 24 hour DOPA.

Figure 14. DOPA-collagen (bottom tube) and pepsin control-collagen gels (top tube) following 24 hours at 37°C and 1 hour at 0°C. A pepsin control gel prior to cooling is also shown (middle tube).



and pepsin-collagen control gel following the degelling phase. The pepsin control gel is completely in solution, while the DOPA-collagen gel is deeply pigmented and rigid.

Discussion.

The results in Figure 13 confirmed the observation that pepsin collagen control gels were completely degelled upon cooling even when incubated at 37°C for extended periods of time. After 1 and 24 hours of incubation at 37°C, the gels were rapidly degelled when cooled, and after 60 minutes destabilization was nearly complete. The introduction of artificial crosslinks into a gel presumably will inhibit the degelling phase. However, following one hour of incubation at 37°C, DOPA-collagen gels degelled completely. It was only after an additional one-half hour of 37°C incubation that the stabilizing effect of DOPA was detected. From this point, the increase in the level of gel stabilization appeared to be progressive, and was at a maximum by 24 hours. Thus, DOPA did stabilize the collagen gels, though an initial 1 to 1.5 hour lag phase preceded the effect. The lag period may indicate that either DOPA, at one hour of incubation, had not been oxidized to the reactive quinone form, and therefore was not capable of binding to the collagen, or that DOPA had bound, but not at a high enough level to cause a stabilization of the gel. The effect of DOPA in this case would be cumulative.

How is the concept of gel stabilization related to crosslink formation? Acetic acid soluble collagen gels become increasingly stable with increasing periods of incubation at 37°C due to aldimine crosslink formation¹⁰⁵. Glutaraldehyde^{53,54} and formaldehyde^{69,106} stabilize collagen fibrils by the introduction of covalent crosslinks

between collagen fibrils. However, Vincent and Hillerton ⁷⁷ have proposed that hardening (a form of stabilization) of the insect cuticle matrix, which has for years been considered a result of quinone crosslink formation, is rather the result of matrix dehydration, not crosslink formation. It seems certain that gel stability and crosslinking are related, though there are better physical measurements of collagen fibril stability which can be related to crosslinking. In the following experiment, the chemical solubility of collagen gels incubated with DOPA was measured.

3. The solubility of DOPA-collagen gels.

Introduction.

Jackson and Bentley ¹⁰⁷ proposed that in any tissue, there exist collagen aggregates with a wide range of susceptibility to solubilizing agents. The degree of insolubility depended upon the relative age of the aggregate and the "strength of cross-linkage". It has since been found that as a tissue ages, the level of detectable reducible crosslinks decreases ¹³. It has long been the contention that these crosslinks are replaced by more stable non-reducible crosslinks and many candidates have been suggested as was described in detail in the introduction. Whatever the structure of the mature crosslink, it is believed that it contributes to the increase in insolubility of the tissue collagen.

When extracting collagen from tissue, several protocols may be employed. Dilute acetic acid hydrolyses immature reducible crosslinks, thus extracting recently laid down collagen ¹⁰⁸. Heating a collagen solution to temperatures approaching 100°C, in dilute acetic acid results in a thermal denaturation of collagen as well as hydrolysis of the aldimine crosslinks ¹⁰⁹. Pepsin treatment, which enzymatically cleaves within the non-helical telopeptide crosslinking region, is used to extract collagen stabilized by mature collagen crosslinks ¹⁰⁴. The type I collagen triple helix, on the other hand, is generally resistant to enzymatic cleavage. The mammalian collagenases, a family of metalloproteases which have been reviewed by Jeffrey ¹¹⁰, cleave at a single site three quarters of the way through the helix, thereby controlling

the physiological turnover of the protein. The helix can, however, be attacked by chemical means. Cyanogen bromide (CNBr) cleaves proteins at the carboxyl side of methionine residues ¹¹¹ and has been used in characterizing the collagens. CNBr treatment releases a series of well defined peptides. Under appropriate conditions ¹¹², the entire collagen content of a tissue can be digested.

In the following experiment, the solubility of DOPA stabilized collagen gels was determined. The solubility in dilute acetic acid under both moderate and harsh temperature conditions, and the susceptibility to cyanogen bromide digestion were determined.

Materials and Methods.

Two buffered collagen solutions were prepared as described in the general methods section (appendix). DOPA was added to one of the solutions at a concentration of 1×10^{-3} M. Nine 2.0 ml aliquots from both solutions were transferred to 10 mm diameter Spectrapor dialysis tubing (M.W. cut off = 12kD - 14kD), and then incubated for 24 hours in a 37°C dry air incubator. The sample bags were exhaustively dialysed against phosphate buffered saline with stirring in the dark over 36 hours. Following dialysis, the gels were removed from the bags and analyzed by the collagen gel resolubilization method described in the general methods section (appendix). In addition to the normal protocol, three samples were autoclaved (15 psi./115°C) in 0.01M acetic acid for 20 minutes.

10 ml aliquots of both the DOPA-collagen and control solutions were incubated in high speed centrifuge tubes at 37°C for 24 hours. Following the

incubation, the collagen gels were homogenized with a Virtis Homogenizer to produce small gel fragments. A fragment of each gel was hydrolyzed in 6.0N HCl for 18 hrs. at 108°C and the hydrolysate analyzed for methionine content by PITC amino acid analysis. The homogenates were digested with cyanogen bromide as described in the general methods section (appendix). Following the extraction, the homogenates were centrifuged at 39,000 x g for 30 minutes in a Beckman J-21 High Speed Centrifuge. The supernatant and pellet were separated and the supernatant was rotary evaporated to remove the excess cyanogen bromide. Equivalent sized aliquots of the supernatants from both samples, and the pellet from the DOPA-collagen sample were hydrolyzed in 6.0N HCl for 18 hours at 108°C. The remainder of the digests were lyophilized and analyzed by SDS-PAGE by the method of Laemli¹¹¹ using a 12.5% acrylamide gel slab. The slab was stained with coomassie brilliant blue R-250 stain as described by Fairbanks¹¹³. All hydrolysates were analyzed for hydroxyproline by the Autoanalyzer method (described in appendix).

Results.

The solubility data for the DOPA-collagen and control collagen gels under the three methods of solubilization is shown in Figure 15. Solubility is expressed in terms of the amount of collagen recovered. Following all treatments, a sizeable pellet remained in the DOPA-collagen samples, but not in the controls. In the boiled and autoclaved samples, the pellet was in the form of a highly contracted, tough, and granular material.

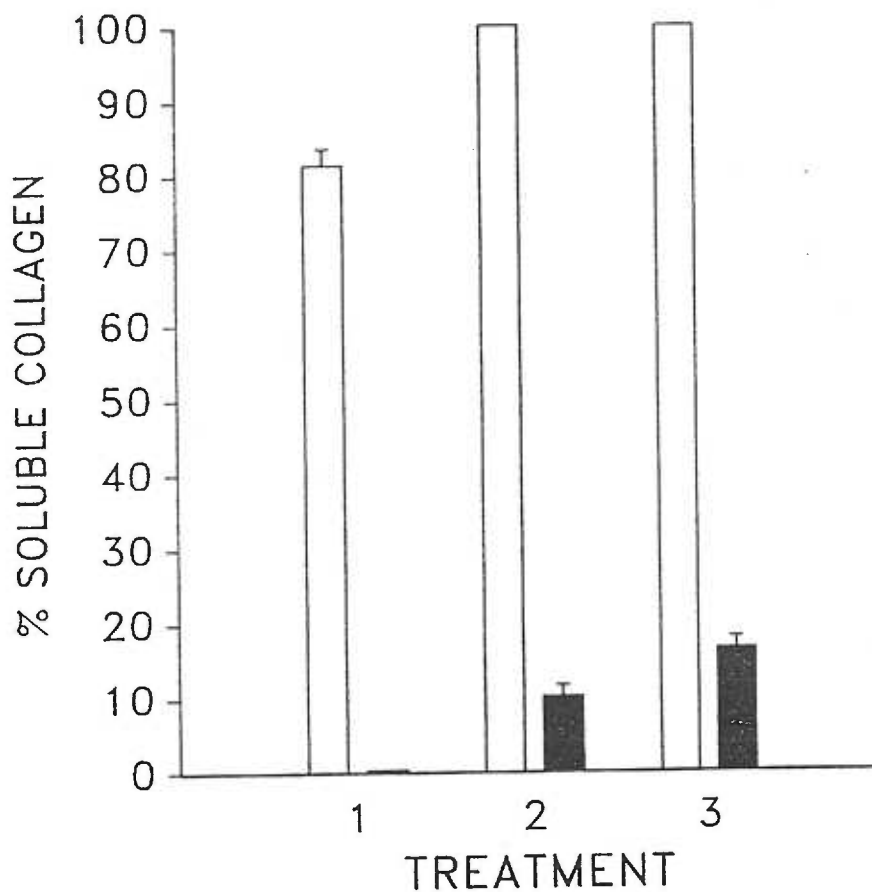


Figure 15. The solubility of DOPA-collagen (■) and control-collagen gels (□) in 0.5N acetic at 4°C for 12 hours (treatment 1), in 0.01 N acetic acid at 100°C for 2 hours (treatment 2), and in 0.01 N acetic acid with autoclaving (treatment 3).

Three replicates were run for each sample. Variation is expressed as the standard error of the mean.

The DOPA-collagen gel had a methionine content of 1.7 ± 0.2 residues per α -chain and the control-gel had a methionine content of 3.5 ± 0.1 residues per α -chain. Following the cyanogen bromide digestion procedure and centrifugation, a sizeable pellet remained for the DOPA-collagen gel, while no pellet remained for the control gel. 100% of the control collagen gel was recovered with CNBR digestion, while $49.6 \pm 0.2\%$ was recovered from the DOPA treated gel. In Figure 16, separation of the components of the CNBr digests for the DOPA and control samples by SDS-PAGE is shown.

Discussion.

The decrease in dilute acetic acid solubility of the DOPA-collagen gels when compared to the acetic acid soluble collagen control gels was dramatic. Acetic acid soluble collagen was used as a control in this experiment to maintain the fibrillar structure of the gel during the dialysis step. Pepsin soluble gels would likely have been even more soluble if tested. As Figure 15 demonstrates, using a typical collagen extraction protocol of dilute acetic acid at 4°C , the DOPA-collagen gel was completely insoluble. However, greater than 80% of the control collagen gel was recoverable under the same conditions. Even under the extremely harsh conditions of boiling and autoclaving in dilute acetic acid, which normally converts collagen to gelatin, the DOPA-collagen gels were very insoluble when compared with the completely soluble control. No more than 12% of the DOPA-collagen gels were recovered. The ability to withstand the extreme conditions employed in the acid

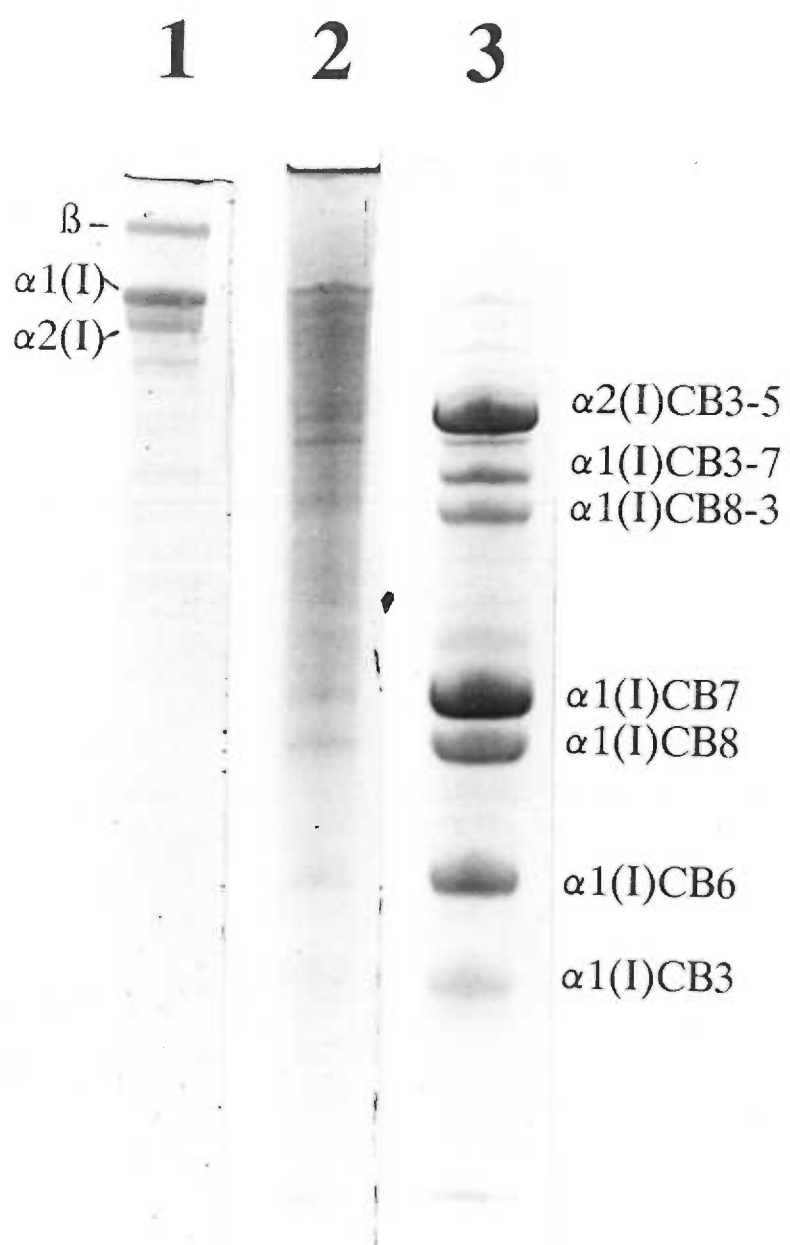
Figure 16. SDS page of cyanogen bromide digested DOPA-collagen gels.

Lane 1: Type I collagen.

Lane 2: Cyanogen bromide digest of 1×10^{-3} M DOPA-collagen gel.

Lane 3: Cyanogen bromide digest of a control-collagen gel.

* β notation indicates aldol crosslinked collagen α chain dimers.



solubility experiment, which would have completely gelatinized collagen in normally crosslinked tissues, as well as to the contracted state of the pellets was significant in that these results appeared to support a covalent model of crosslinking rather than a model which would assume much weaker intermolecular forces.

DOPA treatment also decreased the amount of collagen digestible by cyanogen bromide treatment of collagen gels. The well characterized CNBr peptides of type I collagen, identifiable by SDS-PAGE are shown in lane 3 of Figure 16. A much fainter pattern with certain similarities was seen in material extracted from the 1×10^{-3} M DOPA-collagen gel (lane 2). The majority of coomassie stainable material recovered was in the form of higher molecular weight species at the top of the gel or near the size of the collagen α chains shown in lane 1. This high molecular weight material may represent incomplete cleavage products. The presence of strong oxidizing agents such as dopaquinone during the crosslinking process could possibly oxidize the methionine residues of type I collagen to methionine sulfoxide^{114,115}. When in this oxidized form, cyanogen bromide cleavage does not occur¹¹⁶ and incomplete cleavage products (fused peptides) would result. This oxidation end product is also poorly derivatized by phenyl isothiocyanate, the derivatizing agent used in the PITC amino acid analysis system¹¹⁷. PITC amino acid analyses of DOPA-collagen gel hydrolysates demonstrated a decrease in the methionine content with respect to control collagen gels. These results suggest that methionine residues had been oxidized. An alternative explanation for the predominant high molecular weight material in lane 2, is that it could represent chains of cyanogen bromide peptides linked together by DOPA crosslinks. To address this possibility, the high molecular weight material could be extracted from the gel slab, treated with trypsin

to produce much smaller peptides, and sequenced. If peptides were crosslinked, then two or more sets of sequences would result.

The presence of a sizeable pellet in the DOPA treated gel, which contained approximately 50% of the original collagen, might also have resulted from incomplete cleavage and/or complex crosslinking between cleaved peptides.

In conclusion, the solubility of collagen gels in dilute acetic acid and under the conditions of cyanogen bromide extraction was dramatically decreased. The results strongly support a model of a highly stable cross-linking system.

4. The thermal stability of DOPA-collagen matrices.

Introduction.

Possibly the first collagen related observation was that of the thermal contraction of skin. When heated to temperatures exceeding 60°C, skin and other collagenous tissues contract to more than one half the original length ¹¹⁸. The contraction or "shrinkage" is due to a disruption of labile bonding forces between collagen fibrils ¹⁰⁹. These forces are thought to include salt bridges and hydrogen bonds between amide linkages. The increase in temperature provides the energy necessary to overcome the bonding energies, and the collagen chains are free to assume the energetically favorable randomly coiled conformation. The thermal energy has, thus, been conserved in the form of an increase in entropy content ³. Anything that increases the overall stability of a tissue increases the shrinkage temperature (T_s°), a measure of thermal stability. Tanning agents increase T_s° by introducing additional bonding forces between collagen fibrils ¹⁰⁹. Covalent crosslinks stabilize the matrix ¹¹⁹, and as a result, greater amounts of heat are required to overcome the cumulative bonding energy.

Large polymers, both charged and uncharged, can increase the shrinkage temperature of rat tail tendons without forming covalent crosslinks ¹²⁰. Polymers with an effective radius of 0.6nm are excluded from the fibrils and are not allowed to bind. The increase in shrinkage temperature may be due to a dehydration of the matrix due to the osmotic pressure exerted by the excluded polymers. The result,

based upon the tanning model of Vincent and Hillerton⁷⁷ would be a more compact native fibrillar matrix. Solute molecules with radii below the minimum level can fit within the fibrillar matrix at the gap regions, and have been shown to disrupt the fibrillar structure. This effect seems not to be affected by binding of solute to the fibrils. The result is a significant decrease in the shrinkage temperature of the tendon.

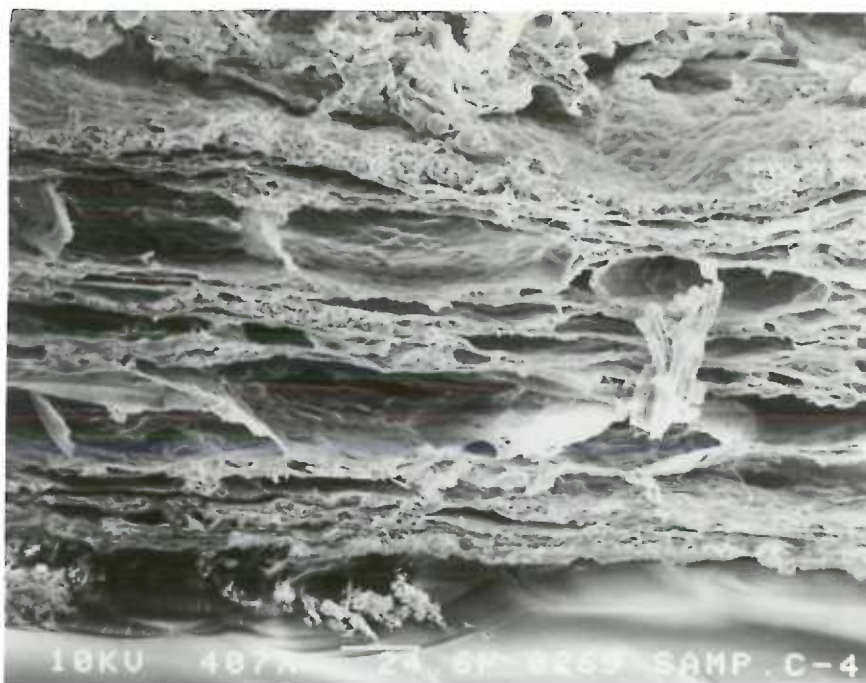
The thermal shrinkage phenomenon has been used in the study of collagenous tissues. Verzar^{12,31,121} in a series of studies measured the magnitude of contraction forces of tendons and strips of skin. The tissues were clamped at one end, immersed in buffered saline, and attached to a kymograph at the other end. The relative forces of contraction for varying samples were proposed to depend upon age related changes in protein crosslinking. Leather chemists typically measure the shrinkage temperature as that temperature at which shrinkage occurs¹⁰⁹. The effectiveness of synthetic crosslinking by tannins has been typically measured in this manner. In general, however, anything that increases the overall stability of a tissue increases the shrinkage temperature.

The following experiment measured the shrinkage temperatures of reconstituted collagen fibrils in the presence of DOPA. Reconstituted collagen fibrils, which appear identical to native collagen fibrils at the electron microscopic level¹⁰³, when quick frozen and then freeze dried retain a fibrous appearance and are given the trivial name, collagen felt. Figure 17 shows a scanning electron micrograph of a pepsin treated collagen felt. Collagen felts, or sponges, have been used frequently as skin grafting material¹²² since the retention of a native fibrillar structure allows host cells a natural environment to invade, and this enhances wound

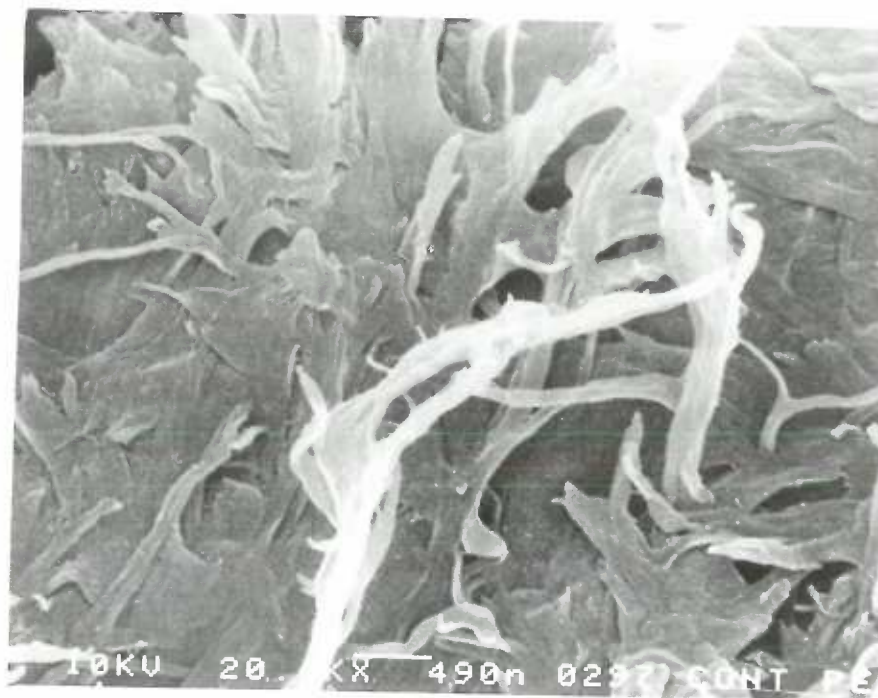
Figure 17. Scanning electron micrographs of: (a) the broken edge of a pepsin treated collagen, and (b) the internal structure of a pepsin collagen felt, exhibiting a random fibrous structure.

Micrographs courtesy of Douglas Keene, Shriners Hospital Research Center, Portland, Oregon.

a.



b.



healing¹²³. The effects of crosslink and melanin like polymer formation on the shrinkage temperature of collagen felts was considered.

Materials and Methods.

The effect of $1 \times 10^{-3}M$ DOPA.

Two buffered collagen solutions were prepared as described in the general methods section (appendix). DOPA was added to one solution at a concentration of $1 \times 10^{-3}M$. Collagen felts were prepared as described in the general methods section (appendix). The collagen felts were cut into 1 cm x 0.4 cm strips. The strips were soaked for 1 hour in preheated 37°C phosphate buffered saline. In addition, tendons of varying diameters were dissected from rat tails, and these were also immersed in 37°C PBS. The shrinkage temperatures of the felt and tendon samples were then determined by the method of shrinkage temperature measurement described in the appendix.

The effect of a lowered DOPA concentration.

The $1 \times 10^{-3}M$ DOPA-collagen solution was incubated at 37°C for one hour in the presence of $3\text{-}^{14}\text{C}$ -DOPA (21mCi/mmol, Amersham Corp.), and then cooled in an ice bath for an additional hour. A 2.0 ml aliquot was lyophilized, and the remainder was transferred to Spectrapor dialysis tubing (M.W. cutoff = 12kD - 14kD) and exhaustively dialyzed against phosphate buffered saline, at 4°C and in the

dark. DOPA-collagen felts were prepared and tested for shrinkage temperature, as described above. The lyophilized sample was dissolved in 2.0M low U.V. absorbance guanidine-HCl (U.S. Biochemical Corp.), 50mM tris (ph7.5), and chromatographed by gel filtration HPLC on the system described in the general methods section (appendix). Fractions were radioassayed by liquid scintillation counting, and assayed for hydroxyproline content, and a DOPA binding constant was calculated.

Results.

The effect of $1 \times 10^3 M$ DOPA.

Figure 18 shows the increase in shrinkage temperature over the first 24 hours of incubation. Values for the pepsin collagen control solutions were not included because they broke under the weight of the small mass during preincubation at 37°C. Rat tail tendons of various diameters had a shrinkage temperature of $60.9 \pm 0.7^\circ\text{C}$.

The effect of a lowered DOPA concentration.

Figure 19 shows the increase in breakage temperature for the collagen felts prepared from the exhaustively dialyzed DOPA-collagen solutions. After one hour of incubation at 37°C, 4.1 moles of DOPA were bound per collagen α chain as determined by the HPLC method described in the appendix.

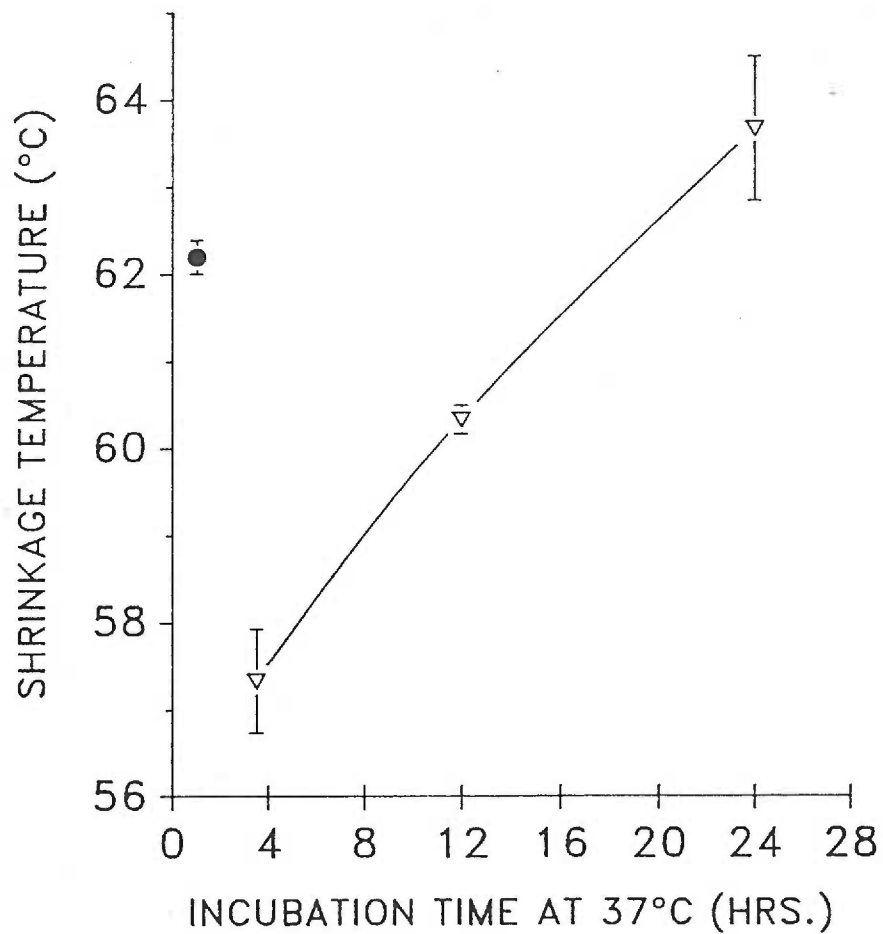


Figure 18. Shrinkage temperatures of 1×10^3 M DOPA-collagen felts (▽), and rat tail tendons (●) following varying incubation periods at 37°C.

A minimum of three replicates were run at each time point. Variation is expressed as the standard error of the mean.

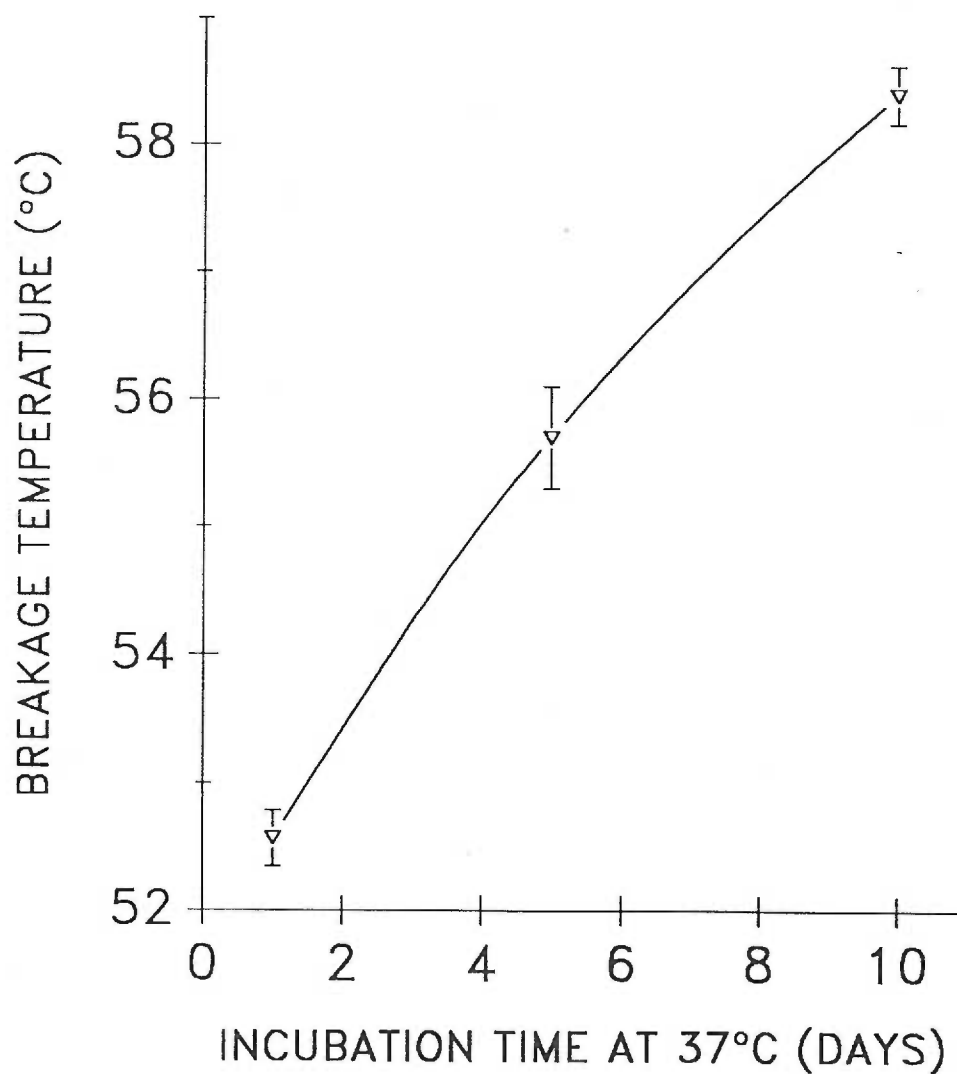


Figure 19. Breakage temperatures (∇) of collagen felts prepared at lowered DOPA concentrations, following varying periods of incubation at 37°C.

A minimum of three replicates were run at each time point. Variation is expressed as the standard error of the mean.

Discussion.

The results of the $1 \times 10^{-3}\text{M}$ DOPA-collagen shrinkage temperature experiment shown in Figure 18, demonstrate the effect of elevated DOPA concentrations on the thermal stability of reconstituted collagen fibrils. Following three hours of incubation at 37°C the DOPA treated felts shrank at temperatures well above the temperature at which the control felts break (37°C). The increase in shrinkage temperature was linear over the incubation time periods shown, and by 24 hours, the DOPA-collagen felts shrank at a temperature (63.5°C) significantly greater than that of rat tail tendons (61.5°C). Over the same time period, control felts broke consistently at 37°C . Therefore, DOPA at $1 \times 10^{-3}\text{M}$ enhanced the thermal stability of reconstituted collagen fibrils to levels surpassing that of a naturally crosslinked collagen tendon. At this concentration, approximately 65 moles of DOPA were available to bind to every collagen α chain. Later in this thesis, it will be hypothesized that there are only a limited number of DOPA binding sites per collagen α chain. At $1 \times 10^{-3}\text{M}$, these sites would be saturated. What is the effect of DOPA when the concentration is below that necessary to saturate all available binding sites?

The effect of lowered DOPA concentrations.

Figure 19 shows the effect of DOPA, bound at a molar ratio of 4 moles per collagen α chain, on the thermal stability of reconstituted collagen fibrils. The values are expressed as breakage temperatures rather than shrinkage temperatures

because the samples broke prior to shrinking. The relationship between the concepts of shrinkage and breakage temperatures is not clear. Both properties are clearly associated with a perturbation of the molecular stabilizing forces of the fibril system. Unlike the samples that shrink, however, the samples which break may not have the tensile properties necessary to withstand these perturbations. Thus, the breakage temperature might be equivalent to the shrinkage temperature, but may also indicate decreased tensile properties of the sample. At this lower DOPA concentration, the breakage temperatures between one and ten days of incubation at 37°C increased linearly and significantly and were higher than the consistent 37°C breakage temperature for the control felts. At no point did the thermal stability of the felts prepared at the lower concentrations approach that of those prepared at a concentration of 1×10^{-3} M DOPA. The progressive increase in the breakage temperature over the 10 day period may indicate that crosslink formation between the bound DOPA monomers was occurring in an equally progressive manner over this time period.

The effect of DOPA on the T_s of reconstituted collagen fibrils was concentration dependent, and may have been related to the likelihood of covalent crosslink formation. At 1×10^{-3} M DOPA, there were approximately 16 times as many moles of DOPA available per collagen α chain, as compared to the samples prepared at the lower DOPA concentration. It seems likely that this difference is related to the number of DOPA monomers which had bound to collagen. At higher concentrations, more DOPA was bound to the collagen and, thus, more interfibrillar crosslinks could be formed. The role that covalent crosslink formation plays in fibril stabilization is the topic of Part III of this thesis.

5. Tensile strength of collagen felts prepared in the presence of DOPA.

Introduction.

The mechanical properties and specifically the tensile strength (TS) of collagenous tissues depend upon the integrity of the natural collagen crosslinking system. BAPN, which disrupts normal collagen crosslinking by inhibiting the activity of lysyl oxidase, causes a decrease in the tensile strength of connective tissue³⁹. Peacock⁴¹ demonstrated that the tensile strength of healing wounds could be enhanced by inserting methylene and amide crosslinks into scar tissue. Collagen disorders such as Ehlers Danlos VI^{29,30} and Ehlers Danlos VII^{32,36}, where normal crosslinking is disrupted by different mechanisms, are characterized in part by decreased tensile strength which is expressed outwardly by tissue fragility and hyperextensibility.

Viidik¹²⁴ has written a review of the functional properties of collagenous tissues. The tensile properties of collagenous tissues can be measured using a tensiometer. The tensiometer pulls a tissue with a constantly increasing breaking load producing a load-deformation or stress-strain curve with the breaking load on the y-axis and the deformation or extensibility of the x axis. Three values are readily definable from the curve. These are the "ultimate" tensile strength expressed in terms of the load per cross sectional area of the sample at the maximum breaking load, the extensibility of the tissue taken directly from the x axis, and the tensile

energy absorption which is the area underneath the stress-strain curve and a function of both the tensile strength and the extensibility of the tissue. Tissue samples with small cross sectional areas, in which all collagen fibrils share the load equally give the most representative values, and thus, uniformly thin samples can be expressed in terms of the load/width.

In the following experiment, the tensile strength, and the tissue extensibility of DOPA-collagen felts with respect to control felts, saturated at the time of testing, were measured.

Materials and Methods.

Pepsin soluble collagen felts were prepared as described in the general methods section of this thesis (appendix). The felts had been prepared either in the presence or absence of 1×10^{-3} M DOPA, and incubated for 1, 2, 4, 6, 10, and 25 days at 37°C. All felts were prepared in the presence of 50 μ g/ml gentamicin sulfate. At the end of the incubation period, small fragments of the 25 day DOPA and control gels were removed from the periphery. These were used to inoculate thioglycolate and nutrient broth to test for anaerobic and aerobic bacterial contamination, respectively. The felts were cut into rectangular samples with dimensions of 2.0 cm in width and 3.5 cm in length. The somewhat fragile samples were protected from premature fracturing with paper folders. Tensile strength measurements were performed by me on tensiometers located at the Weyerhaeuser Physical Testing Center in Tacoma, Washington. The tensiometer, a Instron Series IV Automated Materials Testing System V4.01C, is shown in Figure 20.

Figure 20. Instron Series IV Automated Materials Testing System V4.01C, used for testing collagen felts for tensile properties.



Testing was performed in a climate controlled facility. The humidity was maintained at 50% and the temperature at 23°C. The samples were stretched with a crosshead speed of 25.4mm/min. The full scale load range in kilograms was 1.000 for the dry samples and 0.200 for the wet samples. Sample gauge lengths were at a constant 25.4 mm, and sample widths were between 34.0 and 38.0mm for the dry samples, and 20.0mm for the wet samples. The samples were placed between the upper and lower jaws of the tensiometer and once in place the paper folder was cut and pulled away from the felt. The samples were moistened with deionized water using a fine mist spray bottle. The samples were run only after the sample was completely saturated. Eight to twelve replicate samples were tested for the 1 day and 10 day time points. Two to four replicates were run for those time points between 1 day and 10 days.

Stress-strain curves were collected for each sample, and from these the TS (Load/Width at Maximum Breaking Load), and the extensibility (% Strain at Maximum Breaking Load) were calculated. Samples were excluded when flaws in the matrix were visually detected.

Results.

A typical stress-strain curve for 10 day wet samples of DOPA incubated and pepsin control collagen felts is shown in Figure 21. The tensile strength was calculated simply from the peak maximum. Figure 22 shows the tensile strength

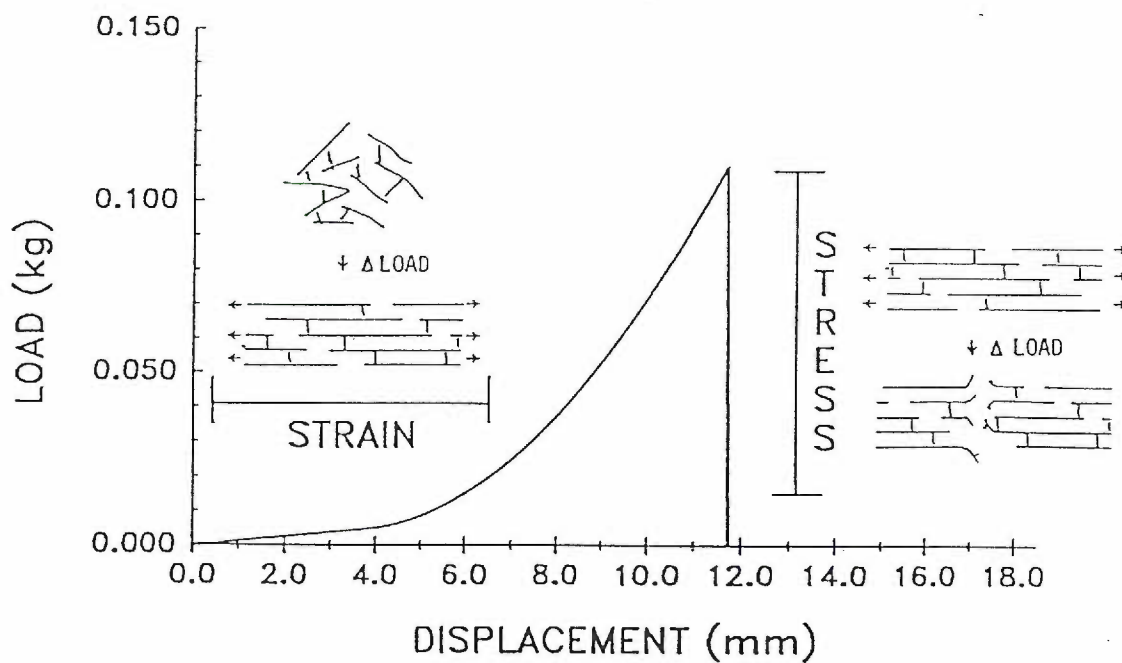


Figure 21. The stress-strain curve of a 1×10^{-3} M DOPA-collagen felt incubated for 4 days at 37°C . The stress and strain phases of the curve are defined. As a pulling force ($\leftarrow \rightarrow$) is applied to the felt, randomly oriented collagen fibrils are forced into a parallel alignment (strain). Once in a parallel alignment, pulling forces with increasing magnitude overcome bonding forces, breaking the fibrillar matrix.

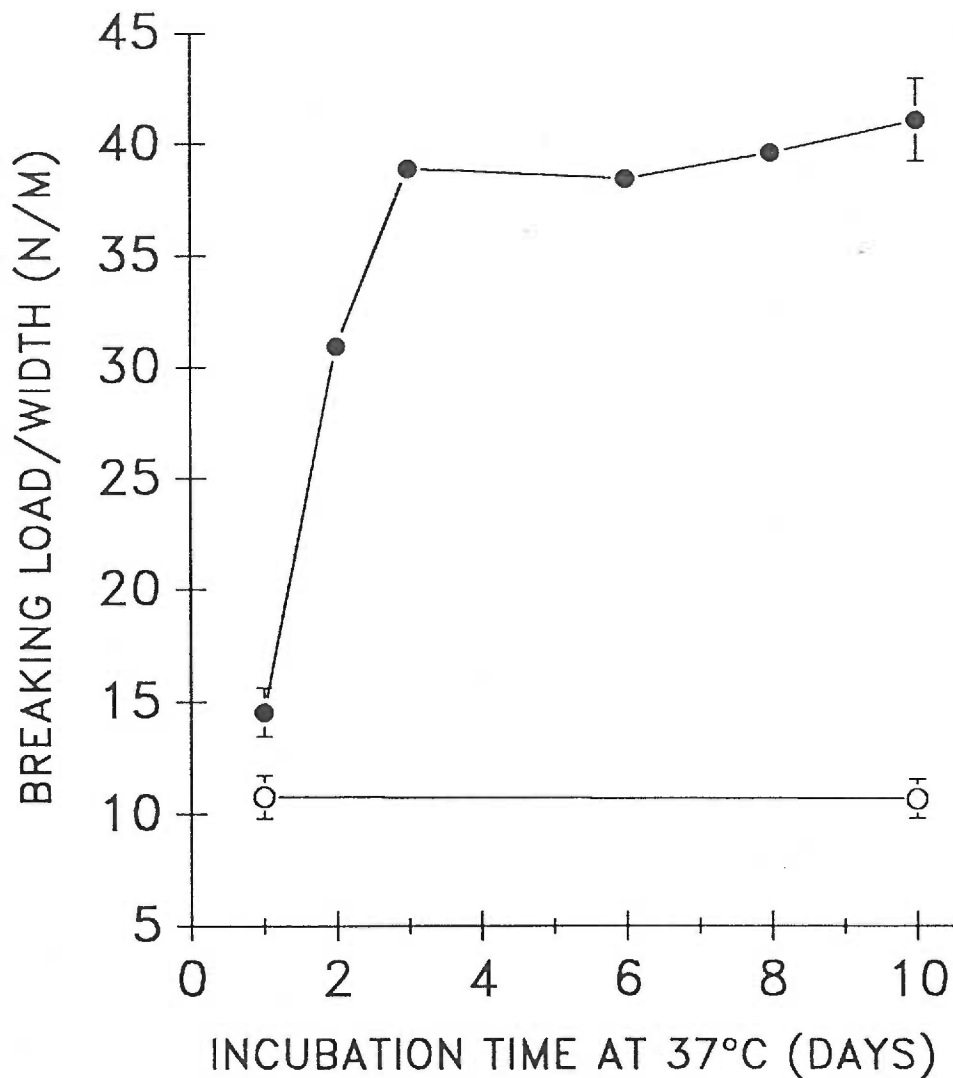


Figure 22. The wet tensile strengths of DOPA-collagen felts (●) and control-collagen felts (○), after varying periods of incubation at 37°C.

A minimum of six replicates were run at the 1 and 10 day time points and the variation is expressed in terms of the standard error of the mean. Two to four replicates were run at the 2,3,6 and 8 day time points and the results are expressed as means with no indication of error.

for both wet DOPA and pepsin control felts over 10 days of incubation at 37°C. Standard errors of the mean are given for the 1 and 10 day time points. Statistical error was not calculated for the time points between 1 and 10 days due to fewer replicates. The effect of incubation time at 37°C on the extensibility of the collagen felts is shown in Figure 23. The values are expressed in terms of % strain at the maximum breaking load.

Discussion.

The tensile strength of a tissue provides a physical measurement of stability. Physiological tissues which consist of collagen abnormally crosslinked due to disease demonstrate decreased tensile strength properties^{29,30}. Glutaraldehyde which introduces covalent crosslinks into a collagen fibril system, can dramatically increase the tensile strength of the tissue¹²⁵. Thus, the tensile strength of a tissue can be related to, and thereby provide a way of measuring the introduction of covalent crosslinks into a tissue, whereas shrinkage temperature data provides more of a general picture of overall stabilization of the tissue.

A typical stress-strain curve for a collagenous matrix can provide clues in itself, to the properties of the tested tissue. The curve shown in Figure 21 can be divided into the two phases. The first, or stress phase is associated with the tissue extensibility. As a collagenous tissue "stretches", randomly oriented collagen fibrils are forced into a parallel alignment¹²⁶. When this realignment is complete, the second, or strain phase of the curve occurs. This phase is associated with the tensile

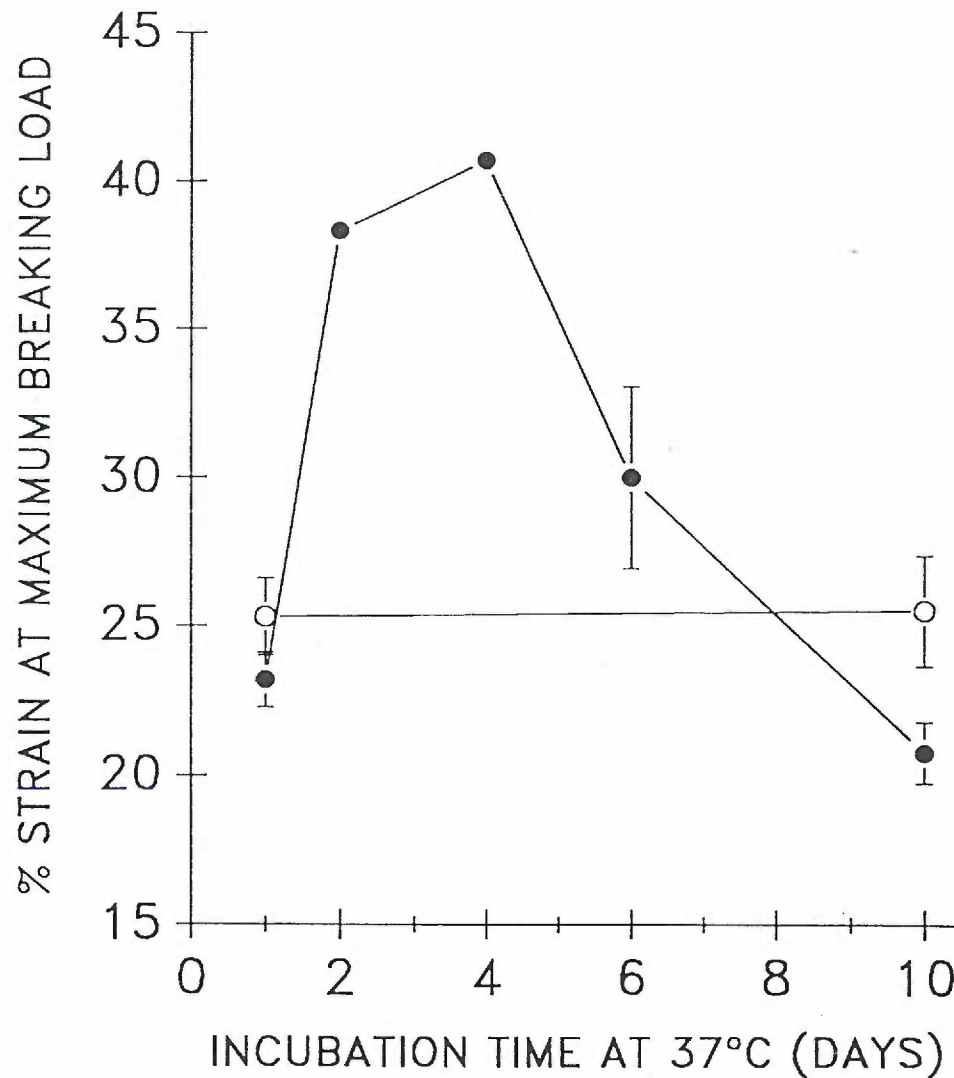


Figure 23. The extensibility of DOPA-collagen felts (●) and control-collagen felts (○) following varying periods of incubation at 37°C.

A minimum of six replicates were run at the 1, 6, and 10 day time points and the variation is expressed as the standard error of the mean. Two replicates were run at the 2 and 4 day time points and the results are expressed as means with no indication of error.

strength of the tissue and depends upon the intermolecular forces which stabilize the tissue. Thus covalent crosslinks enhance the tensile strength of the tissue.

The extensibility of the wet DOPA felts increased much in the same manner as did the tensile strength (Fig. 23). At one day of incubation, the extensibility was near that of the control which did not change during the ten day incubation period. At 4 days of incubation at 37°C, the DOPA sample stretched to approximately 1.4 times the initial length prior to breaking. However, this maximum extensibility was followed by a decrease to below that of the control at 10 days of incubation. These results suggest that the extensibility of the DOPA-collagen felts decreases with ageing. This may be the result of an increase in the complexity and thus the rigidity of the crosslinking system which develops with time. As the complexity of the crosslinking system increased between randomly aligned collagen fibrils, the ability of these fibrils to align in a parallel manner would decrease. The fibrils would, thus, be locked in the randomly aligned state. In a subsequent section of this thesis, the mechanism of crosslink formation will be discussed in detail, and a melanin like polymerization model will be advocated in which individual crosslinks can polymerize with other neighboring DOPA derived crosslinks. The rate of melanin formation is dependent upon the available oxygen concentration. Due to the diversity of the *ortho*-quinones which can be formed by oxidation of DOPA, the molecular interactions between the quinones will be complex. The system under which the felts were prepared was devised to closely mimic physiological pH, ionic strength, and temperature conditions which favor DOPA polymerization.

Based upon the shrinkage temperature data described in the previous experiment, the expected results of the tensile strength experiment was the

attainment of a maximum tensile strength by day one, followed by no additional increase in the ensuing 24 days of incubation. However, the surprising outcome of this experiment was that at one day incubation, the tensile strength was only slightly greater than the control. As Figure 22 shows, the maximum was not reached until 3 days of incubation while at 2 days tensile strength of 30.9 N/m represented a rise to a level of only 66.5% of the maximum. The wet tensile strength was consistent through ten days of incubation after the maximum had been reached, unlike the tissue extensibility which decreased with age. The gradual rise in the tensile strength of the collagen matrix, between one and three days of incubation at 37°C, was again suggestive of a polymerization model of crosslink formation. An increase in crosslink complexity would not have affected the tensile strength of the tissue as it apparently did the extensibility, because the total number of crosslinks between fibrils would have remained consistent with ageing.

In summary, the results of this experiment demonstrated increased tensile and extensible properties of fibrous collagen matrices incubated in the presence of DOPA. Both properties were enhanced in a time dependent manner, supporting a gradual polymerization model of covalent crosslink formation. Extensibility, unlike tensile strength decreased at later timepoints to below control levels. The decrease in extensibility may have been due to continuous though gradual increase in the complexity of the melanin polymer formed. Therefore, this study provided indirect evidence of a polymerization mechanism of DOPA crosslinking of type I collagen. In Part III of the Experimental Section of this thesis, chemical means were used to produce direct evidence in support of this mechanism.

6. Transmission electron microscopy of DOPA stabilized reconstituted collagen fibrils.

Introduction.

Type I collagen is normally found in the connective tissue matrix in the form of 30 - 300nm diameter fibrils which show a distinct 67nm(D) banding pattern ¹²⁷. When negatively stained, alternating light and dark banding regions, can be detected by electron microscopy ¹²⁸.

When type I collagen fibrils are reconstituted, the fibrils formed are very similar if not identical at the E.M. level, to native fibrils ¹⁰³. The formation of the natural aldimine crosslinks, both *in vivo*, and in reconstituted acetic acid extracted collagen where the crosslinking telopeptides remain intact, serves to stabilize the fibrillar matrix. In pepsin soluble collagen, the absence of the non-helical telopeptides affects fibril assembly. However, periodic banding of the pepsin collagen fibrils still occurs, though the pattern may be irregular ^{129,130}. The derivatization of type I collagen during fibril formation, especially if the derivatives added are bulky, might be expected to disrupt the normal D banding of the reconstituted collagen fibrils. Glutaraldehyde causes alterations in the negative staining of collagen fibrils. Light bands are more numerous, and the axial extent of the overlap zone increases by what appeared to be 0.1D. Meek and Chapman ¹³¹, by studying the fine structure of the collagen fibril, have proposed that the

alterations are due to phosphotungstate exclusion by polymeric complexes of glutaraldehyde at the site of crosslink

formation. This experiment was designed to investigate the effect of DOPA binding on collagen banding, and thus fibrillar structure, by electron microscopy.

Materials and Methods.

Buffered pepsin treated collagen solutions were prepared either in the presence or absence of 1×10^{-3} M DOPA. An acetic acid soluble collagen solution was prepared in the same manner but lacked DOPA. The DOPA-collagen and control solutions were incubated for varying periods of time at 37°C. At the end of the incubation period, the collagen gels were homogenized using a Virtis Homogenizer to produce small gel fragments, and then negatively stained by the method of Williams, *et al*¹⁰³. In short, a copper grid (200 mesh) coated with a carbon film (Polysciences, Inc.) was placed on a drop of the gel homogenate for 30 seconds, and then drained with filter paper. The grid was then placed on a large drop of 1% phosphotungstic acid (Malinckrodt, Inc) (pH 7.5) for 10 minutes and again drained and allowed to completely dry. A 37°C temperature was maintained throughout the staining procedure.

The grids were scanned by transmission electron microscopy at a magnification of 30,000 x, with a JEOL JEM 100S Electron Microscope. Areas of collagen fibrillar material were viewed for detection of D-banding, and photographs of the findings reproduced.

Results.

The pepsin control and acetic acid control gel transmission electron micrographs are shown in Figure 24. In Figure 25, the transmission electron micrographs of the 2 day and 63 day DOPA-collagen gels are shown.

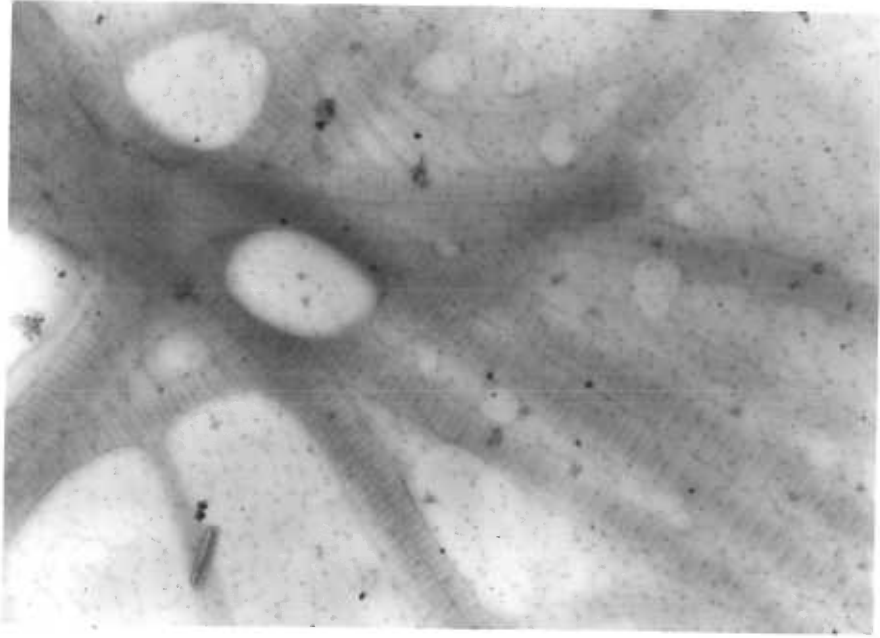
Discussion.

In comparing the TEM's of the control and DOPA treated gels, no major differences in the fibrillar banding pattern could be detected. In both cases, banding was generally consistent throughout the field. Both the pepsin collagen and acid collagen controls tended to stain less intensely with the phosphotungstate, than did the DOPA-collagen gels at any of the time points shown. The maintenance of the fibrillar banding over extended periods of time provided evidence of fibrillar stabilization through crosslink formation.

Thus, this experiment demonstrated that collagen solutions exposed to DOPA at a concentration of $1 \times 10^{-3}\text{M}$ form fibrils which appear identical to control collagen fibrils at the E.M. level.

Figure 24. (a). Transmission electron micrograph of an acetic acid soluble collagen gel (50,000X).
(b). Transmission electron micrograph of a pepsin treated collagen gel (90,000X).

a.



b.

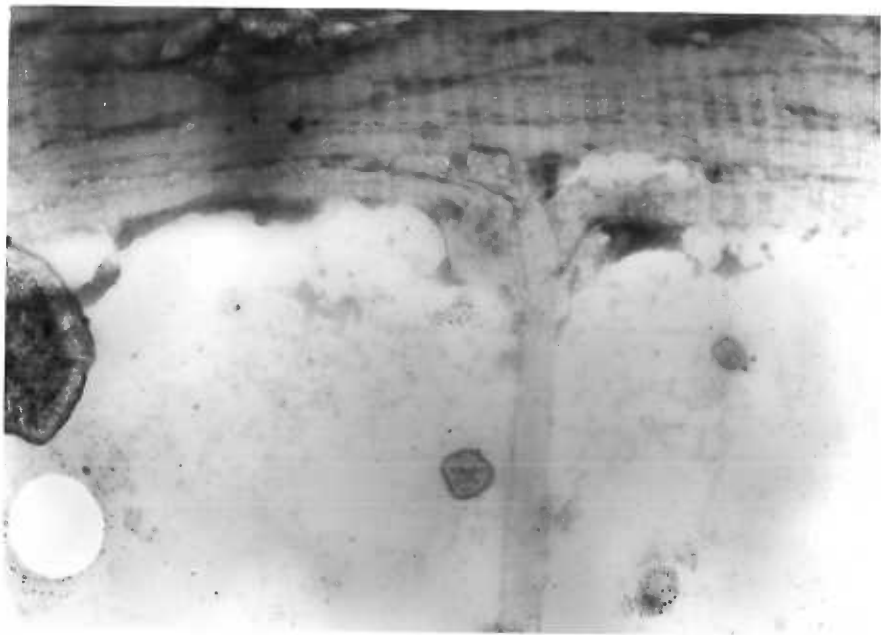
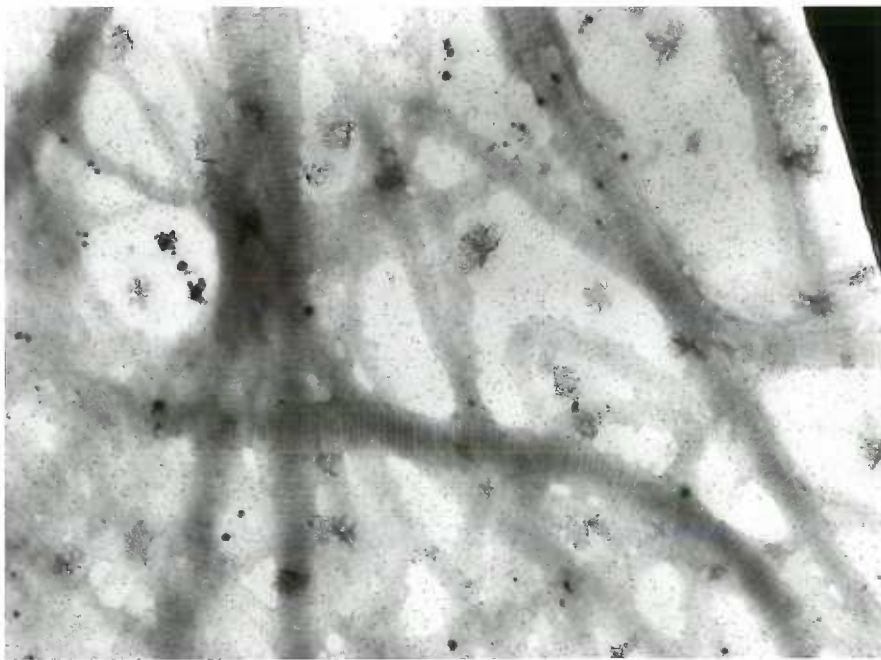


Figure 25. (a). Transmission electron micrograph of a DOPA-collagen gel following a 2 day period of incubation at 37°C (40,000X).
(b). Transmission electron micrograph of a DOPA-collagen gel following a 70 day period of incubation at 37°C (80,000X).

a.



b.



7. The DOPA induced stabilization of preformed Type I Collagen fibrils.

Introduction.

Matrices of collagen fibrils reconstituted in the presence of DOPA are less soluble and have higher thermal stabilities than controls. How does DOPA affect the stability of a collagen fibrillar matrix if DOPA is allowed to interact only after fibrillogenesis is complete? Fibril self assembly depends upon the electrostatic and hydrophobic interactions between groups of the collagen triple helical domain¹³². Therefore, when collagen molecules are in the fibrillar form, many of the reactive groups of the molecule may not be as available to interact with ligands, such as DOPA, simply as a result of molecular shielding. Less interactions may result in a decrease in the stabilizing forces which DOPA adds to the collagen matrix. The following experiment was designed to investigate the ability of DOPA to stabilize pre-formed non-crosslinked collagen fibrils. Collagen felts served as a model fibril system.

Materials and Methods.

A buffered pepsin treated type I collagen solution was prepared as described in the general methods section of this thesis (appendix). Collagen felts were prepared from this solution by the method described in the appendix and incubated for 24 hours at 37°C in physiological saline. The physiological saline for the test

felts contained DOPA at a concentration of $1 \times 10^{-3}\text{M}$. Shrinkage temperatures of incubated $1.0 \times 0.4\text{cm}$ felt strips were measured as described previously in this thesis following an additional one hour pre-incubation period in physiological saline, and the felts were tested for solubility by the collagen gel solubility assay described in the general methods section (appendix).

Results.

The pepsin soluble type I collagen felts were deeply pigmented after having been incubated with DOPA. The stabilizing effect of DOPA with respect to degree of solubility is shown in bar graph shown in Figure 26. During the shrinkage temperature test, the control felts broke at 37°C . The felts soaked in $1 \times 10^{-3}\text{M}$ DOPA had a shrinkage temperature of $59.3 \pm 0.6^{\circ}\text{C}$ (not shown in a figure).

Discussion.

Figure 26 shows the dramatic decrease in solubility of collagen felts exposed to DOPA with respect to control felts soaked in saline. There was a significant difference in solubility both at 4°C and 100°C . However, unlike collagen fibrils formed in the presence of DOPA, and then incubated for 24 hours at 37°C as demonstrated previously in this thesis, the difference in solubility at the harsher conditions was not as pronounced. The reason for this decreased degree of stabilization may be the molecular shielding phenomenon described above. The reactive groups which interacted with DOPA in the stabilizing process may have

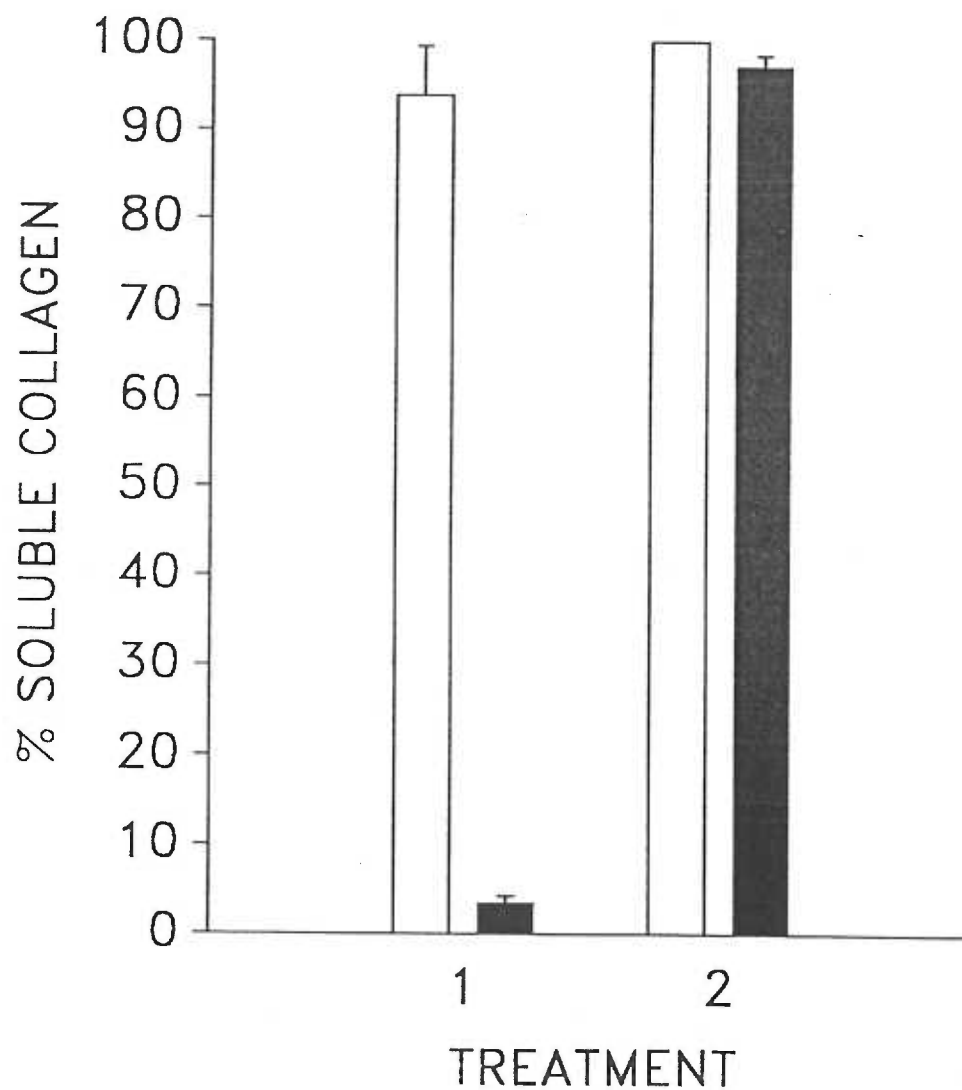


Figure 26. The solubility of DOPA-exposed- (■) and pepsin-control-collagen felts (□) in 0.5M acetic acid at 4°C for 12 hours (treatment 1), and in 0.01M acetic acid at 100°C for 2 hours (treatment 2).

Three replicates were run for each sample. Variation is expressed as the standard error of the mean.

been partially shielded when collagen was in the fibrillar form. The result would have been decreased DOPA-collagen interaction, and decreased stability. One implication of this explanation is that the lag period of *in vitro* collagen fibrillogenesis, which is extended for pepsin treated collagen^{128,132}, might be an important time period for DOPA-collagen interactions to occur.

The shrinkage temperature, as previously described, provides an indication of the degree of thermal stabilization of a connective tissue matrix^{109,119}. The shrinkage temperature value for the collagen felts incubated for 24 hours in the presence of DOPA (59.3) was much higher than the temperature at which the control felts broke, though decreased with respect to the collagen fibrils reconstituted in the presence of DOPA and held at 37°C for 24 hours (63.5°C) as well as intact rat tail tendons (61.5°C) as described previously in this thesis. Again, the decrease in thermal stability with respect to collagen fibrils formed in the presence of DOPA may have been due to decreased numbers of available DOPA binding sites.

Thus, DOPA interacted with preformed collagen fibrils, and in doing so effectively stabilized the matrix with respect to solubility and thermal stability. The effect was, however, diminished with respect to collagen fibrils formed in the presence of DOPA. The mechanism by which the stability was enhanced is not clear from this work. One possibility is the formation of covalent crosslinks between collagen fibrils. *Ortho*-quinones are thought to covalently crosslink proteins⁷². Based upon this speculation, the clinical implications of this work are intriguing. The ability to introduce covalent crosslinks into pre-existing poorly crosslinked collagen fibrils could prove useful in treating crosslinking disorders.

8. Summary.

The previous set of experiments demonstrated that collagen fibrils prepared in the presence of DOPA, or exposed to DOPA when intact, formed highly stable matrices. Collagen gels prepared in the presence of 1×10^{-3} M DOPA demonstrated increased stability with respect to controls beginning at 1.5 hours of incubation at 37°C , and were at maximum stability within 24 hours, based upon turbidimetric measurements of fibril dispersion. At one hour of incubation, DOPA was bound covalently to collagen yet did not affect collagen gel stability, suggesting a biphasic mechanism of fibril stabilization in which DOPA binds initially and then forms covalent crosslinks. DOPA treatment also decreased the solubility of collagen gels in dilute acid and under harsh denaturing conditions and the extractibility with cyanogen bromide. Intact collagen fibrillar matrices, exposed to DOPA at a concentration of 1×10^{-3} M also demonstrated decreased solubility. Cyanogen bromide treatment released only high molecular weight material, which may have represented crosslinked CNBr peptides.

DOPA treatment also enhanced the physical stability of collagen fibrillar matrices. The thermal stability of collagen felts prepared in the presence of 1×10^{-3} M DOPA increased over a 24 hours period of incubation at 37°C . At lower DOPA concentrations, the collagen felts were again stabilized with respect to controls, though the effect was much reduced and occurred over a much longer time period. The thermal stability of intact collagen fibrillar matrices exposed to 1×10^{-3} M DOPA for 24 hours was significantly increased with respect to controls. The wet tensile strength of collagen felts prepared in the presence of 1×10^{-3} M

DOPA reached a maximum after three days of incubation at 37°C. At the maximum, the tensile strength of the DOPA-collagen felts was approximately 2.5 times that of control felts. The extensibility of the DOPA-collagen felts was maximum after four days of incubation at 37° (1.4 times that of control), but decreased to below control levels after ten days of incubation. This indicates development of a complex crosslinking system which "stiffens" the collagen matrix.

DOPA treatment did not affect the native fibrillar structure of collagen gels. DOPA-collagen gels demonstrated normal D-banding at the electron microscope level even after extended periods of incubation at 37°C.

The results of these experiments support a covalent crosslinking model of collagen fibril stabilization involving DOPA polymerization. The next experimental section focused on the mechanism by which these crosslinks were formed.

B. Part II. The Mode of Interaction of Catechol Derivatives and Collagen Reactive Groups.

1. Introduction.

Collagen fibrillar matrices incubated in the presence of DOPA demonstrate decreased solubilities, increased thermal stability, and increased tensile properties. What is the mechanism by which these properties were affected? If stability is achieved by the formation of crosslinks derived from DOPA, then first DOPA must bind to collagen. Catecholamines bind in some manner to both intact connective tissue specimens ¹³³ as well as to reconstituted collagen fibrils ⁸³. The nature of interaction on the other hand is not as well established. That which is known is based largely on very early work where model compounds were synthesized from quinones and amine containing compounds, and these studies have been reviewed by Gustavson ⁷¹. Theoretically, the quinones of catechols form covalent bonds with the available Lewis bases including free ϵ -amino groups of lysine residue side chains, the sulfhydryl groups of reduced cysteine residues, and N-terminal amino groups ^{72,88,95}. Previous studies have used fluorometric techniques to detect interaction ^{101,133}, but have failed to provide firm evidence of covalent modification of the proteins studied. The following series of experiments analyzed the mode of interaction of DOPA, a model catechol-derivative, with purified type I collagen. Covalent adducts of proteins were identified, and the nature of the reactive group on collagen which binds to DOPA was investigated.

2. Quantitative binding of DOPA to collagen.

Introduction.

One of the simpler and more established techniques for measuring binding of a ligand to a protein is an "equilibrium dialysis" experiment¹³⁴⁻¹³⁶. Here, a radiolabeled ligand is exposed to a protein or receptor under the appropriate conditions, and then unbound ligand is removed from the protein by dialysis against buffer to achieve a 200,000 fold dilution (exhaustive dialysis). Ligand which remains bound to the protein through some form of molecular interaction, is measurable and binding coefficients are readily determinable. In the following experiment, the quantitative binding of DOPA to collagen was measured by this technique.

Materials and Methods.

A buffered collagen solution was prepared as described in the general methods section (described in appendix). DOPA was added to the solution at a concentration of $1 \times 10^{-3}M$ labeled with $4.76 \times 10^{-2} \mu Ci/ml$ $3\text{-}^{14}C$ DOPA (21mCi/mmol, Amersham Corp.). 2 ml aliquots were transferred to each of Spectrapor 10 mm x 6.4 mm id (M.W. cut off = 12kD - 14kD) dialysis tubes. The samples were incubated for 24 hours in a humidified 37°C air incubator. At the end of the incubation period, each sample was transferred to a 10 x 15 cm thick walled

test tube containing 20 ml of dialysis buffer [30 mM phosphate (pH7.5), 0.135 M NaCl], and dialyzed in the dark at room temperature. The dialysis bath was stirred continuously, and changed a total of 5 times at 24 hour intervals.

0.5 ml aliquots were taken from each of the dialysates and radioassayed by liquid scintillation counting (appendix). The collagen gels were removed from the dialysis membrane, and both the gel and the membrane were suspended in Soluene 350 tissue solubilizer (Packard) and incubated overnight at 37°C. All samples were radioassayed by scintillation counting.

Results.

33.7% of the original label was accounted for in the dialysate. 31.8% remained inside the dialysis bag following exhaustive dialysis, and 15.2% of the original label was recoverable from the dialysis membrane after soaking in Soluene 350 overnight. The bag remained visibly pigmented even after soaking in the tissue solubilizer for 24 hours. 19.7% of the original label was not accounted for, and probably remained bound to the membrane. 21.4 moles of DOPA were retained in the gel per collagen α chain.

Discussion.

The fact that DOPA was retained in the collagen gel incubated at 37° for 24 hours following exhaustive dialysis was visibly evident. DOPA metabolites readily polymerize to form a brown to black pigmented melanin like polymer. The gel,

even after dialysis was deeply pigmented suggesting that DOPA had, in fact, polymerized and may have been bound. This visual observation agreed with the quantitative data of label retention. The heavily pigmented collagen gel retained 31.8% of the original label. Even after soaking the dialysis membrane in solouene 350, it remained pigmented and probably retained the label unaccounted for. The loss of label was, therefore, not significant with respect to the overall conclusions of this experiment.

The amount of DOPA which remained in the collagen gel was determined using two methods. The first method, compared the moles of DOPA retained in the gel with the moles of collagen originally added. In the second method, a DOPA-collagen gel was hydrolyzed, and the collagen content and specific activity measured and compared. The values of binding agreed nicely. Based upon the deep pigmentation of the collagen gel, it seems unlikely that all of the 21.4 mols of DOPA were bound directly to the collagen molecule. Instead, the data suggested that large polymers were bound to the collagen. In such a mechanism, a single DOPA would bind to the collagen, and then additional monomers would be added. Alternatively, the retained DOPA may have been in the form of free DOPA polymers, which due to their large size, could have been trapped within the gel. Such polymers could also have been larger than the dialysis tubing molecular weight cutoff, though the maximum molecular weight at which a melanin like polymer is soluble is unknown.

Thus, this experiment provided an indication that DOPA can interact with collagen with relatively high affinity. However, alternative explanations associated with the ability of DOPA to form large polymers could account for the results. In

the following experiment, these alternative explanations were addressed. The binding affinity of DOPA for non-fibrillar collagen was investigated.

3. Binding of DOPA to soluble Type I Collagen.

Introduction.

The preceding experiment demonstrated the affinity of DOPA for type I collagen fibrils. What the experiment was unable to demonstrate, however, was the importance of fibril structure in this binding. Collagen, as previously discussed, is capable of forming regular and unique fibrils with a well defined 3-dimensional structure. Does the fibril structure provide the appropriate environment for DOPA interaction with collagen reactive groups? If so, then in the absence of fibrils, DOPA interaction would not occur. This experiment addressed this question by incubating DOPA with collagen at a temperature (4°C) which inhibits collagen fibrillogenesis and slows melanin-like polymer formation. Therefore, both the effects of fibril structure, as well as temperature on DOPA interaction were described.

Materials and Methods.

A buffered type I collagen solution was prepared as described in the general methods section. DOPA was added to the solution at a concentration of $1 \times 10^{-3} \text{M}$, and labeled with $4.76 \times 10^{-2} \mu\text{Ci/ml}$ $3\text{-}^{14}\text{C}\text{-DOPA}$ (21mCi/mmol, Amersham Corp.). Two sets of six-6.0 ml aliquots were transferred to Spectrapor 10 mm diameter dialysis membrane (MW cutoff 12kd-14kd) and incubated in the dark at 4°C for either 24 or 72 hours. Under these conditions, the collagen remains in solution and

fibrils do not form. At the end of the incubation period, the samples were exhaustively dialyzed against four changes of 10 volumes of dialysis buffer (30 mM phosphate [pH 7.5], 0.135 M NaCl), in the dark.

The samples were removed from the membranes. 0.5 ml aliquots were radioassayed by liquid scintillation counting (appendix), and an additional 0.5 ml was analyzed for collagen content by the autoanalyzer method of hydroxyproline analysis as described in the general methods section of this thesis. The remaining 4 ml aliquots from each sample were incubated at 37°C for 24 hours, in spectrophotometer tubes (Bausch & Lomb, Inc.) and assayed for gel stability (described in appendix). The gels were then homogenized and transferred to cellulose nitrate ultracentrifuge tubes and centrifuged at 161,000 g with a Beckman Model L Ultra-Centrifuge. The supernatant was decanted and 0.5ml aliquots taken for liquid scintillation counting (appendix), and collagen content by hydroxyproline analysis. The pellet was assayed for the gel solubility (described in appendix). The supernatants from the various extractions were also analyzed by liquid scintillation counting.

Results.

After 24 hours of incubation at 4°C, 2.4% \pm 0.4% of the original label was retained while at 72 hours, 3.7% \pm 0.1% was retained. 1.56 and 2.38 moles of DOPA were retained in the dialysis bag per collagen α chain for the 24 hour and 72 hour samples, respectively. Figure 27 shows the results of the gel stability experiment for both the 24 hour and 72 hour samples.

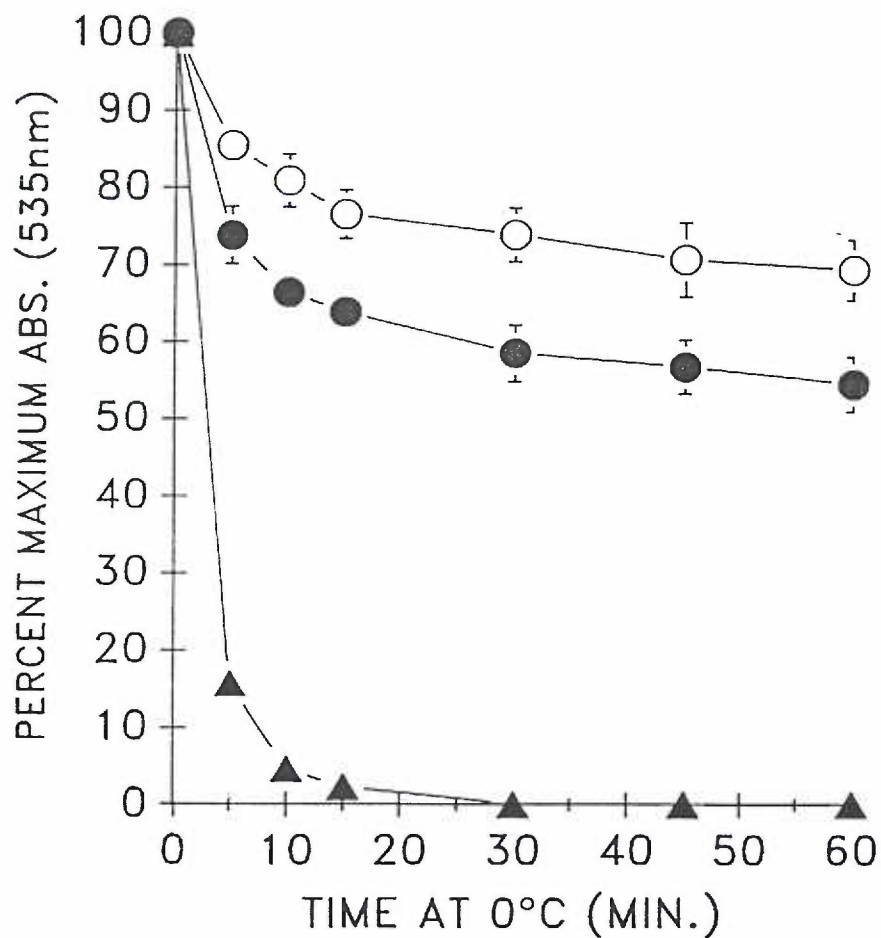


Figure 27. The stability of collagen gels exposed to DOPA at 4°C for 24 hours (●) and 72 hours (○), followed by exhaustive dialysis, and a pepsin control-collagen gel (▲). Following the dialysis procedure, the collagen solutions were incubated at 37°C for 24 hours, and then at 0°C for 60 minutes.

Three replicates were run for each sample. Variation is expressed as the standard error of the mean, and in cases was smaller than the symbol.

Collagen solubility data for the 24 hour and 72 hour incubation samples are shown in Figure 28. The moles of DOPA bound per α chain for the extracted collagens are shown in the Table in the discussion section. 0.6% and 0.7% of the collagen remained in the pellet, or that material remaining following boiling, for the 24 and 72 hour samples, respectively.

Discussion.

The results of the equilibrium dialysis experiment clearly demonstrated the ability of DOPA to bind to soluble collagen, prior to fibril formation. The increased level of binding with increased incubation at 4°C, suggested that binding was random and occurred in an Arrhenius fashion. It is notable, however, that binding was not linear over a 72 hour period. At 24 hours, 2.4% of the original label was retained in the bag yielding a 1.56 mole DOPA/mole collagen α chain. Following 72 hours, if binding had occurred in a linear fashion, the expected binding coefficient would have been three times that at 24 hours, or 4.68. Rather, at 72 hours, the binding coefficient is only 1.5 times that at 24 hours, or 2.38 mols DOPA/mole collagen α chain. This data suggested that either there are only a very small number of reactive sites on a collagen α chain to which DOPA can bind and these were effectively saturated at 72 hours, or, there are different populations of reactive sites with different degrees of reactivity. The most reactive sites would have been occupied at 24 hours, and the less active sites would bind DOPA in the time that followed. There is some evidence of reactive populations of helical lysyl and hydroxylysyl residues in total collagen^{137,138}.

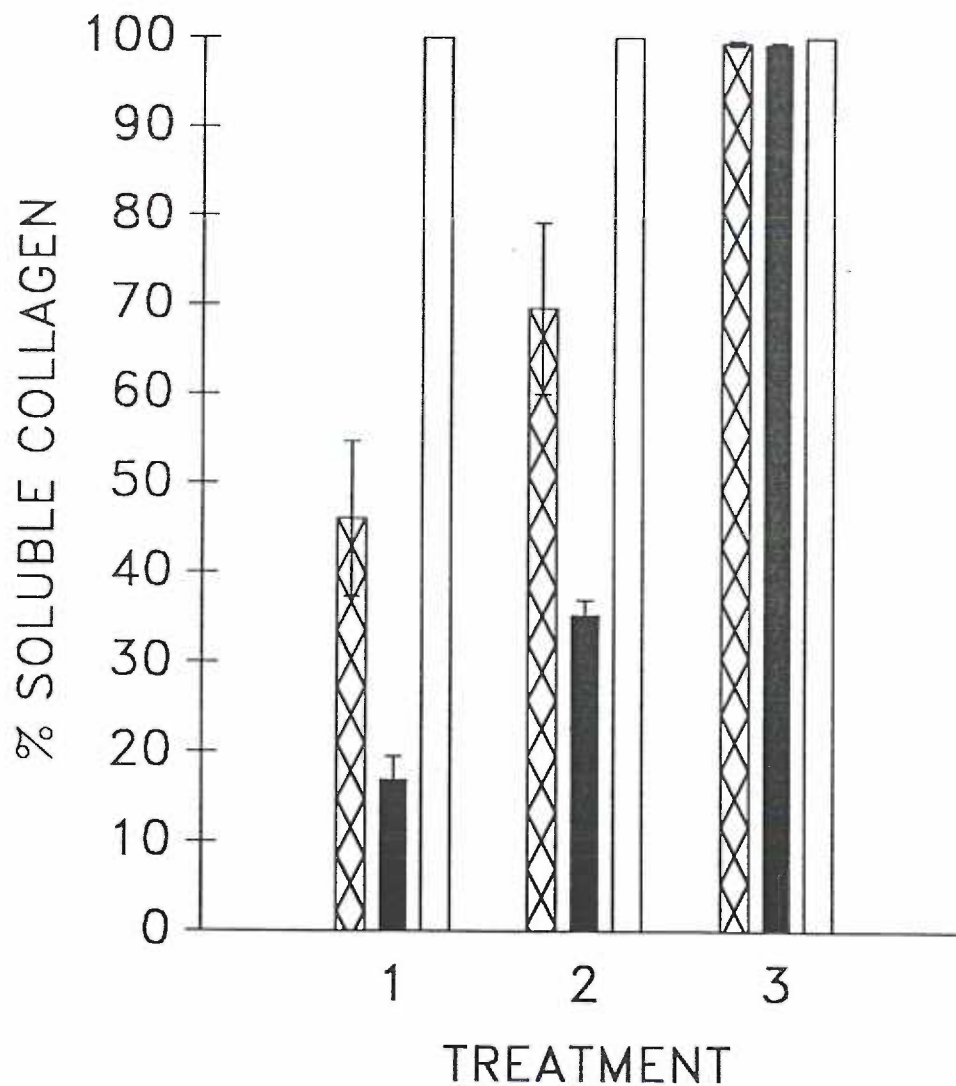


Figure 28. The solubility of collagen gels exposed to DOPA at 4°C for 24 hours (⊠), and for 72 hours (■) followed by exhaustive dialysis, and a control-collagen gel (□). The solubilities in phosphate buffered saline (PBS), 0.05M acetic acid at 4°C for 12 hours, and 0.01M acetic acid at 100°C for 2 hours are shown.

Three replicates were run for each sample. Variation is expressed as the standard error of the mean.

As Figure 27 shows, soluble collagen which had been modified with DOPA prior to fibril reconstitution, was stabilized by DOPA when fibrils were formed. The relative stability of the collagen gel, measured after 60 minutes at 0°C, was related to the amount of DOPA bound to the collagen, as was the collagen gel solubility of the stabilized gels (Fig. 28). In the 24 hour sample, 1.56 moles of DOPA were bound per α chain, and the gel was stabilized 54.5%. The 72 hour sample had 2.38 moles of DOPA bound per α chain, and was 69.3% stable. This represents a 1.4 fold increase in gel stability. Binding can therefore cause collagen fibril stabilization. However, it was not until the collagen was heated to 37°C that this occurred. This is probably not as much a temperature phenomenon as it is the requirement of fibril formation prior to stabilization. Modified fibrils may orient bound DOPA *ortho*-quinones adjacent to collagen reactive groups or other bound *ortho*-quinones resulting in dimerization and thus crosslink formation. Temperature may also play a role in increasing the probability of reaction. The molar binding ratios of the sequential extractants of the gelled 24 and 72 hour solutions following incubation at 37°C for 24 hours might provide additional support for different populations of binding sites. This evidence might also be construed to support a theory of random binding of DOPA to collagen. The amount of bound DOPA was significantly increased with the harshness of the extraction protocol, as shown by the binding values in the Table below. Not only does this data suggest that not all of the collagen bound DOPA at the same level, but it also demonstrates that increased binding of DOPA resulted in increased fibrillar stabilization. The latter concept will be discussed in great detail at a later point in this thesis.

EXTRACTION CONDITIONS	BINDING RATIO	
	24 HOUR	72 HOUR
PBS	0.32	0.57
0.5M ACETIC ACID 12HR @ 4°C	1.57	0.84
0.01M ACETIC ACID 2HR @ 100°C	2.32	3.16

Therefore, the results of this experiment support an Arrhenius mechanism of binding of DOPA to collagen and related binding to gel stabilization, though there is some evidence which supports the existence of a group of high affinity DOPA binding sites on collagen.

4. Is DOPA covalently bound to collagen?

Introduction.

The two preceding experiments provided strong evidence of the affinity of DOPA for collagen. However, this affinity might be explained by many forms of molecular interaction. It has been proposed that polyhydroxyphenols could hydrogen bond through their hydroxyl groups with peptide bonds of the protein ⁵¹. Ionic interactions between the alpha-amino group of DOPA and the multiple charged amino acid side chains of collagen, and hydrophobic interaction between the aromatic ring of DOPA and that of the aromatic amino acids of the proteins could facilitate binding ⁷⁷, though these interactions would be relatively weak. Lewis bases can react with quinones through a 1,4-Michael addition, to form covalently bonded adducts ¹³⁹. The first demonstration of such products was provided through molecular modeling studies which have been reviewed by Gustavson ¹⁴⁰. Mason ¹⁴¹ has provided a detailed review of the spectrophotometric characteristics of the covalent adducts formed by interaction of DOPA with the alpha-amino groups of the major amino acids. The epsilon amino groups of lysine side chains of proteins are thought to covalently interact with quinones in the same manner. Such is the basis of the protein crosslinking model which will be discussed later. The studies which have demonstrated the binding of catechol derivatives to connective tissue proteins ^{101,133}, have failed to provide direct evidence of covalent modification. Rather, binding has generally been measured under non-chaotropic conditions where

weaker interactions could persist, and thus explain the apparent binding to the protein.

The following experiment was designed to provide direct evidence of covalently modified collagen. Free labeled DOPA and DOPA exposed collagen α chains were separated by high performance liquid chromatography under denaturing conditions. This method was also used to measure the number of moles bound to collagen.

Materials and Methods.

A buffered collagen solution was prepared as described in the general methods section, $1 \times 10^{-3}M$ DOPA labeled with $4.76 \times 10^{-2} \mu Ci/ml$ $3\text{-}^{14}C$ DOPA (21mCi/mmol, Amersham Corp.) was added. 5ml aliquots were incubated at $37^{\circ}C$ for one hour, and $4^{\circ}C$ for 24 hours and 72 hours. At the end of the incubation period the gel formed at $37^{\circ}C$ was cooled to $0^{\circ}C$ until the solution had completely degelled. The samples which had been incubated in the cold were transferred to dialysis tubing and exhaustively dialyzed against phosphate buffered saline. All samples were immediately frozen and lyophilized. The lyophilized sample was analyzed by the gel filtration HPLC method described in the appendix.

Results.

The elution of U.V. absorbing and $3\text{-}^{14}C$ labeled material for the collagen sample incubated for one hour at $37^{\circ}C$ is shown in Figure 29. Figure 30

demonstrates the same for the samples incubated at 4°C for 24 hours, followed by exhaustive dialysis. The binding values for the three samples are shown below.

INCUBATION CONDITIONS	MOLES DOPA/ α CHAIN
1hr @ 37°C	4.10
24hr @ 4°C	1.46
72hr @ 4°C	2.40

Discussion.

In a 2.0M Gu-HCl buffer, the separation range of this gel filtration column is between 1kD and 70kD¹⁴². Therefore, in the chromatograms shown in Figures 29 and 30, the U.V. absorbing material at the void volume was presumably the 95kD type I collagen α chain. A large U.V. absorbing peak at the total volume (v_t) of the column presumably represented DOPA, with a molecular weight of 197.2 daltons. The 3-¹⁴C label is shown to co-elute with both U.V. absorbing peaks in Figure 29. Co-elution with the void volume peak is most significant, indicating interaction with the collagen α chains. Due to the chaotropic/denaturing conditions under which the column was eluted, this provided strong evidence for the presence of a covalent link between DOPA and collagen. The same is shown in Figure 30. However, excess DOPA had been removed by exhaustive dialysis.

Though DOPA can condense into large melanin like polymers, it is very unlikely that a large polymer could have explained the peak at the void volume. A

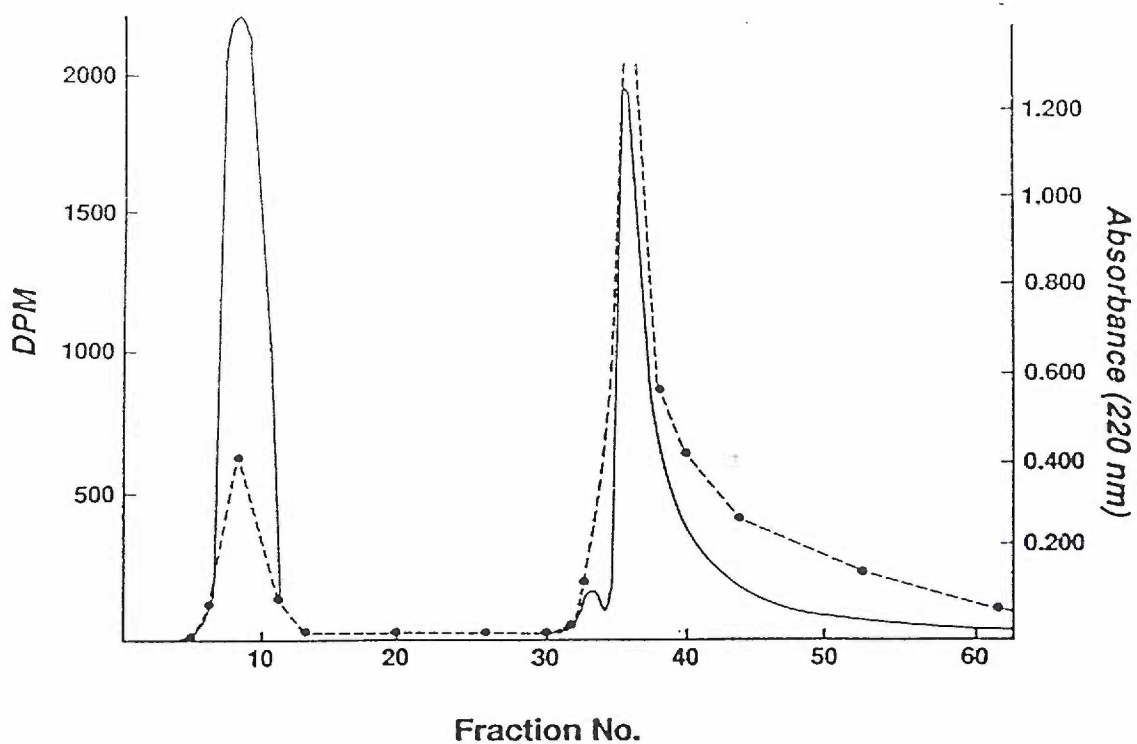


Figure 29. Gel filtration HPLC elution of $3\text{-}^{14}\text{C}$ -DOPA labelled collagen and unbound DOPA under denaturing conditions. Collagen solutions were incubated at 37°C for 1 hour in the presence of $1 \times 10^{-3}\text{M}$ $3\text{-}^{14}\text{C}$ -DOPA and then cooled at 0°C for 1 hour prior to application to the column.

(—): 220nm absorbance of eluant.
(-•-): DPM in elution fractions.

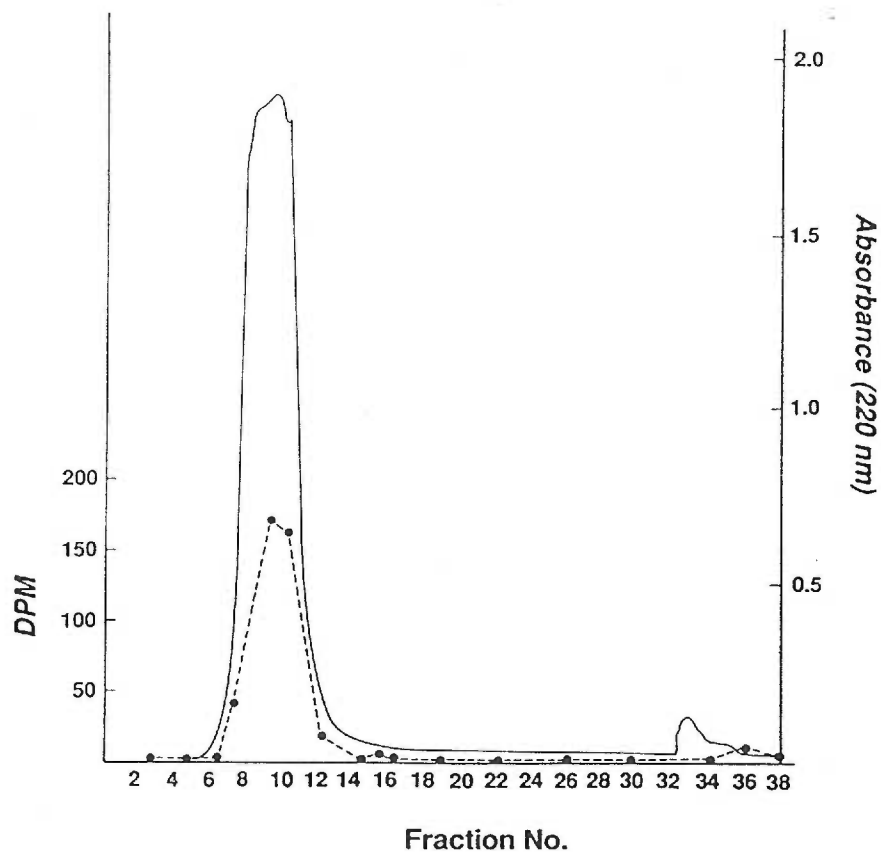


Figure 30. Gel filtration HPLC elution of $3\text{-}^{14}\text{C}$ -DOPA labelled collagen under denaturing conditions. DOPA-collagen gels were incubated at 4°C for 24 hours, and then exhaustively dialyzed to remove unbound DOPA prior to application to the column.

(—): 220nm absorbance of eluant.
(-•-): DPM in elution fractions.

70,000 MW polymer would likely be insoluble, and would have been removed by high speed centrifugation prior to being loaded on the column. In addition, a wide range of polymer sizes would have been expected to fall between the void volume and the total volume. As Figure 30 shows, there was no label evident besides that at the void and total volume. Finally, the experiment was devised to limit DOPA polymerization via both short binding times at 37°C, or the use of cold temperatures.

The calculated binding values provided some insight into the number of moles of DOPA which bind under various incubation conditions. A consistently small number were found to bind under conditions where DOPA polymerization was limited. These results suggested the presence of only a limited number of binding sites along the collagen α helix since there are 32 and 18 lysine residues per $\alpha 1$ and $\alpha 2$ chain, respectively. Elevated binding ratios represented bound DOPA polymers rather than monomers.

5. The involvement of the lysine side chains of collagen in DOPA binding.

Introduction.

The preceding experiments demonstrated the binding affinity of DOPA for collagen. Collagen, like all other proteins, provides reactive amino acid side chains which are capable of interacting with suitable ligands. *Ortho*-quinones are Lewis acids which can react with any available Lewis base. Proteins provide a number of Lewis bases. Thus, DOPA should be able to bind to any protein which has within its amino acid sequence, the specific reactive functional groups that allow binding with collagen. In this experiment, two homopolymeric polypeptides, poly-L-lysine and poly-L-glutamic acid, were analyzed for their ability to bind to DOPA covalently. Homopolymeric polypeptides were chosen to limit the possible types of side chains which aided in the identification of the reactive amino acid side chains. Both lysine and glutamic acid provide multiple charged side chains, though the lysine epsilon amino group is known to react with DOPA through a well characterized 1,4-Michael addition, and DOPA should react less effectively if at all with carboxyl functional groups¹⁴¹. Poly-L-glutamic acid has a single amino terminal group which is highly reactive, and therefore should react with DOPA. If blocked by acetylation, this interaction should be inhibited. Therefore, polylysine and poly-L-glutamic acid should react to varying degrees, and completely N-acetylated poly-L-glutamic acid should not react with DOPA. In this experiment, Gel Filtration HPLC under

denaturing conditions was used to determine whether the polypeptides had been covalently modified.

This study also investigated the amino acid compositions of DOPA collagen hydrolysates, looking for a decrease in the lysine content when compared to the control collagen. The bond formed between DOPA and lysine is non-acid labile, and therefore, should remain intact following strong acid hydrolysis. The lysine will remain bound to the DOPA, and as will be demonstrated at a later point in this thesis, these adducts will be part of a much larger melanin like polymer. Thus, amino acid compositions of proteins to which DOPA has bound should result in a decrease in the lysine content when compared to control samples.

Materials and Methods.

Binding of DOPA to Poly-L-lysine.

Solutions of poly-L-lysine with a molecular weight of 63kD, and poly-L-glutamic acid with molecular weight of 64kD and N-acetylated with acetic anhydride by the method of Ansari, *et al*¹⁴³, were prepared at concentrations of 0.75 mg/ml in buffered saline (polypeptides were purchased from the Sigma Chemical Co.). Three 5.0ml aliquots of each solution were transferred to Spectrapor Dialysis Tubing (MW cutoff = 3.5kd) and incubated in a dry air incubator in the presence of 1×10^{-3} M DOPA labeled with $0.05 \mu\text{Ci/ml}$ $3\text{-}^{14}\text{C}$ -DOPA (21mCi/mmol, Amersham Corp.), at 37°C for 2 hours. Following the incubations, the solutions were exhaustively dialyzed first against running tap water and then against buffered saline. The contents of the

dialysis bags were centrifuged at 20,000 x g for 30 minutes using a Beckman J-21 High Speed Centrifuge. Aliquots were lyophilized and 750 μ g of protein analyzed by the Gel Filtration HPLC method described in the appendix, and the results are shown in Figure 31.

The Fate of Lysine Residues in DOPA-Collagen Hydrolysates.

A buffered pepsin soluble collagen solution, prepared as described in the general methods section, was incubated in the presence and absence of 1×10^{-3} M DOPA at 37°C for a 30 day time period. Under these conditions, one would expect that DOPA binding would be at a maximum, and polymerization would be complete. The gels were then hydrolyzed in 6.0N HCl at 108°C for 18 hours. The hydrolysates were dried under nitrogen, resuspended in deionized water, passed through a 0.22 μ syringe tip filter, and an aliquot analyzed for collagen content by hydroxyproline analysis. An appropriate volume which contained approximately 5000 picomoles of hydroxyproline was lyophilized and derivatized with phenyl-isothiocyanate. A sample containing approximately 200 picomoles of derivatized hydroxyproline was analyzed for lysine content by PITC amino acid analysis¹¹⁷ on an IBM chromatographic system.

Results.

Both of the polypeptide solutions were visibly pigmented at two hours when incubated at 37°C, though the N-acetylated-poly-L-glutamic acid may have been

more so. The two hour incubation samples, following exhaustive dialysis provided visual evidence of a major difference in the ability of the preparations to interact with DOPA. Only the poly-L-lysine solution was visibly pigmented, suggesting that it alone had bound the DOPA. Some black granular material (removed by centrifugation) had precipitated from the N-acetylated poly-L-glutamic acid solutions, but not the poly-L-lysine solutions. The HPLC chromatograms of the two solutions along with the corresponding radiolabel elution pattern is shown in Figure 31. Label co-eluted with the poly-L-lysine but not the N-acetylated poly-L-glutamic acid.

Following hydrolysis of the DOPA-collagen gels, a great deal of black granular material had precipitated and was separated from the hydrolysates by being passed through a 0.22μ syringe tip filter. The amino acid profile for a DOPA collagen hydrolysate is shown in Figure 32. The lysine content in the DOPA-collagen hydrolysates and the control hydrolysates were $26.1 \pm .6$ residues, and 28.3 ± 0.3 residues per type I collagen α chain, respectively. Glycine, proline, hydroxyproline, and hydroxylysine contents were unchanged. Histidine levels were decreased from 5.4 ± 0.4 residues in the control gels to 4.3 ± 0.2 residues in the DOPA-collagen gels.

Discussion.

The *ortho*-quinones of DOPA are thought to react with both amino and sulfhydryl side chains of amino acids through a 1,4-Michael addition⁹⁵. However, in type I collagen, there are no cysteine residues, and therefore sulfhydryl groups are not a consideration in these studies. Poly-L-lysine has an abundance of lysyl epsilon

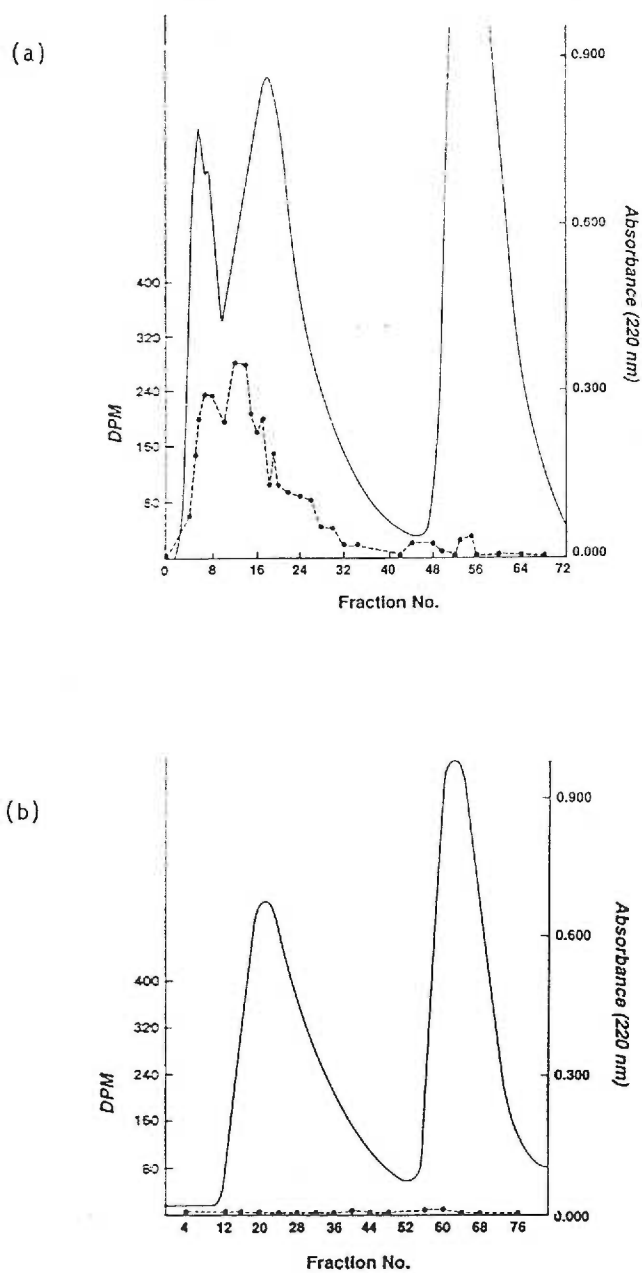


Figure 31. Gel filtration HPLC elution of $3\text{-}^{14}\text{C}$ -DOPA exposed (a) poly-L-lysine and (b) N-acetylated poly-L-glutamic acid under denaturing conditions, following exhaustive dialysis to remove excess DOPA.

(—): 220nm absorbance of eluant.
 (-•-): DPM in elution fractions.

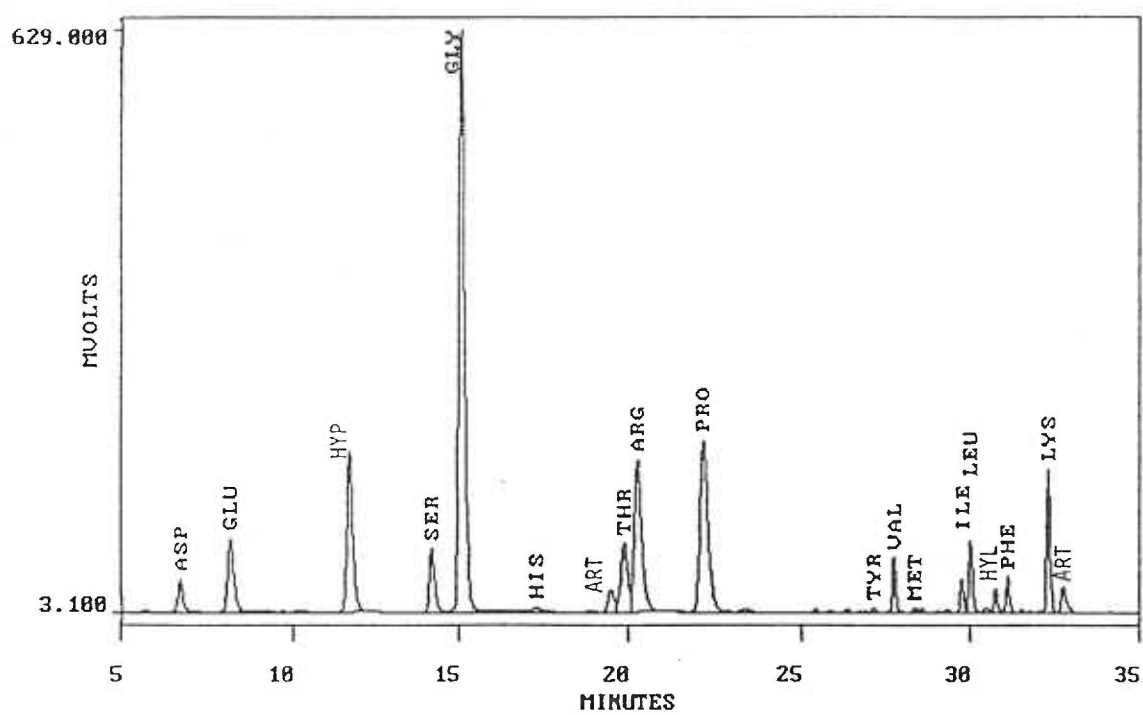


Figure 32. Chromatogram showing the PITC amino acid composition of a DOPA-collagen gel incubated at 37°C for 10 days. Three letter amino acid abbreviations were used and PITC derivatization artefacts are denoted by the abbreviation, ART.

amino groups, and a single alpha-amino group which can react with DOPA. Poly-L-glutamic acid has only the single alpha amino group to which DOPA can bind. If this site is blocked with an acetylating agent, then DOPA should not bind. The binding of DOPA to amine functional groups, and the polymerization of DOPA monomers occur in solution ¹⁴¹, and must be competing reactions. Therefore, if amines are available in a solution containing DOPA, a portion of the DOPA molecules will bind to these amines and will not be available for binding to other DOPA monomers. The relative lack of pigmentation of the poly-L-lysine solution with respect to the N-acetylated poly-L-glutamic acid solution at the end of the 37°C incubation, as described in the results section may have been due to the presence of competing reactions from lysyl amino groups that were abundant in the poly-L-lysine solution. Thus, less moles of *ortho*-quinone would have been available for self polymerization, and the production of a pigmented melanin like polymer.

Poly-L-lysine incubated with DOPA for 2 hours, and then exhaustively dialyzed against physiological saline, like type I collagen (described previously), formed an interaction with DOPA that was stable in guanidine-HCl (Fig. 31). Again, this data supports a covalent model of adduct formation. N-acetylated poly-L-glutamic acid, on the other hand, had no label associated with it's U.V. peaking, indicating lack of binding. The chromatogram showing binding to poly-L-lysine demonstrated more than one molecular wight species. Further studies are now being pursued to determine if these are crosslinked polypeptides.

It is my hypothesis that when DOPA binds to collagen, it polymerizes with both bound and free DOPA to form a melanin like polymer. Visual observations suggest that under strongly acidic conditions, melanin like polymers are precipitated

and can be removed by filtration. DOPA is thought to bind to lysine residues through a non-acid labile covalent bond. Therefore, because this bond should not be broken during hydrolysis, as melanin like polymers precipitate, so should the bound lysine. The expected result was a decrease in the lysine content of the hydrolysate. The results of this experiment demonstrated that DOPA-collagen hydrolysates had two to three fewer lysines per α chain, than did control gels. In comparison, the content of other marker amino acids of collagen (excluding histidine), were unchanged. These results indicated that three lysines were derivatized by DOPA, and were covalently bound to the melanin like polymer that precipitated. This represents approximately 10% of the lysine residues of bovine collagen¹⁴⁴⁻¹⁵⁰. This could indicate that only three lysines did, in fact, covalently bind to DOPA after 30 days at 37°C. A previous binding study measured the number of moles of DOPA bound to collagen after 24 hours of incubation at 37°C. Approximately 20 moles of DOPA were bound per collagen α chain. When taken together, the results of these two separate studies mean that of the 20 moles of DOPA which were bound after 24 hours, 17 were not **directly** linked to lysine but rather are DOPA polymers bound to lysine. Visual evidence again provided a clue that this may actually be the case. DOPA-collagen gels which had been incubated at 37°C for 24 hours, and then exhaustively dialyzed against phosphate buffered saline, retained the dark pigment which indicates the presence of melanin like polymers. An additional explanation for the small lysine loss may be that the DOPA-lysine bond is acid labile, and the lysine would be released. The significant decrease in the histidine content of the DOPA-collagen gel hydrolysates could

indicated that the secondary amine of the imidazole ring is a strong enough Lewis acid to react with the *ortho*-quinone.

Can two to three covalently bound DOPA monomers explain the remarkable stability of the DOPA-collagen fibrillar matrices describe in Part I of this experimental section? The answer may be yes. Naturally crosslinked collagen has only four crosslinking residues per collagen molecule, resulting in a highly stable matrix. In addition, due to possible complexity of a melanin like crosslink (a topic that will be discussed in the following section), the crossbridging effect of these three covalently bound residues, which can react with free DOPA, may be enhanced. Taken together, the results of this experiment, and that previously described, support the role of lysine as the primary amino acid of collagen to which DOPA binds.

In conclusion, this experiment provided evidence of the affinity of DOPA for lysine containing proteins and that two to three lysine residues of collagen bind covalently to DOPA, and thus mediate the stabilizing effect of DOPA. In the following experiment, peptide mapping methods were used in an attempt to identify the specific lysine residues which mediate DOPA binding along the collagen chain.

6. Peptide mapping of Type I Collagen-DOPA reactive lysine residues.

Introduction.

Page and associates ^{137,138}, in the late 1960's, proposed that there existed a small group of highly reactive lysine and hydroxylysine side chains in the collagen α helix which played some role in the processes of natural collagen crosslinking. They based these conclusions on experiments which showed enhanced reactivity with pyridoxal-6-phosphate, resulting in Schiff base formation presumably with epsilon amino groups. Since then, four specific lysine and hydroxylysine residues have been identified in the type I collagen α helix which form aldimine crosslinks in the processes of natural collagen crosslinking ². Whether or not these residues are those which Page identified is not clear. The following experiment was designed to map the site of covalent binding of DOPA on the type I collagen α helix, and to answer the question of whether there are a group of specific reactive lysine and hydroxylysine residues which preferentially bind DOPA. The mapping strategy was based upon the fragmentation of collagen into representative peptides with known sequences. Cyanogen bromide cleavage was chosen to break the collagen helix into representative fragments due to the large body of information on the structure of the cyanogen bromide peptides of type I collagen ¹⁴⁴⁻¹⁵⁰. The peptide maps for the $\alpha 1(I)$ and $\alpha 2(I)$ chains of type I collagen ¹⁵¹ are shown in Figure 33.

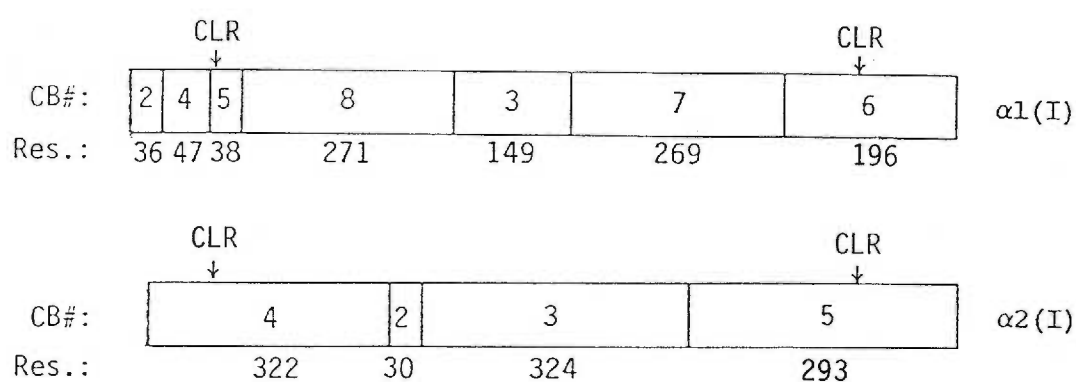


Figure 33. Cyanogen bromide peptide maps of the $\alpha 1$ and $\alpha 2$ chains of pepsin treated type I collagen¹⁵¹. The approximate positions of the crosslinking lysine residues located within the helical domain² are indicated (CLR).

Materials and Methods.

Pepsin soluble collagen was labeled with 3-¹⁴C-DOPA by the following method. A 100 ml collagen solution was prepared at a concentration of 4.5 mg/ml pepsin treated collagen, 0.135 M NaCl, 2.5 mM acetate, 30 mM phosphate (pH 7.5). To this solution was added 20 μ Ci 3-¹⁴C-L-3,4-dihydroxyphenylalanine (21 mCi/mole, Amersham). The solution was thoroughly aerated and incubated in the dark at 37°C for 24 hours. The labelling reaction was terminated by adding 10ml of 0.5M acetic acid, and then the solution was cooled to 0°C with stirring for 1 hour to totally disperse the collagen fibrils. The solution was transferred to dialysis tubing (Spectrapor M.W. cutoff = 12kD - 14kD) and exhaustively dialyzed against 5mM acetic acid. An 0.5ml aliquot was lyophilized and analyzed by Gel Filtration HPLC (appendix). Two additional 0.5ml aliquots were analyzed directly by Liquid Scintillation Counting and hydroxyproline assay to calculate a specific activity of binding. The resulting DOPA-collagen adduct had a measured specific activity of $5 \times 10^2 \mu$ Ci/mg collagen.

40 mg samples of the labeled and unlabeled control collagen were digested with cyanogen bromide by the method of Epstein¹⁵² described in the General Methods section of this thesis (appendix).

SDS polyacrylamide gel electrophoresis and autoradiography.

80 μg of freeze dried CB peptides were separated on a 13% acrylamide SDS-Page gel system as described by Laemli ¹¹¹. In an additional lane, 20 μg of type I collagen α chains were run as a reference. The gel was stained by the Fairbanks method ¹¹³ with coomassie brilliant blue R-250 dye (Biorad Laboratories). The gel was then treated with Fluoro-Hance (Research Products International Corp.), an autoradiographic enhancer, dried under vacuum, and allowed a 2 week period to expose a sheet of X-Omat AR high speed X-ray film (Eastman Kodak Co.).

A duplicate gel was run, and the known type I collagen CB peptide bands cut out and counted in Hionic Fluor (Packard Instruments Co., Inc.) following extraction of the protein from the gel with Soluene 350 (Packard Instruments Co., Inc.).

Gel Filtration High Performance Liquid Chromatography.

2 mg of the labeled CB peptides was eluted by gel filtration HPLC by the method of Miller ¹⁵³, with slight modifications. In short, the peptides were eluted on tandem 30 x 0.75mm Bio-Sil TSK-250 columns, with a 2.0M low U.V. absorbance guanidine-HCl, 50mM tris (pH 7.5) run buffer. The flow rate was maintained at 0.3 ml/min., the elution was monitored at 220nm with a Hitachi variable wavelength detector, and fractions were collected every 1.0 minutes. 200 μl aliquots were counted from each fraction with a Beckman LS-250 Liquid Scintillation Counter.

Results.

The results of the SDS-PAGE separation of type I collagen cyanogen bromide peptides is shown in Figure 34. Coomassie stained unlabeled type I collagen α -chains are shown in Lane 1. Lane 2 is a standard cyanogen bromide peptide map of type I collagen, lane 3 is a cyanogen bromide peptide map of collagen exposed to DOPA, and lane 4 is the autoradiograph of lane 3. The dpm values of the four major α 1(I) CB peptides CB3, CB6, CB7 and CB8 were 29.6, 96.0, 88.6 and 145.0, respectively.

Figure 35 shows the gel filtration HPLC elution profile of the labeled and unlabeled CB peptides. Both the UV and radiographic tracings are shown for the labeled peptides. In addition, for reference the elution position of type I collagen α -chains is shown.

Discussion.

The results of this experiment were in many ways anticipated, though in other ways enlightening. Lanes 3 and 4 of the SDS-PAGE gel in Figure 34 demonstrates that label co-migrated with the four largest peptides of the α 1 chain of type I collagen. Label also seemed to co-migrate with the large peptides (CB3, CB4, and CB5) of the α 2 chain, though this was not distinct. A great deal label which was not associated with any of the known peptides, may have represented high molecular weight material, and resulted in a high background in the region of this band. These results were in no way surprising in that they agreed with previous data which

Figure 34. SDS-Page gel and autoradiograph of cyanogen bromide (CB) peptides of $3\text{-}^{14}\text{C}$ -DOPA labelled collagen.

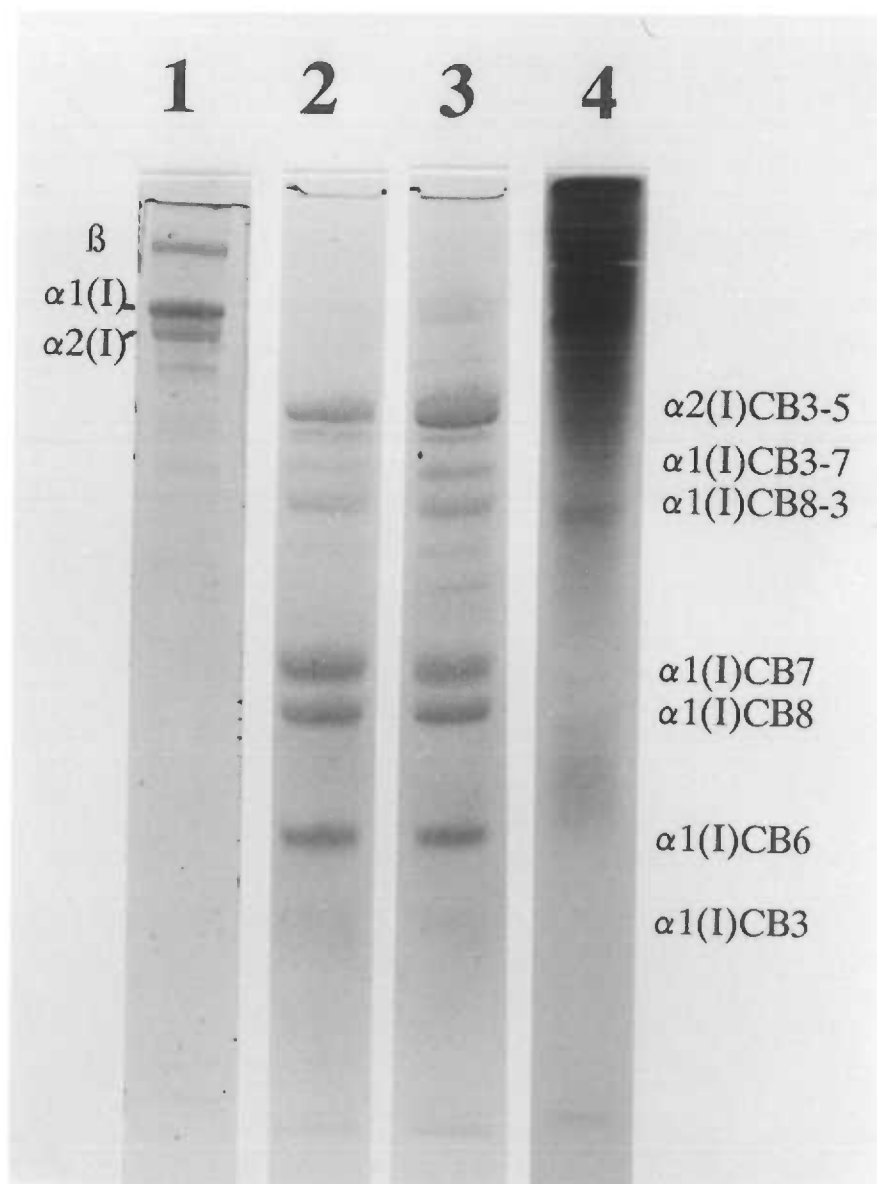
Lane 1: Undigested type I collagen.

Lane 2: Coomassie stained unlabelled type I collagen CB peptides.

Lane 3: Coomassie stained CB peptides of $3\text{-}^{14}\text{C}$ -DOPA exposed type I collagen (low molar ratio binding).

Lane 4: The autoradiograph of Lane 3.

* β notation indicates aldol crosslinked collagen α chains.



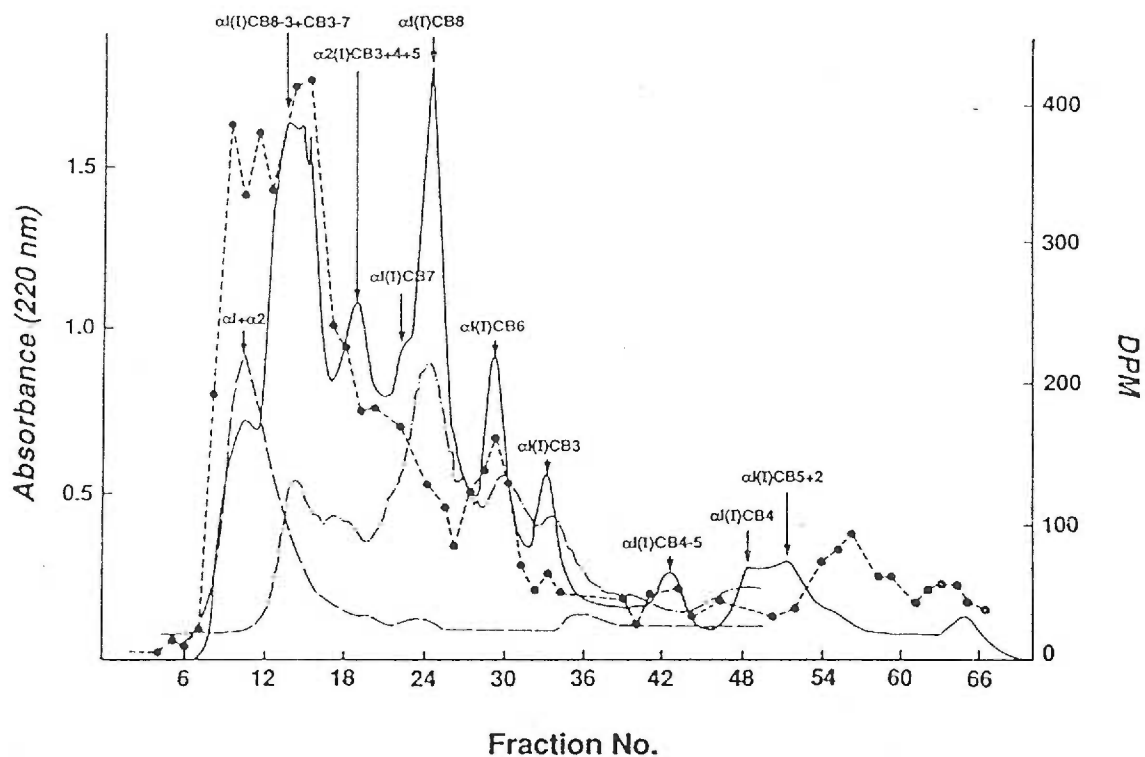


Figure 35. Gel filtration HPLC elution of $3\text{-}^{14}\text{C}$ -DOPA exposed type I collagen cyanogen bromide peptides under denaturing conditions.

- (—): 220nm absorbance of eluant of DOPA-collagen CB peptides.
- (•---•): Radioactivity of eluant fractions of DOPA-collagen CB peptides.
- (---): 220nm absorbance of eluant of CB peptides from type I collagen not exposed to DOPA.
- (-·-·-): Undigested type I collagen.

demonstrated the covalent interaction of DOPA and collagen lysine side chains. Cyanogen bromide digestion, even under the strongly acidic conditions employed in this experiment would not have been expected to have cleaved the 1,4-Michael addition product of DOPA and lysine since the mechanism of hydrolysis requires a thiol-ether functional group¹¹¹. Cyanogen bromide cleavage is specific for hydrolysis of amide bonds on the carboxyl side of methionine residues¹¹¹, and could not, therefore, have hydrolyzed the bond. In addition, the bond formed is not acid labile.

What was of surprise was the upper portion of the autoradiograph. The method by which the DOPA was bound to the collagen was not expected to form crosslinks between the collagen α chains. Labeled DOPA was added at a molar ratio of 0.2 moles/mole collagen α chain. Though 2/3 of the label was retained with the collagen, it seemed likely that this was not in the form of bound polymers. The likelihood that any two DOPA molecules were close enough to polymerize and form a crosslink should have been low. However, lane 4 shows that the majority of the label loaded on the gel either did not, or only slightly penetrated the gel. In lane 3, the material that did not penetrate the gel was stained with coomassie blue and therefore should be collagen. In contrast, there was no coomassie stainable material at the top of the lane in the control peptides run in lane 2. These findings strongly suggested the presence of highly crosslinked proteinaceous material in the labeled DOPA treated collagen. Also, there was a higher abundance of high molecular weight coomassie stainable material in lane 3 than there was in lane 2 (Figure 34). The implication of this finding was that either cleavage was being hindered by the presence of DOPA residues in close proximity to the methionine residues, or DOPA crosslinks were linking together neighboring peptides.

The results of the gel filtration HPLC elution of the labeled and unlabeled CB peptides (Fig. 35) confirmed the SDS-PAGE results. The CB3, CB6, CB7 and CB8 peptides of the $\alpha 1(I)$ chain were again labeled, and an abundance of high molecular weight UV absorbing material other than uncleaved α chains elutes and was highly labeled. The benefit of this technique over the SDS-PAGE technique was that the lower molecular weight peptides of the $\alpha 1(I)$ chain as well as the $\alpha 2(I)$ peptides were resolved. As a result, the proportional labeling of the specific CB peptides of the type I collagen α chains could be investigated and compared with number of lysine residues per peptide. The lysine content of each $\alpha 1(I)$ peptide are compared with the total number of amino acid per peptide in the Table below. The $\alpha 1(I)$ CB6 peptide, a 217 residue peptide at the C terminus of the protein, contains only 4 out of the total 32 lysine residues of the $\alpha 1$ chain. As is demonstrated by

PEPTIDE	AMINO ACIDS/PEPTIDE	LYSINES/PEPTIDE
CB2	36	0
CB3	149	5
CB4	47	2
CB5	38	2
CB6	196	4
CB7	269	10
CB8	271	9

comparing the U.V. and radiographic profiles, the CB6 peptide had a relatively high level of label bound in comparison to, for example, the CB3 peptide, which had a higher lysine content. This agreed with the results of extraction of protein from the electrophoresis gel slab. Greater than three times the amount of radioactivity extracted from the $\alpha 1(I)CB3$ band was extracted from the $\alpha 1(I)CB6$ band. The large CB7 and CB8 peptides, which contain more than twice the number of lysines, appeared to be labeled to the same degree. In fact, when looking at the data of extraction from the gel slab, only the $\alpha 1(I)CB8$ peptide band had a higher amount of extractible radioactivity. One of the two crosslinking lysines derived residues located within the collagen helical region is localized to $\alpha 1(I)CB6$ peptide, as is shown in Figure 33². Could this lysine or hydroxylysine residue be one of the reactive groups proposed by Page^{137,138}. If so, would DOPA be more likely to bind to this residue? The apparent increased affinity of DOPA for the CB6 peptide might provide evidence in support of this hypothesis. However, sequence analysis of the derivatized peptide would be required for substantiation. The other helical crosslinking lysine residue lies within the $\alpha 1(I)CB5$ peptide. Elution of label with the fused peptide $\alpha 1(I)CB4-5$ but not with the $\alpha 1(I)CB4$ peptide suggested that the CB5 portion of the fused peptide had bound label. This peptide did not show the same level of labeling with DOPA. Only the $\alpha 1(I)CB2$ and $\alpha 1(I)CB4$ peptides appeared not to have bound DOPA. The larger peptides of the $\alpha 2(I)$ chain were not readily separable using either of these techniques. However, they were separable from the peptides of the $\alpha 1$ chain. The HPLC peak representing the $\alpha 2(I)CB3+4+5$ peptides co-eluted with label under denaturing conditions indicating that the $\alpha 2$ chain did bind DOPA.

In summary, this experiment demonstrated that DOPA binds to most of the cyanogen bromide peptides of the $\alpha 1$ chain of type I collagen, as well as the peptides of the $\alpha 2$ chain, though which peptides of the latter could not be determined. The CB6 peptide of the $\alpha 1$ chain appeared to have a high affinity for DOPA which may indicate the presence of a highly reactive lysine residue. Generalized labeling of most peptides, however, indicated that binding was random, which agreed with data presented previously in this thesis. Thus, to explain this apparent paradox, it is hypothesized that DOPA can bind through what is a simple organic reaction to any available lysine residue of collagen. There may exist, however, one or more highly reactive residues which can bind DOPA with a higher affinity. Finally, this study seemed to indicate the formation of crosslinked collagen molecules even at low DOPA concentrations. These crosslinks could link together adjacent CB peptides, and might sterically hinder the hydrolysis reaction of cyanogen bromide at neighboring methionine residues.

7. Summary.

The results of the previous set of experiments supported the hypothesis that DOPA binds covalently to collagen through lysine side chains. Approximately 21 moles of DOPA were bound per collagen α chain of a 1×10^{-3} M DOPA-collagen gel, following 24 hours of incubation at 37°C. Binding also occurred when collagen fibril formation was inhibited by incubation at cold temperatures. The number of moles of DOPA bound was reduced 10 fold, and appear to reach a maximum number of approximately three moles following 72 hours of incubation. These results suggested that when collagen is in the soluble form, DOPA monomers react with only a small number of binding sites. At 37°C, where fibril formation occurred, the binding of increasing numbers of moles of DOPA indicate polymer formation.

The binding of DOPA to collagen was shown to be covalent in nature by separating DOPA-collagen adducts and free DOPA under denaturing conditions. Lysine side chains were implicated as the specific site of DOPA binding. DOPA was covalently bound to poly-L-lysine, but did not react with N-acetylated poly-L-glutamic acid. In addition, the lysine composition of DOPA-collagen hydrolysates was decreased by approximately three moles.

The site of DOPA binding along the collagen molecule was mapped to specific cyanogen bromide peptides. The $\alpha 1$ (I) CB6 peptide which contains one of the four specific crosslinking lysine side chains, had a higher affinity for DOPA with respect to the lysine content. In addition, the $\alpha 1$ (I)CB7 and α (I)CB8 peptides, but not the $\alpha 1$ (I)CB3 peptide appeared to bind DOPA with a high affinity. These

results support the presence of a population of reactive lysine side chains capable of reacting and forming covalent adducts with DOPA with high affinity. Generalized labeling of most of the other peptides of type I collagen suggests that there is also a much larger population of lysine residues with a lower affinity for DOPA.

B. PART III. Studies on the Mechanism of Crosslinking of DOPA Derivatized Type I Collagen Alpha Chains.

1. Introduction.

Work previously described in this thesis provided evidence that DOPA could covalently modify collagen α chains as well as other proteins. The modified collagen chains formed collagen fibrillar matrices which were highly insoluble, resistant to cyanogen bromide digestion, and had enhanced thermal stabilities and tensile properties. How did bound DOPA monomers increase the chemical, thermal, and physical stabilities of collagen gels? Two very different models of quinone or vegetable tanning have been proposed to explain the increased stability of protein matrices exposed to this class of compounds, and these have been described in the general introduction. The first is a covalent crosslinking model in which a quinone monomer interacts with two polypeptide chains through a series of oxidation-reduction reactions⁵¹. The second model⁷⁷, which has been described in the insect cuticle, proposes that the increased stability is the result of weak interactions of the quinone compounds with lysine side chains, as well as other hydrophilic groups. The quinone compounds can then polymerize to form large hydrophobic groups within the matrix. The result would be a dehydration of the matrix which would cause an inward collapse, and resulting stabilization of the matrix. The actual quinone tanning mechanism may occur through a combination of these two

processes. DOPA binds covalently to collagen, and in doing so may initially block hydrophilic groups and cause a small scale dehydration and matrix stabilization. Polymerization of the covalently bound quinones would not only increase the stability of the matrix through crosslink formation, but would in addition increase the dehydration phenomenon by increasing the hydrophobicity of the polymer formed. The following series of experiments were designed to investigate the mechanism by which covalently bound DOPA monomers stabilize collagen gels. The role of DOPA polymerization in this mechanism was determined. The spontaneous nature of DOPA metabolite polymerization^{87,141} poses a question of what role this process might have in crosslink formation. Bound monomers might react with other bound monomers to give dimer crosslinks. There definitely seemed to be a time where DOPA has bound to collagen fibrils, but stabilization of the gel has not occurred. This occurred at one hour of incubation in the DOPA-collagen gel stabilization experiment. If this lack of stabilization indicated a lack of crosslink formation then it would follow that binding and crosslink formation are two events separable by time. Melanin is a totally uncharacterized family of polymers derive from DOPA. It is insoluble in even the harshest reagents and is resistant to acid hydrolysis. For these reasons, direct proof that lysyl-DOPA condenses to form crosslinks is virtually impossible to obtain. The following experiments were, therefore, designed to provide "circumstantial" evidence by manipulating the DOPA/collagen interaction conditions in ways known to affect melanin like polymer formation. For melanin formation to occur, oxygen must be available to produce the highly reactive *ortho*-quinone precursors of the melanin. Two of the precursors of melanin absorb strongly in the visible and ultraviolet range, and can therefore be detected, and

decarboxylation of DOPA occurs in the synthesis of 5,6-indole-quinone, one of the three or more melanin subunits ¹⁴¹. Finally, the reactive sites at which polymerization occurs are known ⁹⁷. Blocking these sites with large hydrophobic groups should inhibit melanin formation. In the following experiments, these concepts were addressed.

2. The concentration dependency of DOPA.

Introduction.

In an experiment described previously, the thermal stability of collagen fibrils reconstituted in the presence of DOPA was decreased if the extent of binding was limited. The tensile strength at decreased DOPA concentrations was also decreased with respect to fibrils exposed to 1×10^{-3} M DOPA. These results suggested that the stabilizing effect of DOPA was concentration dependent. The majority of the preceding experiments have investigated the interaction of collagen fibrils with DOPA at a concentration of 1×10^{-3} M. At this concentration, there are more than 65 moles of DOPA available for binding to each collagen α chain. According to the laws of molecular kinetics, as the number of moles of DOPA bound increases, the likelihood that bound monomers will come in close proximity to additional bound monomers also increases. *Ortho*-quinones can, through a series of spontaneous reactions, form melanochrome dimers and higher melanin like polymers^{87,89,141}. Bringing monomers into close proximity should increase the frequency of occurrence of these reactions. Thus, by raising the concentration of DOPA, dimerization of bound and oxidized DOPA monomers to form covalent crosslinks between collagen fibrils should increase, and the result should be a more stable gel. The following experiment investigated the concentration dependent nature of the stabilizing effect of DOPA on reconstituted collagen fibrils.

Materials and Methods.

Buffered pepsin soluble type I collagen solutions were prepared as described in the general methods section of this thesis. From a starting concentration of $1 \times 10^{-3}\text{M}$, serial dilutions of DOPA were added to each of 10 solutions giving a concentration range of $1.95 \times 10^{-6}\text{M}$ to $1 \times 10^{-3}\text{M}$. At each concentration, three 4.0 ml DOPA-collagen solutions and controls lacking DOPA were incubated for 18 hours at 37°C in spectrophotometer tubes (Bausch & Lomb, Inc.). Following this incubation period the tubes were measured for absorbance at 535 nm, and the cooled to 0°C for 1 hour. The absorbance at 535 nm was again read, and the degree of destabilization based upon % Maximum Absorbance (following the warm incubation) was determined. The cooled collagen gels were analyzed for collagen gel solubility by the method described in the general methods section (appendix).

Results.

Pigmentation was most dramatic at $1 \times 10^{-3}\text{M}$ and appeared to decrease in a near linear fashion with respect to the serial dilutions, and was virtually absent in the 10^{-5}M concentration range. Both the change in collagen gel stability and solubility are shown in Figure 36. Gel stability is expressed in terms of percent of the optical density prior to cold incubation, and solubility is expressed as percent of the total collagen in the original gel. The effect of the pigment on the optical density at 535nm of the collagen gels was cancelled by comparing concentrations

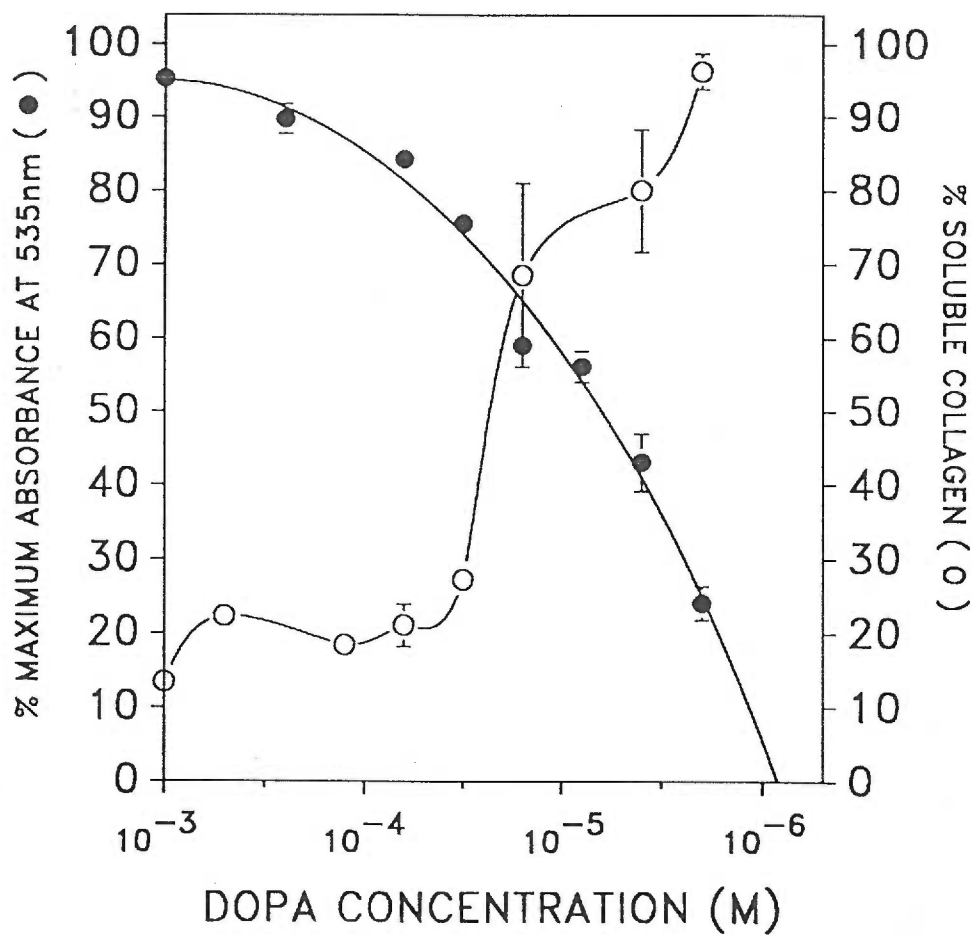


Figure 36. Collagen gel stability (●) and solubility (○) at varying concentrations of DOPA. DOPA-collagen solutions were incubated at 37°C for 18 hours, and then cooled at 0°C for 1 hour. The solubility in 0.5M acetic acid is shown.

Three replicates were run at each concentration. Variation is expressed as the standard error of the mean, and in cases was smaller than the symbol.

against a maximum absorbance at the end of the 37°C incubation period. Both are plotted against DOPA concentration.

Discussion.

The results of this experiment were extremely informative. Here, the phenomenon of gel stabilization, which can be, but is not necessarily related to the formation of covalent crosslinks, was related to gel solubility. As Figure 36 shows, gel **stabilization** decreased as the DOPA concentration decreased. The decrease was not linear and appeared to become more pronounced in the 10^{-5} M range. The calculated x-axis intercept indicated that at a concentration of 8.57×10^{-7} M, DOPA could no longer exert a stabilizing effect on the collagen matrix. At this concentration, a molar binding ratio of 0.05 mols of DOPA / mole of collagen α chain was calculated.

The gel **solubility** data in Figure 36 shows a more defined critical concentration. As in the gel stabilization data, the effect of DOPA was greatest at 1×10^{-3} M, the highest concentration tested. However, unlike the previous data, between the concentrations of 1×10^{-3} M and 3.1×10^{-5} M, the effect of DOPA did not decrease significantly. On the other hand, between the concentrations of 3.1×10^{-5} M and 1.65×10^{-5} M, a dramatic increase in solubility occurred. These concentrations corresponded to molar binding ratios of 1.97 and 0.99 respectively. The extremely large variability in the 1×10^{-5} M concentration range was suggestive of a "transition point" with respect to the insolubilization effect of DOPA on collagen gels.

In light of the combined data in Figure 36, several conclusions could be drawn and speculations made. First, the effect of DOPA on collagen gels was concentration dependent. Higher concentrations of DOPA yielded more stable and less soluble collagen gels. Secondly, gel stability data could be generally related to solubility data, though the latter appeared to provide a more defined picture of the effect of DOPA. Finally, these data suggested that the mechanism of the stabilizing effect of DOPA involves more than one distinct step. Even at the very low concentrations tested, DOPA was capable of affecting the stability of the collagen matrix. Molar binding ratios less than 1.0 mole / mole of α chain at these low concentrations effectively precluded the possibility of crossbridge formation through dimerization. Yet, the effect was demonstrable. Vincent and Hillerton⁷⁷ proposed that the insect cuticle becomes insoluble when quinones react with and block hydrophilic lysine side chains, which under physiological conditions would interact with water. DOPA quinone, when bound would expel water and increase the hydrophobicity of the protein due to the phenyl ring. Thus, the matrix would be forced, through hydrophobic interactions to collapse upon itself. In this sense, as in the case of lipids, the hydrophobic groups attempt to shield themselves from the aqueous environment. This same mechanism could have accounted for the effect that DOPA had at the low concentrations. Such hydrophobic bonding forces could have accounted for the gel stabilizing effect of DOPA even at concentrations in the 10^{-5} M range. At higher concentrations of DOPA, the effect was more pronounced. As all DOPA binding sites on the collagen chain became occupied, and an excess of DOPA surrounded these bound groups, I speculate that crossbridging between the bound quinones occurred.

3. The reactions of DOPA during collagen gel stabilization.

Introduction.

In the presence of oxygen and collagen, and at a neutral pH, DOPA is oxidized through a series of spontaneous reactions to form a group of at least three *ortho*-quinones capable of either 1) self polymerization, 2) derivatization of collagen at specific reactive sites, or 3) polymerization with the *ortho*-quinones bound directly to the collagen reactive sites. These processes would lead to the growth of unbound or bound melanin like polymers (Fig. 37). When DOPA is present in a stoichiometric excess with respect to the number of collagen reactive sites, all reactions should affect the final stability of the collagen gel formed.

In the following experiment, the polymerization of DOPA to form melanin like polymers in DOPA-collagen gels was investigated. DOPA-collagen hydrolysates were micro-filtered to remove melanin like granules, and the recovery of non-polymerized DOPA was determined.

Materials and Methods.

3-¹⁴C-DOPA Recovery From DOPA-collagen Hydrolysates.

Buffered pepsin treated collagen solutions were prepared as described in the appendix, transferred in 1.0ml aliquots to parafilm capped tubes, and incubated in

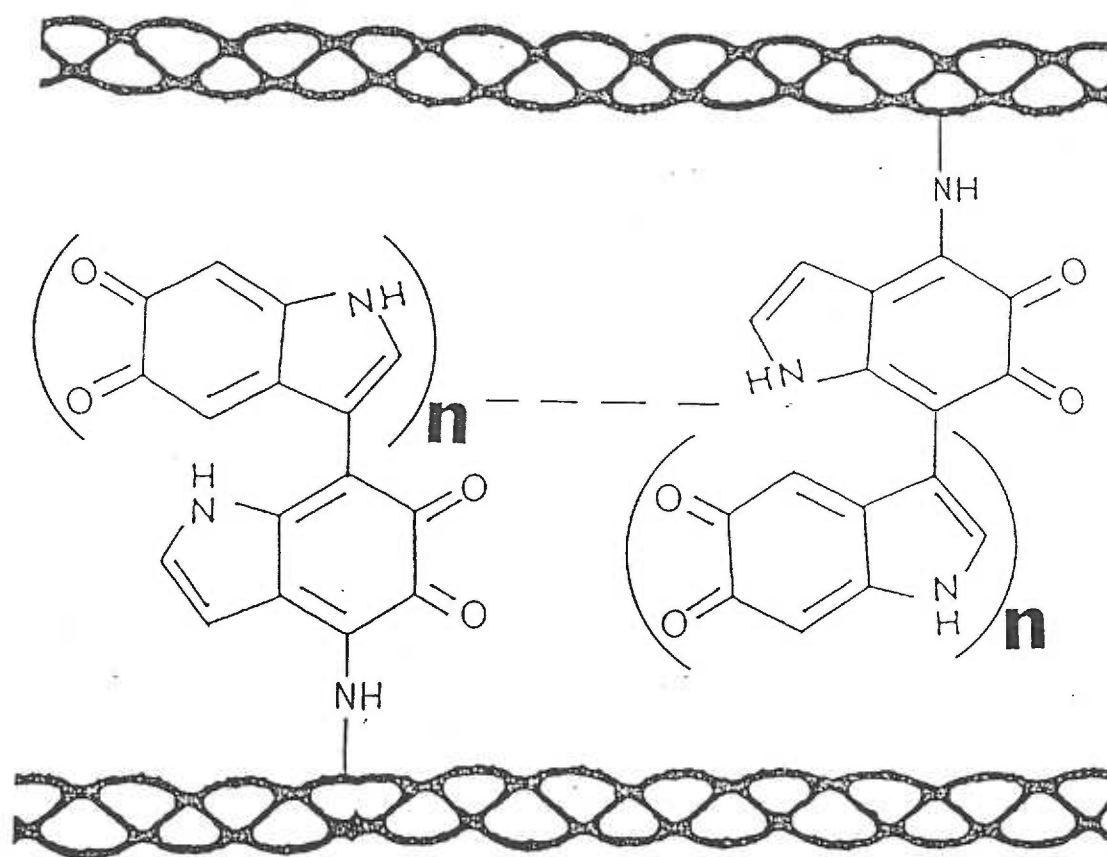


Figure 37. Proposed interaction of collagen bound melanin polymers. In this manner, bound DOPA is hypothesized to react with excess DOPA to form melanin like polymers.

the presence of 1×10^{-3} M DOPA labeled with $0.3 \mu\text{Ci } 3\text{-}^{14}\text{C-DOPA}$ (21mCi/mmol) at 37°C for time periods of 0 hour, 1 hour, 14 hours, 1 day, 3 days, 5 days, 7 days, and 16 days. Following the incubation, the samples were hydrolyzed in 6.0N HCl for 18hrs at 108°C . The hydrolysates were passed through a sterile 0.22μ syringe tip filter, and the supernatants radioassayed by liquid scintillation counting and assayed for collagen content by hydroxyproline analysis (both methods described in appendix).

Results.

The recovery of label with respect to incubation time at 37°C from the hydrolyzed collagen gels is shown in Figure 38. Collagen was consistently recovered at 100% of that in the 0 hour time point solution (not shown graphically).

3-¹⁴C-DOPA Prelabeling of Type I Collagen.

A 100 ml collagen solution was prepared at a concentration of 4.5 mg/ml pepsin treated collagen, 0.135 M NaCl, 2.5 mM acetate, 30 mM phosphate (pH 7.5). To this solution was added $20 \mu\text{Ci } 3\text{-}^{14}\text{C-L-3,4-dihydroxyphenylalanine}$ (21mCi/mole , Amersham). The solution was thoroughly aerated and incubated in the dark at 37°C for 24 hours. The labelling reaction was terminated by adding 10ml of 0.5M acetic acid, and then the solution was cooled to 0°C with stirring for 1 hour to totally disperse the collagen fibrils. The solution was transferred to dialysis tubing (Spectrapor M.W. cutoff = 12kD - 14kD) and exhaustively dialyzed against 5mM

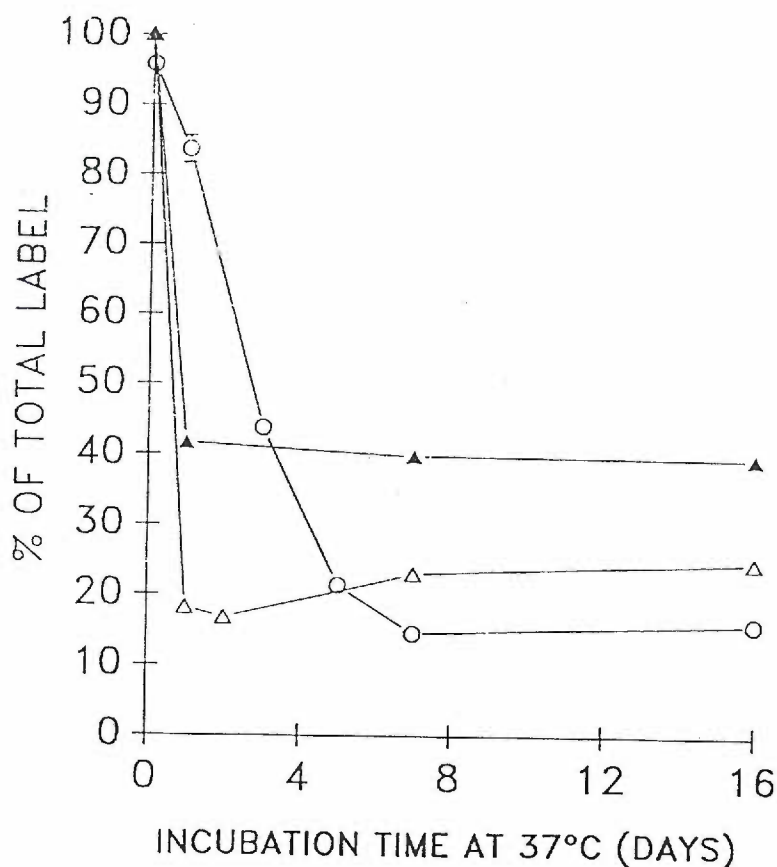


Figure 38. The reactions of DOPA which lead to the formation of melanin like polymers in DOPA-collagen gels.

- (O): Collagen incubated for varying periods of time at 37°C with 3^{14}C -DOPA labelled DOPA.
- (Δ): Collagen prelabelled with DOPA and incubated for varying periods of time at 37°C with unlabelled DOPA.
- (▲): Collagen prelabelled with DOPA, and incubated for varying periods of time at 37°C in the absence of additional DOPA.

Collagen gels were hydrolyzed and the hydrolysates microfiltered to remove melanin-like polymers. The filtrate was radioassayed and the percentage of polymerized and non-polymerized DOPA calculated.

Three replicates were run at each time point. Variation is expressed as the standard error of the mean, and in cases was smaller than the symbol.

acetic acid. An 0.5ml aliquot was lyophilized and analyzed by Gel Filtration HPLC (appendix). Two additional 0.5ml aliquots were analyzed directly by Liquid Scintillation Counting and hydroxyproline assay to calculate a specific activity of binding.

Results.

The HPLC elution of the 3-¹⁴C-collagen is shown in Figure 39. Labeled DOPA co-eluted with the U.V. absorbing collagen peak at the void volume indicating that DOPA and collagen were covalently bound. The specific activity of the collagen was calculated at $5 \times 10^2 \mu\text{Ci}/\text{mg}$ collagen.

Label Recovery From DOPA-collagen Gels Prelabelled with 3-¹⁴C-DOPA.

A Buffered collagen solution was prepared as described in the appendix using the 3-¹⁴C-DOPA labeled collagen solution prepared as described above. 1.0 ml aliquots were incubated either in the presence or absence of cold DOPA at a concentration of $1 \times 10^{-3}\text{M}$. These samples were incubated for periods of 1, 7, and 16 days at 37°C. At the termination of the incubation, all solutions were hydrolyzed in 6.0N HCl at 108°C for 18 hours. The hydrolysates were dried under nitrogen, resuspended in deionized water, and the suspensions filtered through 0.22 μ syringe tip filters. The filtrate was analyzed for collagen content by hydroxyproline analysis (appendix) and radioassayed by liquid scintillation counting (results shown in Figure 39).

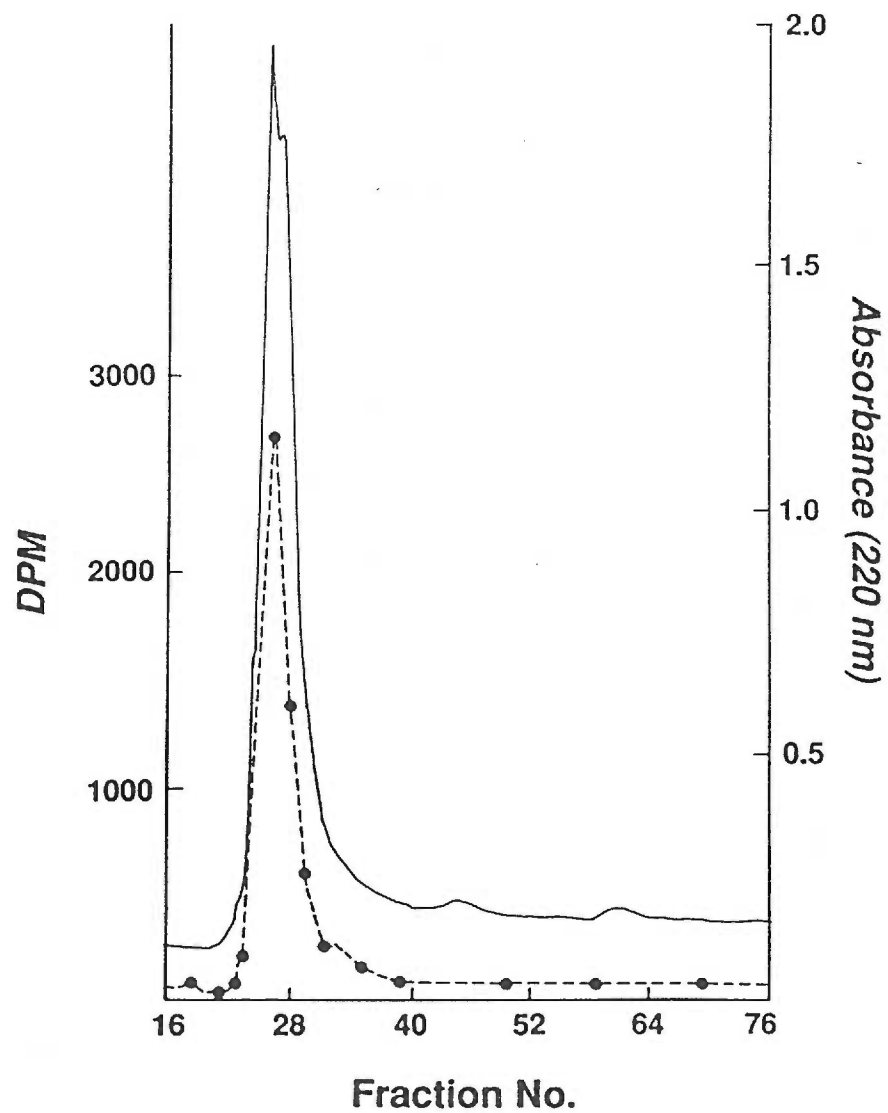


Figure 39. $^3\text{-}^{14}\text{C}$ -DOPA labelled collagen isolated by gel filtration HPLC under denaturing conditions. The absorbance at 220nm (—) and the specific activity of the eluant (---) are shown.

Results.

The recoveries of prebound 3-¹⁴C-DOPA with respect to incubation time at 37°C from the prelabeled DOPA-collagen gels exposed to cold DOPA at a concentration of 1 x 10⁻³M (open triangles), and those not exposed to cold DOPA (closed triangles) is shown in Figure 38. Collagen recovery was consistently 100% of the 0 hour time point solution (not shown graphically).

Discussion.

The interpretation of the results of this experiment is based upon two assumptions. First, acid hydrolysis was assumed not to drive DOPA monomers to polymerize into large melanin-like polymers. Rather, the strong acid conditions precipitated melanin-like polymers which existed in solution prior to hydrolysis. The results support this assumption in that more than 95% of the total DOPA pool is recoverable after one hour of incubation, and the collagen gel showed no visible evidence of melanin formation. However, when the gels became deeply pigmented (24+ hours), indicating the presence of melanin-like polymers, a black granular precipitate resulted from acid hydrolysis, and a smaller percentage of the total DOPA pool was recovered.

The second assumption is that all melanin-like polymers which precipitated upon acid hydrolysis were removed by the micro-filtration step. The radioactivity which remained in solution is ascribed to free, non-polymerized DOPA. Thus, two

pools of DOPA existed. One pool was free, non-polymerized DOPA, which was large at the initiation of the incubation and declined as free quinones added to growing melanin-like polymers. The second, or polymer pool, was very small initially, and was precipitated upon acid hydrolysis and removed by micro-filtration. This second pool increased in size as additional free quinones added to the growing polymers.

When unlabeled collagen was exposed to low specific activity DOPA for varying periods of time and then hydrolyzed, the amount of non-polymerized DOPA recoverable declined in a linear fashion over the first seven days (Fig. 38, open circles). Between 7 and 15 days, 12 - 15% of the original label was consistently recovered. These results reflect the rate of melanin-like polymer formation, the rate of which is limited by the availability of oxygen.

If collagen was initially pulsed with high specific activity DOPA at a low concentration, and then chased with cold DOPA at a concentration of $1 \times 10^{-3}M$, the radioactivity which was recoverable decreased to a minimum after one day of incubation at $37^{\circ}C$ (Fig. 38, open triangles), this result was consistent over the entire 16 days of incubation. The loss of radioactivity from the hydrolysate reflected the polymerization of the DOPA bound directly to collagen binding sites, and subsequent removal by filtration. The consistent recovery of a small percentage of prebound and non-polymerized DOPA following hydrolysis, may have been due to the strongly acidic conditions of hydrolysis which can decompose melanin-like polymers⁹¹, or could have indicated that a percentage of the DOPA bound to collagen was protected from and could not react with the growing melanin-like polymers. This DOPA would have been consistently recovered as soluble monomers

or oligomers bound to lysyl residues. This does not preclude the possibility that these bound monomers could react with other bound monomers to form soluble polymer crosslinks, but inhibit such crosslinks from reacting with the insoluble melanin-like polymers. The manner in which some, but not all of the bound DOPA monomers could be protected from the growing melanin-like polymers is not clear. These monomers may form intramolecular crosslinks between collagen α chains, and could be sterically shielded from reacting with the melanin-like polymers.

Finally, if the high specific activity labeling was not chased with cold DOPA, approximately 38% of the radioactivity was consistently recovered over the entire 16 days of incubation (Fig. 38, closed triangles). The interpretation of these results is that 62% of the DOPA bound directly to collagen reacted to form melanin-like polymers. The ability of excess cold DOPA in the previous experiment to increase the percentage of bound DOPA which polymerized over that in this experiment suggested that the DOPA not directly bound to collagen and the bound DOPA had reacted and polymerized.

If taken together, these three experiments demonstrated that with time, the majority of DOPA in a DOPA-collagen gel, including most of the DOPA bound directly to collagen reactive groups, reacted to form melanin-like polymers. A small percentage of the DOPA which derivatized collagen was consistently non-recoverable and may have formed intramolecular crosslinks sterically shielded from reacting with the growing melanin-like polymers.

In conclusion, this experiment supports the hypothesis that DOPA which has derivatized collagen can react with excess DOPA to form melanin-like polymers. This is a very dynamic system where many reactions occur simultaneously. As

dopaquinone reacts with Lewis bases of collagen, excess *ortho*-quinones of DOPA polymerize to form melanin-like polymers. The *ortho*-quinones bound directly to collagen can react with excess DOPA or preformed melanin-like polymers. The resulting melanin-like polymers bound to collagen can in turn react to form much larger polymers which crosslink adjacent fibrils. The simplest crosslink would be a dimer or melanochrome though the complexity of the crosslink with respect to both the number of subunits involved, and the diversity of *ortho*-quinones should be unlimited. This proposed complexity could explain the gradual increase in tensile strength over a three day period, and the decrease in extensibility of collagen felts with increasing incubation periods demonstrated at an earlier point in this thesis. As the *ortho*-quinones bound directly to collagen are gradually incorporated into the melanin-like polymers, the interconnections between collagen fibrils becomes more complex yielding a stronger yet less extensible matrix. The rate limiting feature of this system may be the oxygen availability. This feature will be addressed in the following study.

4. The Role of Oxygen in DOPA Stabilization of Collagen Gels.

Introduction.

Oxygen is known to play a crucial role in melanogenesis^{87,141}. It provides the key oxidation potential which drives the formation of the highly reactive *ortho*-quinones which are the building blocks of melanin, and which react with amino acid side chains. It follows that, in the absence of oxygen, quinones would not be produced, and unreactive DOPA would be unable to bind to collagen amino acid side chains, and to polymerize into melanin-like polymers. As a result, collagen gel stabilization should be inhibited. The hypothesis that anaerobic conditions inhibit the stabilization of collagen gels with DOPA was tested in this experiment by purging the system of soluble oxygen, and determining the effect on the gel stabilization model discussed previously.

The oxygen requiring enzyme tyrosinase (previously named the phenolase complex by Mason¹⁴¹) catalyzes the oxidation of DOPA to dopaquinone as well as the prior hydroxylation of tyrosine to DOPA. It should, therefore, follow that tyrosinase should be able to not only trigger the stabilizing effect of DOPA when coincubated with DOPA in a buffered collagen solution at 37°C, but it should also accelerate the process. The following study also investigated this hypothesis.

Materials and Methods.

Three buffered pepsin soluble type I collagen solutions (1.47 mg/ml) were prepared. Solution #1 was incubated in the absence of L-DOPA, solution #2 was incubated in the presence of 1×10^{-3} M DOPA, but was deaerated by purging with N_2 for 30 minutes, and solution #3 was again prepared in the presence of 1×10^{-3} M DOPA, and aerated for 30 minutes. 4.0 ml aliquots of each solution were transferred to spectrophotometer tubes (Bausch & Lomb, Inc.) and held at 37°C for 3 hours. Following the incubation, the tubes were immersed in an ice bath. The change in absorbance at 535nm was monitored using a Bausch and Lomb Spec 20 Visible Spectrophotometer over 21 hours.

Two buffered collagen solutions (1.47 mg/ml) were prepared in the presence of 1×10^{-3} M DOPA. To one of the two solutions was added 2200 units/ml of mushroom tyrosinase (2000-4000 units per mg, Sigma Chemical Co.). The solutions were incubated at 37°C for 60 minutes. At the end of this period, the solutions were immersed in an ice bath for an additional 60 minutes. At the surface of the solution containing the tyrosinase, a firm black collagen "cap" remained. This was removed and the solutions were incubated at 37°C for an additional 2 hours. Again the solutions were immersed in an ice bath for one hour, at the end of which time the absorbance at 535 nm was measured using a Bausch and Lomb Spec 20.

Results.

The results of the DOPA-collagen gel deaeration experiment over the first 60 minutes at 0°C is shown in Figure 40. Solution #3, unlike the other two solutions was visibly pigmented. After 21 hours at 0°C, only solution #2 showed an additional decrease in % maximum absorbance to a mean value of 16.7. The results of the tyrosinase experiment are given in the form of an illustration in Figure 41.

Discussion.

The very different effects of aeration and deaeration on the stabilization of the collagen gels was seen both visually and spectrophotometrically. Pigmentation was inhibited in the deaerated DOPA-collagen gel, indicating that melanin-like polymer formation was not occurring to the extent of that in the aerated gel. The important role of oxygen in the collagen gel stabilizing effect of DOPA is plainly demonstrated in Figure 40. Under the deaeration conditions described (and it follows a low pO_2), the collagen gel stability in the presence of DOPA was approximately 20% of that of the aerated gel. Due to the viscosity of the solution, complete removal of oxygen was difficult if not impossible. The lowered O_2 concentration, which remained following the near complete deaeration, was proposed to result in the modest stabilization above that of the control gel.

The initial effect of tyrosinase was to rapidly oxidize DOPA to dopachrome This was demonstrated by the development of the orange chromophore, with a

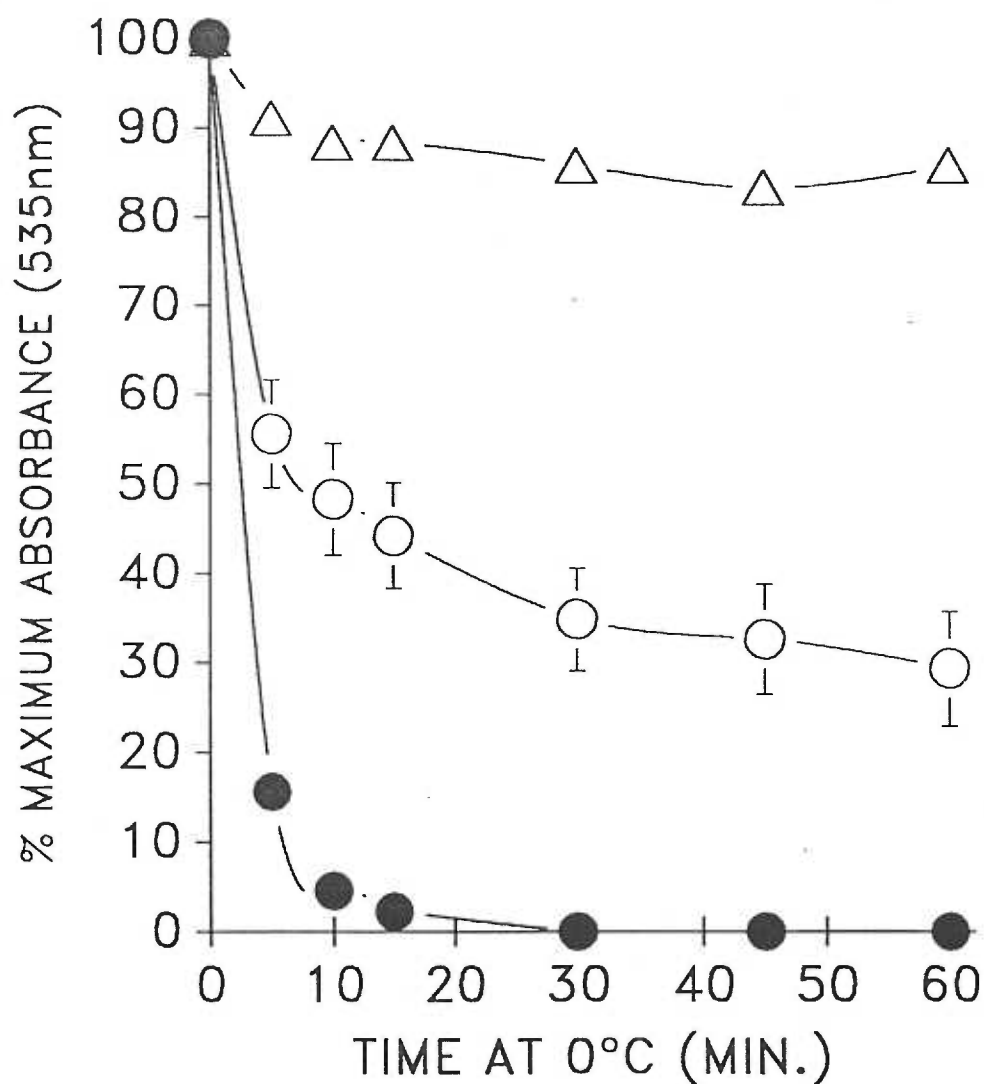


Figure 40. DOPA-collagen gel stability after 3 hours at 37°C under varying conditions of aeration.

- (●): Control-collagen solution aerated for 30 minutes.
- (○): DOPA-collagen solution O₂ purged with a steady stream of N₂ for 30 minutes.
- (△): DOPA-collagen solution aerated for 30 minutes.

Three replicates were run for each sample. Variation is expressed as the standard error of the mean.

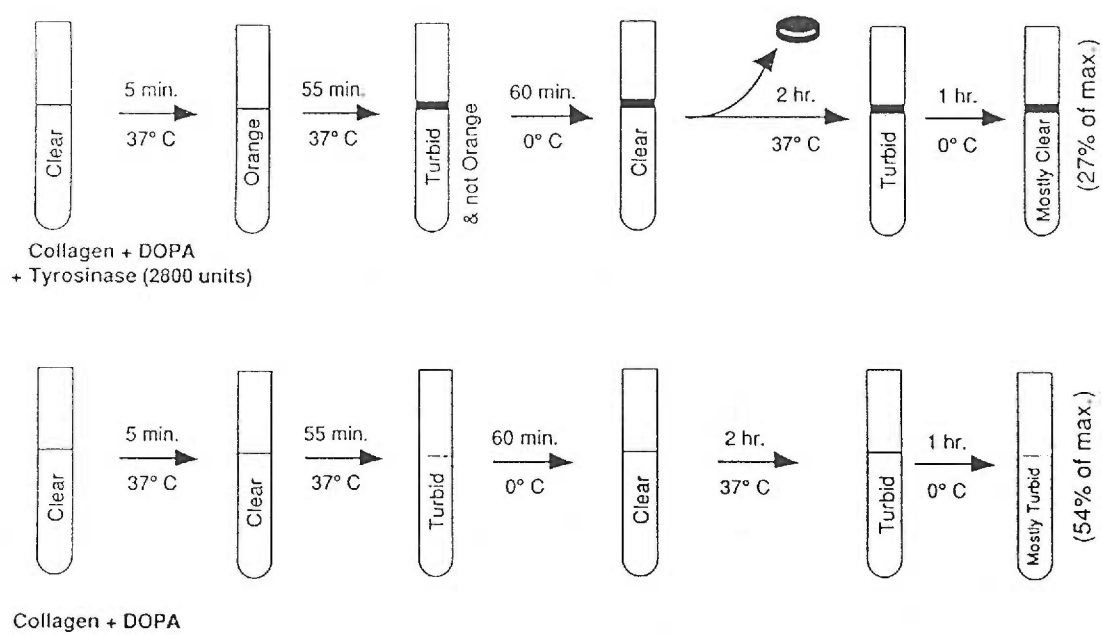


Figure 41. The effect of mushroom tyrosinase on DOPA-collagen gel solutions incubated at 37°C.

visible wavelength maximum of 475nm¹⁴¹, in solution after 5 minutes of incubation at 37°C. When DOPA-collagen solutions were incubated in the absence of tyrosinase, the orange color was not detectable. This may suggest that the oxidation to the quinone was more gradual, and that low concentrations of *ortho*-quinones were immediately absorbed to the collagen matrix and further oxidized, and therefore, a high concentration of free dopachrome never developed in solution. The loss of the orange color after 60 minutes at 37°C indicated that dopachrome had been further oxidized to a non-chromophore melanin precursor.

Again, the importance of oxygen in collagen fibril stabilization was demonstrated in the appearance of a deeply pigmented fibrous disk, or "black cap" at the surface of the DOPA-collagen solution, following incubation at 37°C. As stated above, oxygen drives not only the oxidation of DOPA to dopaquinone, but also the subsequent steps in melanin formation. In rapidly catalyzing the oxidation of DOPA to dopaquinone, tyrosinase may have depleted the collagen solution of dissolved oxygen. If this were the case, then the only source of oxygen for driving melanin-like polymer formation would have been atmospheric oxygen at the surface of the solution. Thus the ability of oxygen to diffuse into the solution was rate limiting in the development of melanin-like polymers and the resulting gel stabilization. The results of this experiment suggested that where oxygen is available, DOPA polymerization and thus collagen gel stabilization is accelerated in the presence of tyrosinase. Oxygen depletion may also explain the decreased level of collagen gel stabilization below the "black cap" of the tyrosinase solution with respect to the control after a total of 4 hours of incubation at 37°C. Although the

precursors of melanin are available in solution, the lack of oxygen inhibited polymer formation, and therefore, collagen gel stabilization.

In summary, the results of this experiment demonstrated that oxygen was required and, in fact, was rate limiting in the DOPA induced stabilization of collagen fibrillar matrices. Oxygen is required to produce the *ortho*-quinones of DOPA which bind to collagen and form the melanin-like polymers which serve as the interfibrillar crosslinks. In the absence of tyrosinase, DOPA oxidation and polymerization was gradual with the rate controlled by the local oxygen partial pressure.

5. Identification of the precursors of melanin in DOPA-collagen solutions.

Introduction.

One of the strategies of investigating the nature of the melanin polymer is to investigate the precursors of melanin. The Raper-Mason pathway developed out of this strategy. The precursors of melanin can be detected by both chemical and spectrophotometric techniques. Decarboxylation can be measured and indicates the production of 5,6-indole-quinone. This is one of at least three *ortho*-quinones which can polymerize to form melanin-like polymers. Thus, decarboxylation is not a required step, but an option in melanin formation. Dopachrome and melanochrome dimers can be identified spectrophotometrically.

In the following experiment, the decarboxylation of and the appearance of dopachrome and melanochrome in DOPA-collagen gels was investigated.

Materials and Methods.

Decarboxylation of DOPA-collagen gels.

A buffered collagen solution was prepared as described in the general methods section, and exposed to $1\text{-}^{14}\text{C}$ -DOPA at a concentration of 1×10^{-3} M, and a specific activity of 5.4 mCi/mmole (Amersham Corp.). Six 2.0ml aliquots of the solution were transferred to separate pieces of 10mm diameter Spectrapor dialysis

tubing (M.W. cutoff = 12kD - 14kD). The samples were air incubated at 37°C for 24 hours, and an evaporation dish containing 5.0ml of hyamine hydroxide (Amersham/Searle Corp.) was placed in the air chamber to capture any CO₂. Following the incubation, the hyamine hydroxide was radioassayed by liquid scintillation counting (described in appendix).

Results.

26.0% of the label in the 1-¹⁴C-DOPA-collagen was recovered in the hyamine hydroxide.

Spectrophotometric analysis of DOPA-collagen gels.

Two buffered pepsin soluble type I collagen solutions were prepared as described in the general methods section, and incubated in quartz cuvettes at 37°C for 5 hours. One of the solutions was exposed to 1 x 10⁻³M DOPA. At different time points (1hr, 3hr, and 5hr) the DOPA-collagen gel was scanned over a wavelength range of 400nm to 650nm, following baseline subtraction of the pepsin treated collagen control gel, with a Hitachi Model 557 Double Wavelength Double Beam Spectrophotometer.

Results.

In Figure 42 the visible wavelength scan between 400 and 650 nm of the DOPA-collagen gel following baseline subtraction is shown for the various incubation time points.

Discussion.

The collagen gel was deeply pigmented and extremely stable. The recovery of radioactivity in the hyamine hydroxide indicated that DOPA had been decarboxylated during gel stabilization. Only 26.0% of the total DOPA was in the decarboxylated form following 24 hours of incubation at 37°C. This was not a surprising finding since it is well accepted that at least two carboxylated *ortho*-quinones derived from DOPA polymerize to form melanin-like polymers.

The visible wavelength scan of the DOPA-collagen gel shows the time dependent appearance of dopachrome and melanochrome during the stabilization process. At 1 and 3 hours, both chromophores were not detectable. However, at 5 hours, both were detectable, though the wavelength maxima were overlapping due to the production of melanin-like polymers which saturate the visible and ultraviolet spectra. The appearance of the melanochrome wavelength maximum indicated the beginning of dimer, and it follows, higher polymer formation. This is an important stage since collagen gel stabilization, I propose, is due to the formation of melanin-like polymer crosslinks between collagen fibrils.

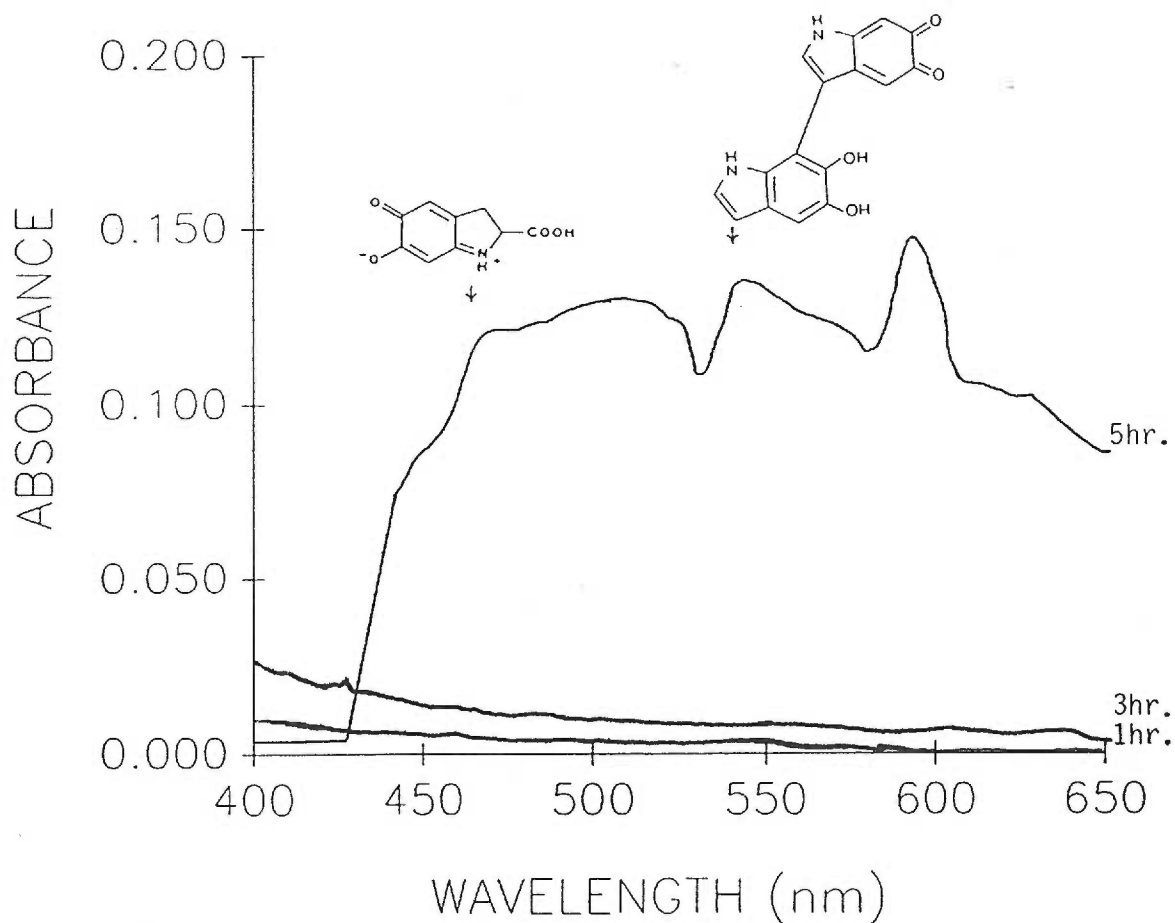


Figure 42. The visible spectrum of a 1×10^{-3} M DOPA-collagen solution (following baseline subtraction of a pepsin-control-collagen solution) after 1, 3 and 5 hours of incubation at 37°C . The absorbance maxima of two of the precursors of melanin are identified by the respective molecular structure.

In summary, this experiment demonstrated the presence of important precursors of melanin-like polymers in DOPA-collagen gels. Dopachrome and the decarboxylated 5,6-indole-quinone can react with Lewis bases to derivatize collagen, and the melanochrome dimer may indicate the production of the simplest of collagen crosslinks. More complex crosslinks can contain both dopachrome and 5,6-indole-quinone as well as the carboxylated form of the latter.

6. Inhibition of catechol polymerization and the effect on collagen gel stability.

Introduction.

To investigate the role of catechol polymerization in crosslink formation, *ortho*-quinones with differing polymerization potentials were chosen. Two such analogs, 4-tert-butylcatechol (TBC) ^{154,155} and 3,5-ditert-butylcatechol (diTBC) are compared structurally with the quinones of DOPA in Figure 43. The presence of large hydrophobic blocking groups around the reactive sites, as well as other structural differences should affect the ability of these compounds to stabilize collagen fibrillar matrices when compared to DOPA. The following experiment investigated the effect of TBC and diTBC on reconstituted collagen fibrils. Many of the methods used in determining the effect of DOPA on fibrillar stability were used in this study, and a comparison with DOPA was made. In comparing the effect of diTBC with other *ortho*-quinones, a concentration was chosen at which all were soluble. DiTBC was the least soluble of those tested, with a limiting concentration of $5 \times 10^{-5}M$, though even at this concentration, 0.5% ethanol was required.

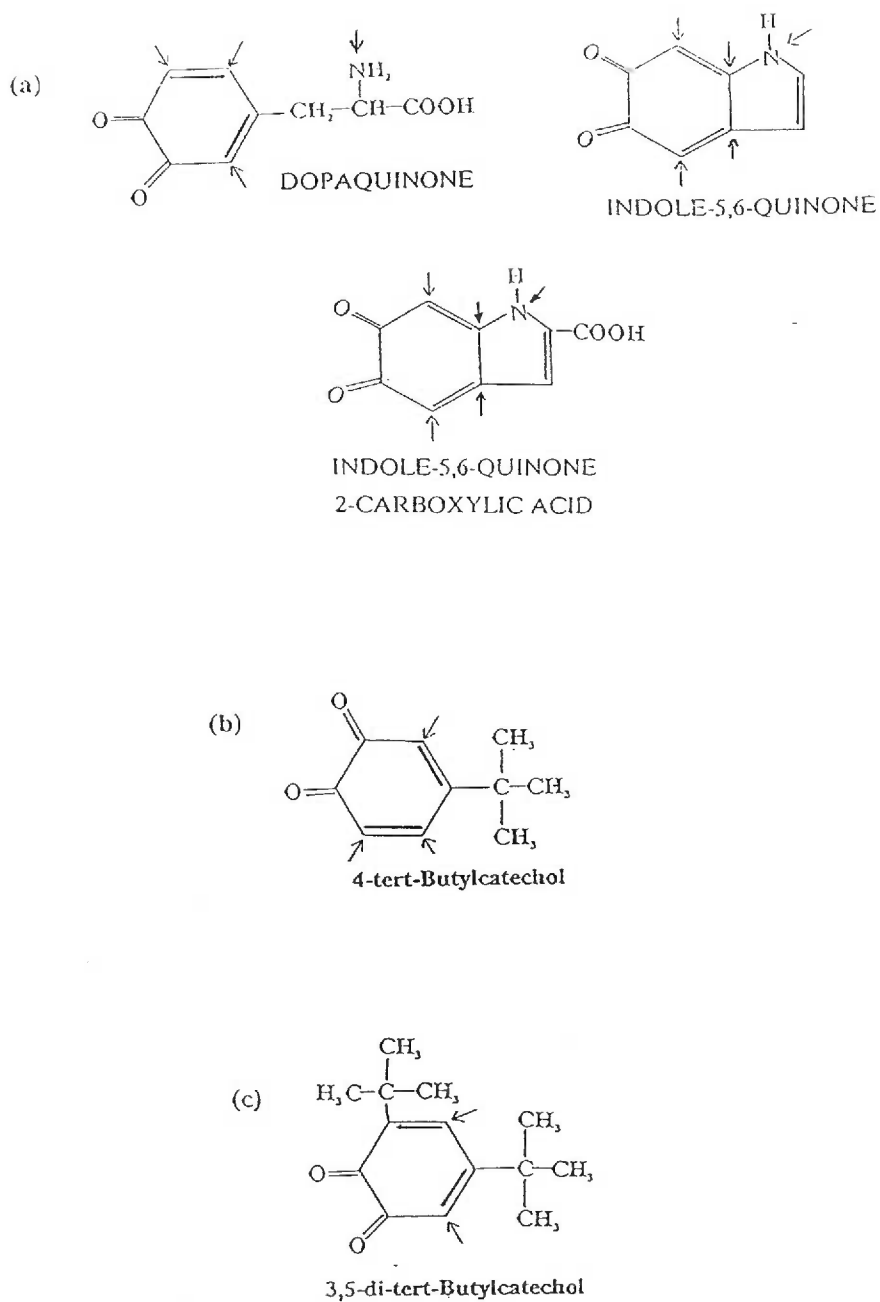


Figure 43. Comparison of the molecular structures of the orthoquinones of (a) **DOPA**, (b) **4-*tert*-butylcatechol**, and (c) **3,5-di-*tert*-butylcatechol** with identification of the reactive polymerization/protein interaction sites (denoted by \downarrow).

Materials and Methods.

4-tert-butylcatechol Binding Assay.

Two 8.0ml buffered collagen solutions were prepared as described in the general methods section of this thesis. 4-tert-butylcatechol (Aldrich Chemical Co.) was added to one of the solutions at a concentration of 1×10^{-3} M. Both solutions were incubated and gelled (the TBC exposed collagen gel was completely stable) at 37°C for 24 hours, followed by cooling at 4°C for 7 days. The samples were homogenized, heated to 100°C for one hour, and the protein precipitated in 95% ethanol. The protein was centrifuged, and the pellet washed with 95% ethanol four additional times. The residual ethanol was removed by heating for 20 minutes at 100°C, and the precipitated protein from the TBC and control solutions were heated to 100°C in 2.0ml deionized water. The samples were transferred to quartz cuvettes and the TBC sample scanned against the control between 260 and 500nm using a Perkin Elmer 557 Double Wavelength Double Beam Spectrophotometer. A buffered 1×10^{-3} M TBC solution was scanned over the same wavelengths.

Collagen Gel Stability.

A buffered pepsin soluble type I collagen solution was prepared in the presence of 1×10^{-3} M 4-tert-butyl catechol. Three 4.0 ml aliquots were transferred to Bausch and Lomb spectrophotometer tubes and assayed for gel stability as

described in the appendix of this thesis. The 37°C incubation period was 24 hours and the 0°C incubation period was 60 minutes.

Buffered pepsin soluble type I collagen solutions were incubated in the presence of either DOPA, Catechol, 4-tert-butylcatechol or 3,5 ditert-butylcatechol (K&K Laboratories) at a concentration of 5×10^{-5} M. The solutions were prepared in buffered saline (0.125 M NaCl, 2.5 mM acetate, 30 mM phosphate) and contained 0.5% ethanol. 4 ml aliquots from each solution were transferred to Bausch and Lomb spectrophotometer tubes. The samples were held at 37°C for 18 hours and then immersed in an ice bath for 24 hour period during which time the change in optical density was monitored.

Collagen Gel Solubility.

Six 1.0 ml aliquots of the 4-tert-butylcatechol-collagen solution were transferred to Spectra/por 10mm dialysis tubing (MW cutoff = 12kD -14kD). The membranes were sealed and incubated in a humidified air incubator at 37°C for 24 hours. At the end of the incubation period, the samples were exhaustively dialyzed against phosphate buffered saline [0.125 M NaCl, 30 mM phosphate (pH 7.5)].The collagen gels were removed from the dialysis membrane and assayed for collagen solubility (appendix).

The destabilized collagen gels incubated at 5×10^{-5} M with the catechol derivatives, were homogenized in 15 ml 0.5 M acetic acid then transferred to 50 ml high speed centrifuge tubes. The homogenates were assayed for collagen solubility.

Tensile Strength.

Multiple 6.0ml aliquots of the 4-tert-butyl catechol-collagen solution were transferred to 60 x 15mm covered glass Pyrex petri dishes, which had been preheated to 37°C in a foil covered still air model Hova-Bator incubator. Following incubation, the gelled solutions were flash frozen in liquid nitrogen and lyophilized overnight. The resulting "felts" were cut into 2.0 x 3.5 as samples which were tested for tensile strength as described in Part II of this thesis. An additional 1 day TBC-collagen felt was cut into 1.0 x 0.4cm strips which were tested for shrinkage temperature by the method also previously described.

Multiple 6.0 ml aliquots of the 3,5-ditert-butyl catechol and DOPA-collagen solutions were transferred to 60 x 15 mm covered Pyrex petri dishes and incubated for time periods of 1, 8, 10, and 25 days at 37°C in a Still Air Model Hova-Bator incubator. Following incubation, the samples were flash frozen with liquid nitrogen and lyophilized. The resulting felts were cut into several 20 x 35mm samples and tested for tensile strength as described previously.

Results.

The results of the TBC binding assay are shown in Fig. 44, and will be discussed below.

The TBC-collagen gel formed was pigmented a deep yellow. The gel

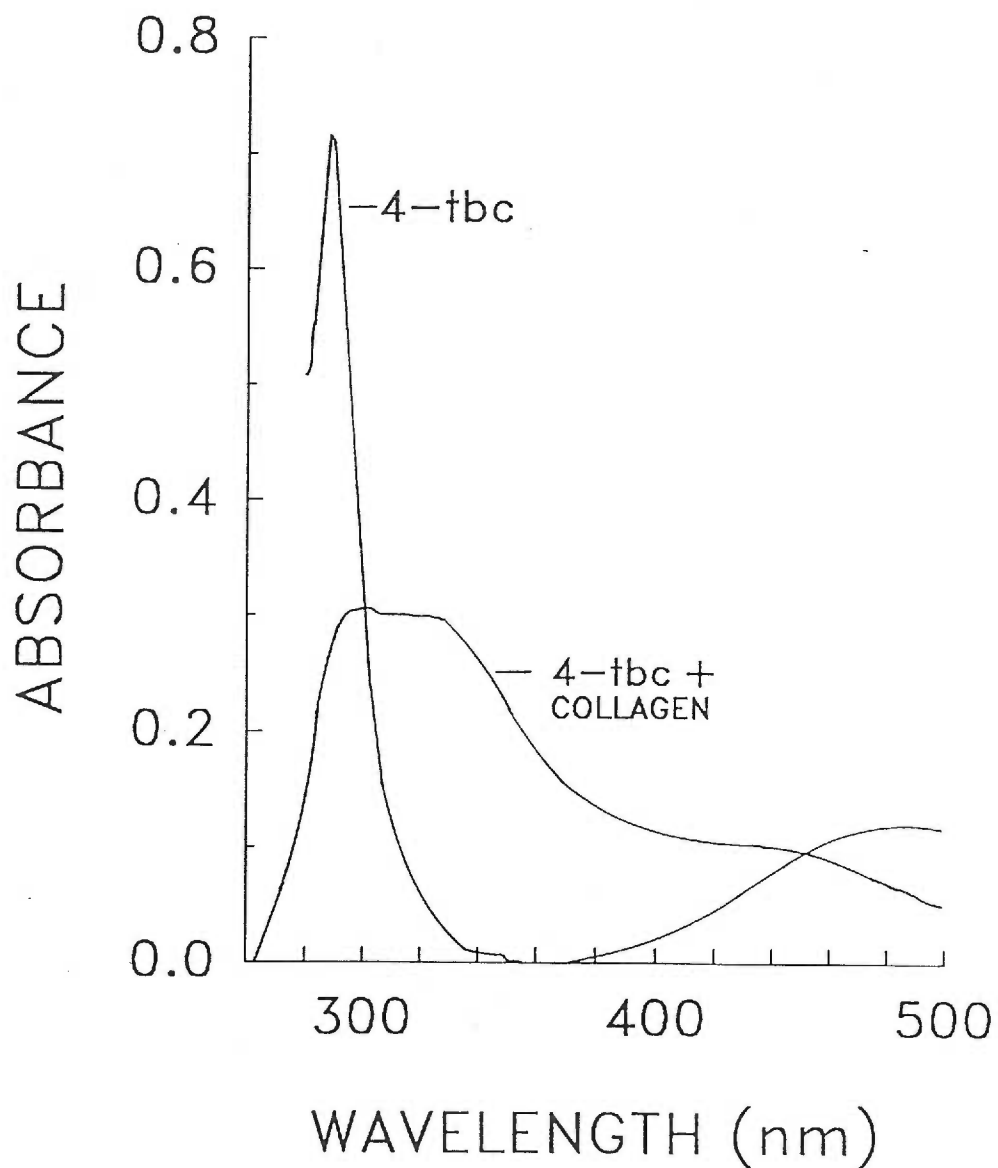


Figure 44. Ultraviolet-visible spectrum of 4-tert-butyl catechol bound collagen prepared as described in the text, and 4-tert-butyl catechol ($1 \times 10^{-3}M$) in phosphate buffered saline, following control-collagen baseline subtraction.

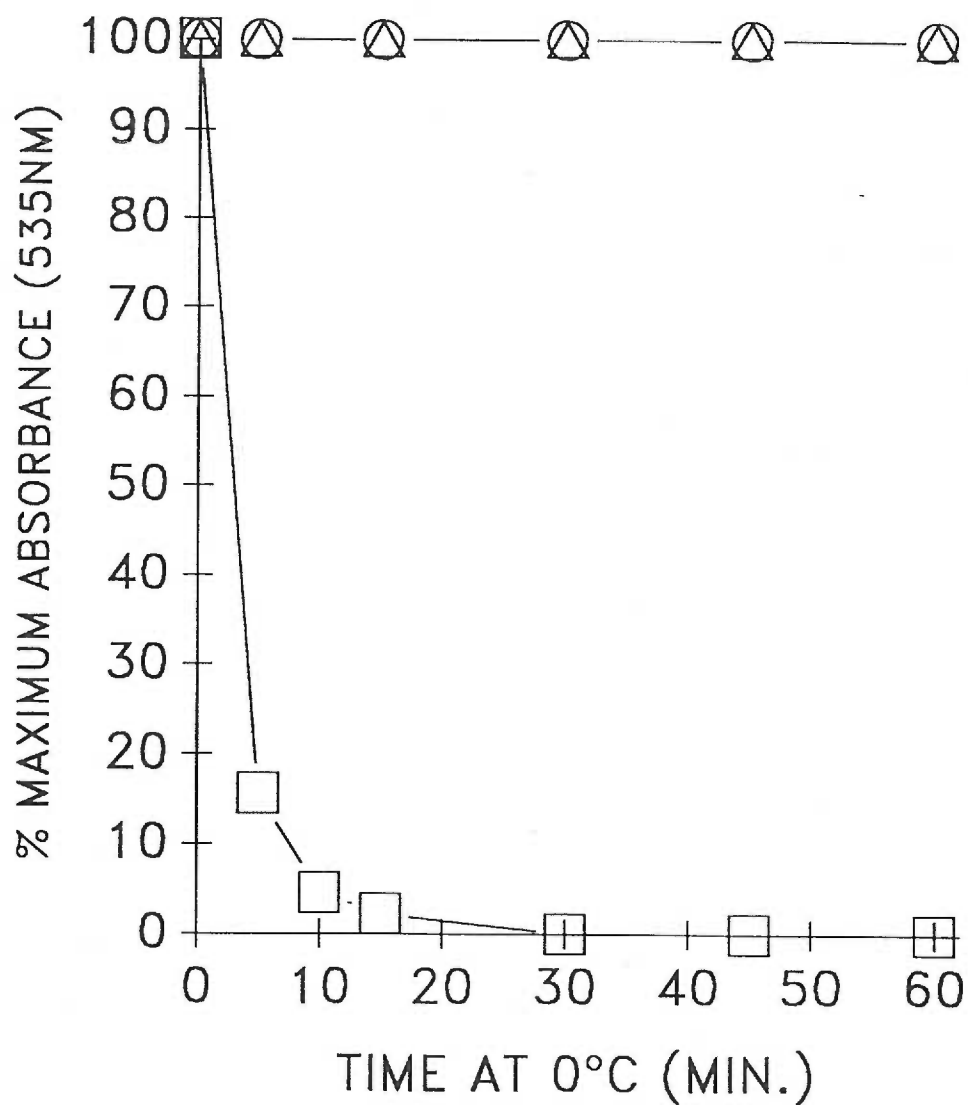


Figure 45. The stability of $1 \times 10^{-3}M$ TBC-collagen (Δ), DOPA-collagen (\circ), and control-collagen gels (\square) after 24 hours of incubation at $37^{\circ}C$.

stabilizing effect of 4-tert-butyl catechol is demonstrated in Figure 45, and it can be seen that TBC exposed collagen gels are completely stable and will not degel. The gel stabilizing effect of lower concentrations ($5 \times 10^{-5}\text{M}$) of TBC, as well as DOPA, catechol, and diTBC is shown in Figure 46. Pigmentation of these gels was far less than noted at higher concentrations. At this concentration catechol, DOPA, and TBC showed similar results whereas diTBC seemed less effective.

Figure 47 gives the solubility data of the $1 \times 10^{-3}\text{M}$ TBC-collagen gels following 24 hours of incubation at 37°C . It appears that TBC and DOPA were equally effective in causing insolubility in cold acetic acid but at 100°C , the TBC exposed collagen gel was completely soluble. The solubility data for the collagen exposed to reagents at $5 \times 10^{-5}\text{M}$ is represented in the form of a bar graph (Fig. 48).

The shrinkage temperature of the TBC felt, incubated for 1 day, was 59.3°C with a standard error of 0.3°C (not shown graphically). The wet tensile properties of the TBC samples were compared with that of 10^{-3}M DOPA-collagen felts prepared in an identical fashion (Fig. 49). Again it was evident that the effect of TBC is equivalent to or even exceeded that of DOPA. The tensile strengths of the DOPA and diTBC samples prepared at a concentration of $5 \times 10^{-5}\text{M}$ are given in terms of Load/Width at Maximum Breaking Load in Figure 50. The control values were also plotted for sake of comparison against baseline tensile strength. While the effect of diTBC is significantly greater than control, there is no difference between the 1 day and 10 day time points. Progressive increases were, however, seen with DOPA even at these low concentrations.

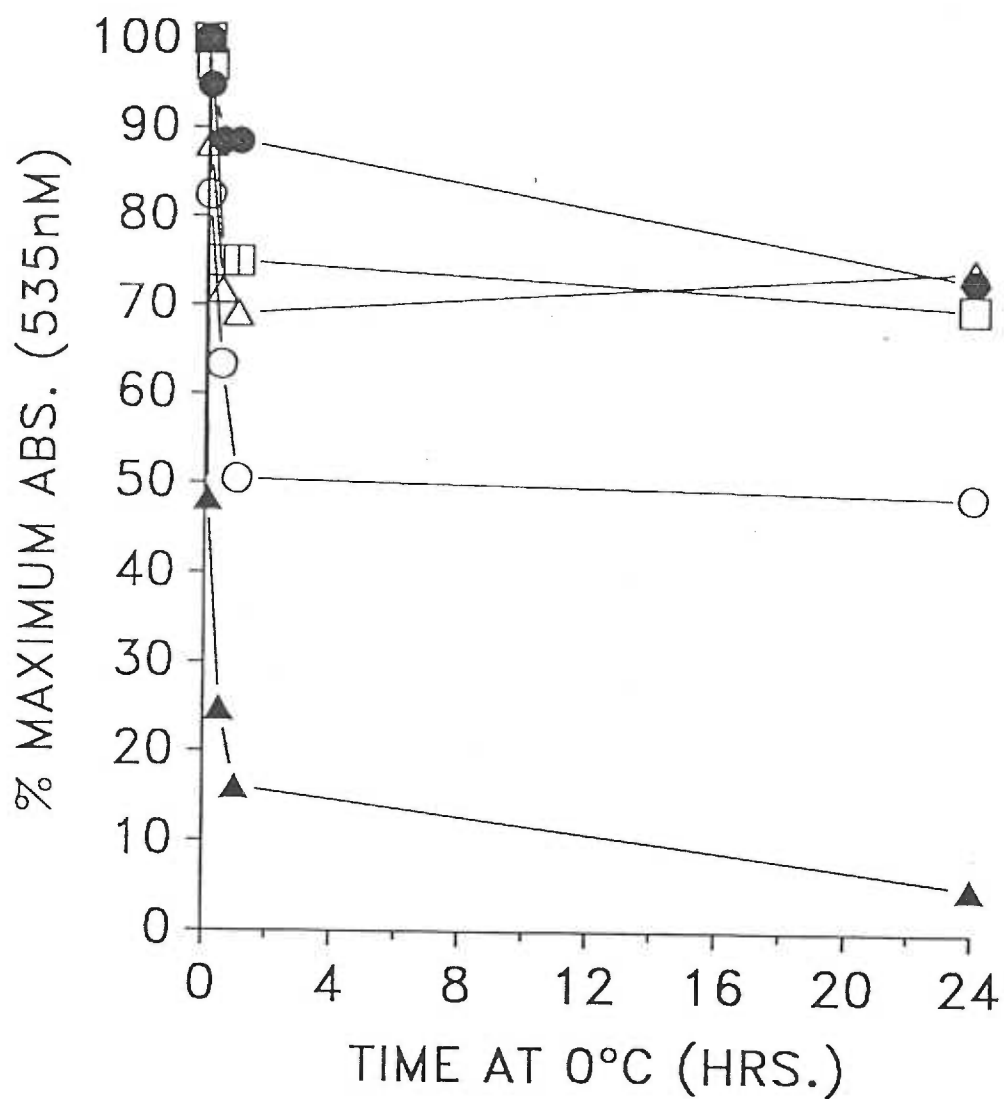


Figure 46. The stability of collagen gels exposed to various catechol derivatives at a concentration of $5 \times 10^5 \text{M}$ for 24 hours at 37°C .

- ▲ - Control Collagen Gel
- - 3,5-ditert-butylcatechol
- - 4-tert-butylcatechol
- △ - Catechol
- - DOPA

Three replicates were run at each time point and the results are expressed as the mean of these values.

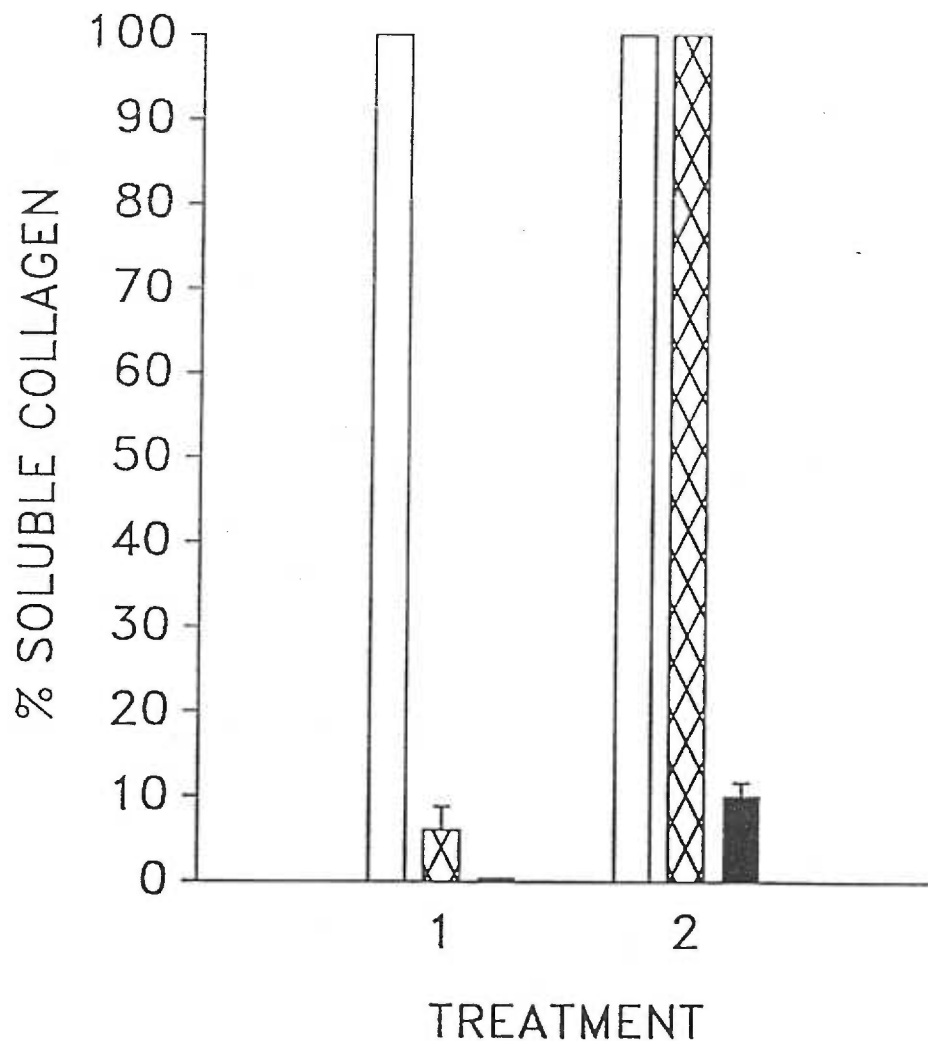


Figure 47. The solubility of 1×10^{-3} M TBC-collagen (▣), DOPA-collagen (■), and control collagen (□) gels following 24 hours of incubation at 37°C. The solubility in 0.5M acetic acid at 4°C for 12 hours (treatment 1), and in 0.01M acetic acid at 100°C for 2 hours (treatment 2) are shown.

Three replicates were run for each sample. Variation is expressed as the standard error of the mean.

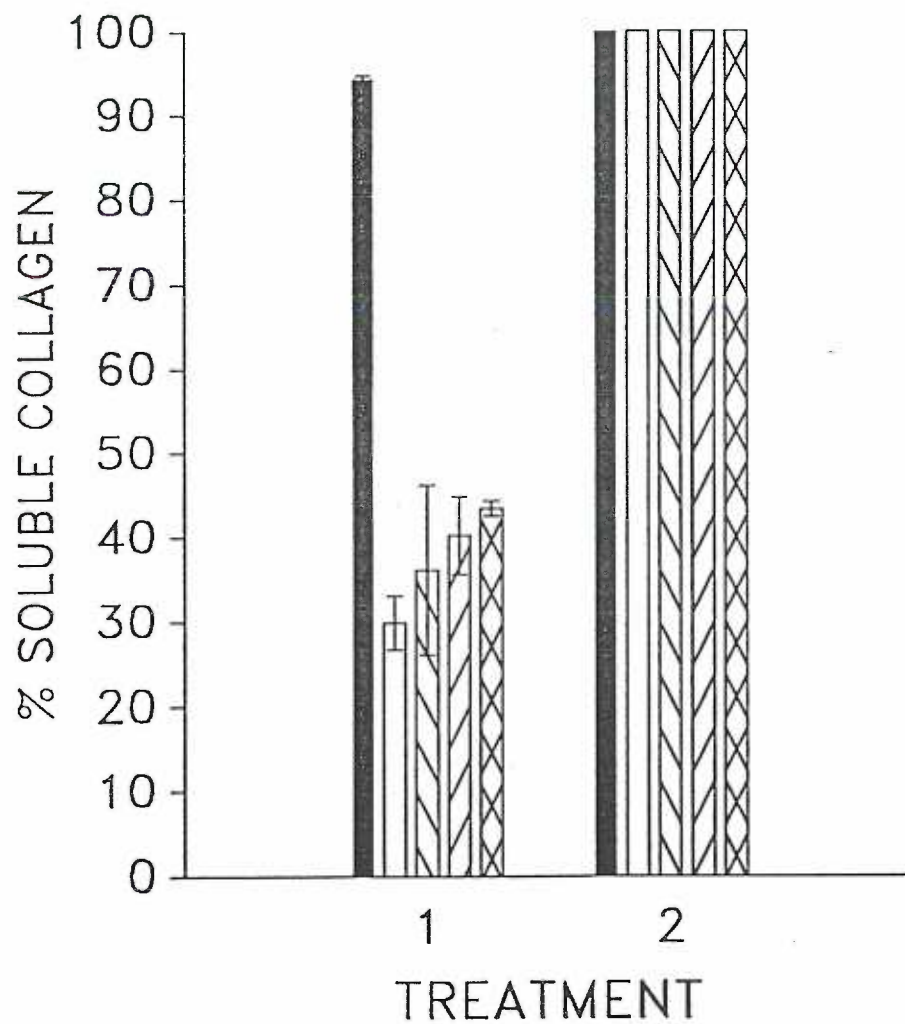


Figure 48. The solubility of collagen gels exposed to various catechol derivatives at a concentration of $5 \times 10^{-5}M$ for 24 hours at $37^{\circ}C$. The solubility in 0.5M acetic acid at $4^{\circ}C$ for 12 hours, and in 0.01M acetic acid at $100^{\circ}C$ for 2 hours are shown for each derivative.

- ⊠ - DOPA
- ▧ - Catechol
- ▨ - 4-tert-butylcatechol
- - 3,5-ditert-butyl catechol
- - control

Three replicates were run for each sample. Variation is expressed the standard error of the mean.

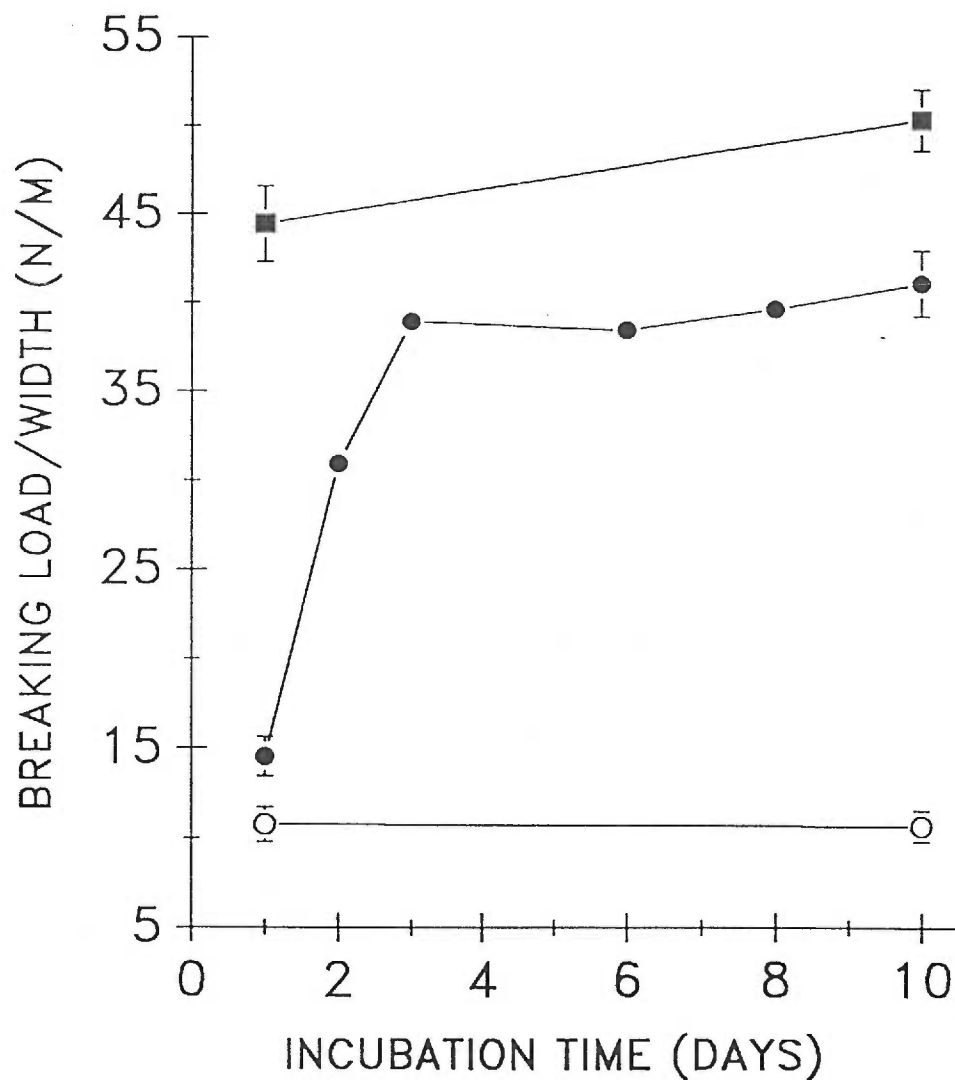


Figure 49. A comparison of the wet tensile strengths of 4-tert-butyl catechol-collagen (■) DOPA-collagen (●), and pepsin control-collagen (○) felts. over 10 days of incubation at 37°C.

A minimum of six replicates were run at the 1 and 10 day time points and the error is expressed in terms of the standard error of the mean. Two to four replicates were run at the 2,3,6 and 8 day time points and the results are expressed as means with no indication of error.

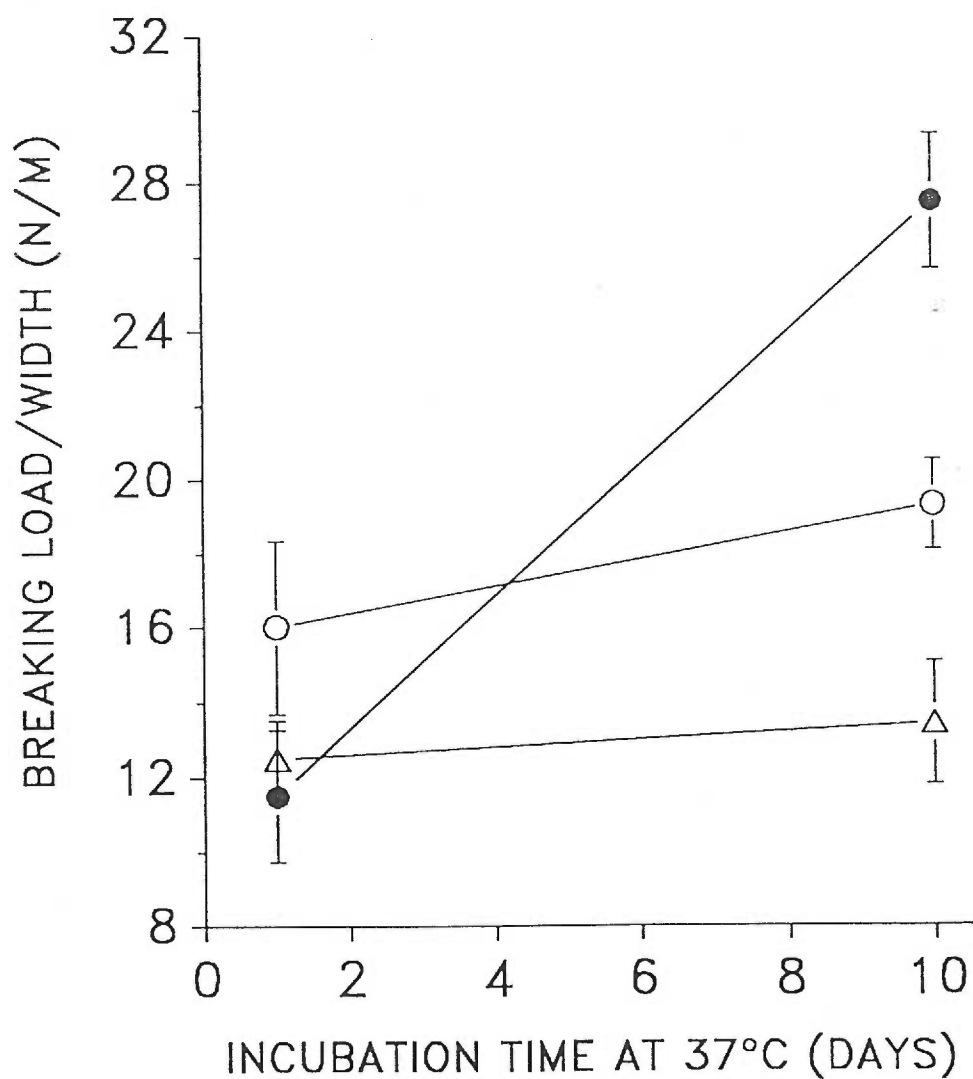


Figure 50. A comparison of the wet tensile strengths of collagen felts exposed to 3,5-ditert-butyl catechol (O) and DOPA (●) at a concentration of 5×10^{-5} M, and control-collagen felts (Δ) of 10 days of incubation at 37°C.

A minimum of six replicates were run at both time points for each sample. Variation is expressed the standard error of the mean.

Discussion.

TBC-collagen gels did not degel at 0°C and were insoluble in acetic acid at 4°C. They were, unlike DOPA-collagen gels, quite soluble at 100°C and the explanation for this paradox is based upon the structural comparisons of the two compounds, shown in Figure 43. TBC has a *para*-oriented tert-butyl group. The molecular structure and chemistry is otherwise similar to that of DOPA. TBC, through a single oxidation reaction, can be converted to the highly reactive quinone form. Once formed, ring positions adjacent to the two quinoidal functional groups as well as the 5-carbon become Lewis acids which can react with any available Lewis base. However, the tert-butyl functional group, which is bulky and quite hydrophobic should limit access to the adjacent reactive site. Lewis bases of proteins should bind less efficiently to this site, but would not be totally blocked. The lack of a similar bulky group adjacent to the other reactive site, allows free access. Thus, the overall decrease in binding affinity is probably minimal, and in fact as Figure 44 demonstrates, TBC (abs. max. 294-314nm) did bind to collagen, and the adduct formed was stable under denaturing conditions. Therefore, TBC and DOPA appeared to form covalent adducts with collagen at approximately the same rate.

TBC quinones can form polymers by a mechanism similar to that of DOPA polymerization, as was indicated by the deep yellow pigmentation of the TBC-collagen gels. The absence of the alanine group of DOPA limits the number of

reactive quinones which can be formed from TBC. DOPA-melanin is a heteropolymer of three *ortho*-quinones, dopaquinone, 5,6-indole quinone, and indole-5,6-quinone-2-carboxylic acid (Fig. 43), whereas TBC derived polymers are homopolymers of the quinone of TBC. Limiting the diversity of the monomers, would result in a decreased complexity of the polymer structure formed, and crosslinking would be limited to long chains rather than complex branched structures as occur with DOPA derived melanins. This decreased complexity, I propose, may explain the solubility differences between DOPA and TBC exposed gels. A complex 3-dimensional and hydrophobic polymer such as DOPA-melanin would limit the access of water to the protein matrix, limiting protein solubility.

Whereas the crosslink complexity of TBC polymers was decreased by the absence of the alanine group, the rate of polymer, and thus, crosslink formation seemed to be enhanced. The results of the tensile strength experiment in Figure 49 demonstrate that the rate of gain in the tensile strength of TBC-collagen felts is increased with respect to that of DOPA. The tensile strength of TBC-collagen felts was at a maximum following 1 day of incubation at 37°C. DOPA-collagen felts attained a maximum tensile strength only after an additional two days of incubation. These results support the observation of Bentley and Fellman¹⁵⁶ that the stability of catechol-collagen gels was greater than DOPA-collagen gels after 4 hours of incubation at 37°C, though these authors did not test for insolubility and tensile strength. The explanation of these results may be based upon the oxygen

requirement of catechol gel stabilization described in an earlier experiment. Each reaction in the conversion of DOPA to the three *ortho*-quinones which comprise the melanin-like polymer requires oxygen. TBC has the same requirement though the amount of oxygen consumed is less since only a single oxidation reaction is required to produce the sole quinone of TBC polymers. The production of DOPA-polymers may simply deplete the available oxygen, as did the tyrosinase catalyzed oxidation of DOPA to dopachrome. Thus, the rate limiting factor would be the diffusion of atmospheric oxygen into the gel.

The maximum tensile strength of TBC-collagen gels was comparable to and appeared even to exceed that of the DOPA-collagen gels. Similarly, the shrinkage temperature of TBC-collagen gels after 1 day of incubation at 37°C was nearly at the level of DOPA-collagen gels. Thus, like DOPA, TBC enhanced the physical properties of collagen fibrillar matrices through the formation of polymer crosslinks.

The catechol derivative 3,5-ditert-butylcatechol, pictured in Figure 43, differs from 4-tert-butylcatechol in that an additional bulky and hydrophobic tert-butyl group has been added to the ring. Also, the positions on the catechol ring to which the group has been added have shifted. One group inhabits one of the strategic reaction sites, and the other group lies adjacent to the other. Ring carbon number 4 is also a potential Lewis acid, but is effectively shielded by the two bulky tert-butyl groups. The result is two-fold. First, Lewis base addition can occur at only one site on the ring. Second, the remaining reactive site, the six carbon position, is slightly less accessible to addition due to the steric hindrance and the hydrophobic nature of the adjacent tert-butyl group at position five on the ring. These features

provide an unique tool for studying the role of polymerization in crosslink formation. Since one potential reactive site is available, diTBC can react with and derivatize proteins. However, this reaction is "suicidal" in the sense in that following binding, the *ortho*-quinone is no longer reactive. Therefore, protein crosslinking is inhibited.

As pointed out earlier, diTBC is insoluble at concentrations above $5 \times 10^{-5}M$ and it is, thus, difficult to make exact comparisons between this compound and DOPA since the effect of this latter compound has been shown to be concentration dependent. However, even at this lower concentration, 3.2 moles of the *ortho*-quinones were available for every 1 mole of collagen α chain (stoichiometry based upon initial concentrations). Depending upon the efficiency of reaction, enough moles of *ortho*-quinone would be bound to the protein to allow the formation of crosslinks. Thus, if the *ortho*-quinone was an effective crosslinking agent, an effect would be detectable at this concentration.

The gel stability data for the collagen gels incubated in the presence of all catechol derivatives at this low concentration (Fig. 46) shows that all of the putative ligands used in this experiment were capable of stabilizing reconstituted collagen fibrils to a certain extent, though diTBC seemed less effective. Similarly all the ligands decreased the solubility of collagen gels in cold 0.5M acetic acid with respect to control, though all were completely soluble in boiling 0.01M acetic acid. Again diTBC was the least effective at decreasing the gel solubility.

The clearest contrast between DOPA, a potential crosslinking agent, and diTBC, an agent incapable of forming crosslinks is found in the tensile strength data in Figure 50. It is evident in this figure that the tensile strength of diTBC-collagen felts, though significantly greater than control levels, did not increase over a 10 day

incubation period. The wet tensile strength of DOPA-collagen felts prepared at the same concentration increased from control values to three times that of control and approximately twice that of the diTBC felts over the same incubation period. One might speculate that over a 10 day time period, more and more DOPA crosslinks will form simply due to the increased probability of reaction with time. In the case of diTBC, no reaction was possible once the monomer was bound, and therefore an increase in tensile strength would not have been expected.

It is curious that diTBC had any effect at all on the stability of collagen fibrillar matrices in light of the structural considerations discussed above. Vincent and Hillerton's ⁷⁷ matrix dehydration mechanism of quinone tanning of the insect cuticle could provide an explanation, however. DiTBC monomers can bind covalently to hydrophilic lysine ϵ -amino groups and the quinoidal groups of monomers and dimers can interact with additional amino acid side chains through weak hydrogen bonds, and in doing so expel water from about these groups. The consequence would be a partial dehydration, collapse, and compaction, and resultant stabilization of the matrix. It is in fact, part of my hypothesis that the initial effect (observed as gel stabilization) of bound DOPA monomers occurs via a dehydration of the matrix. Higher levels of stability (observed as insolubility and elevated tensile strength) are brought about by the subsequent formation of dimer and higher polymer crosslinks between these bound monomers.

This experiment has, therefore, provided supporting evidence of a polymer crosslinking model of DOPA-collagen matrix stabilization. Structural modifications

which enhanced the rate of polymer formation were found to enhance the rate of attaining higher levels of matrix stability, and those which inhibited crosslinking inhibited stabilization greater than that brought about by matrix dehydration.

7. Summary.

The previous set of experiments have provided evidence of a polymerization model of DOPA crosslink formation in collagen fibril stabilization. DOPA stabilized collagen gels over a wide concentration range. It appeared that at a binding ratio of 1 mole of DOPA per mole of collagen α chain, DOPA was capable of stabilizing collagen gels. At ratios below this critical value, large decreases in the gel stability suggested that a dimer rather than a monomer may represent the actual structure of the crosslink. As the number of collagen binding sites were exceeded, excess *ortho*-quinones were available to be oxidized and to interact with bound DOPA to form a melanin-like polymer structure. These increasingly complex interactions could cause a gradual increase in the tensile properties, and a decrease in the extensibility of the collagen fibrillar matrix. It, however, appeared that a small percentage of the DOPA which was bound was protected from interacting with this melanin-like structure, and may in fact have been involved in intramolecular crosslinking of collagen α chains.

Oxygen was shown to be essential for gel stabilization to be achieved. Oxygen provides the oxidation energy required to produce the precursors of melanin-like polymers and to drive polymerization of these precursors. Tyrosinase, which catalyzes the oxidation of DOPA to dopaquinone, accelerated collagen gel stabilization in an oxygen rich environment.

Decarboxylation of DOPA-collagen gels indicated the synthesis of one of the *ortho*-quinone subunits of melanin, 5,6-indole quinone, and the appearance of two

visible wavelength absorbing precursors of melanin during collagen gel stabilization provided further support of a melanin-like polymer crosslinking model of collagen gel stabilization.

The stabilization of collagen gels associated with crosslink formation was inhibited by the addition of hydrophobic blocking groups at the reactive polymerization sites of catechol, a DOPA analogue. Tert-butyl groups added to the 3 and 5 ring positions of catechol decreased the stability as well as the degree of insolubility of reconstituted collagen fibrils. Also, the tensile strengths of collagen matrices prepared in the presence of this catechol derivative were not enhanced as was the case for DOPA treated collagen matrices. Addition of a single blocking group at the *para*-position of catechol decreased neither the collagen gel stability, nor the tensile strength. In fact, the rate of increase in the tensile strength of 4-tert butyl catechol matrices with respect to DOPA-collagen matrices prepared under the same conditions, was greater, due likely to the simple one step oxidation of TBC-quinone prior of polymer formation. DOPA, on the other hand, has a much higher oxygen requirement to produce the multiple *ortho*-quinone subunits of melanin-like polymers. The rate phenomenon may, therefore, be dependent upon the oxygen availability in solution. TBC treated collagen felts, unlike the felts exposed to DOPA, were completely soluble in boiling acetic acid. This difference was due to the decrease in complexity of the TBC polymer crosslink with respect to DOPA-melanin-like polymers.

V. CONCLUSIONS AND SIGNIFICANCE OF RESULTS.

The hypothesis tested in this thesis was that DOPA and other catechol derivatives stabilize collagen fibrils through what is a two step mechanism. In step 1, *ortho*-quinones bind covalently to lysine side chains, and in doing so cause a dehydration, collapse and compaction with a resulting stabilization of the collagen matrix. In step 2, the bound *ortho*-quinones polymerize with excess *ortho*-quinone to form melanin-like covalent crosslinks. At the beginning of this thesis, three questions were posed to test this hypothesis. The first question was what effect did DOPA exposure have on the stability of collagen fibrillar matrices. The second question was what is the mode by which *ortho*-quinones interact with collagen. This question was broken down into three specific questions: is the interaction of a covalent nature, to what reactive groups of collagen does DOPA bind, and where along the collagen molecule are these reactive groups located? The final question posed was how do bound DOPA monomers form covalent crosslinks between collagen molecules to produce a stable fibrillar matrix. In the following pages, these three questions will be addressed through a summary of the experimental results which have been previously discussed.

DOPA exposure stabilized collagen fibrillar matrices. When collagen fibrils were prepared in the presence of 1×10^{-3} M DOPA, the effect was dramatic. Collagen gels exposed to DOPA for 24 hours at 37°C were highly insoluble even when autoclaved in dilute acetic acid. The gels were also resistant to cyanogen bromide digestion conditions designed for total tissue extraction¹¹². DOPA also

enhanced the physical properties of pepsin treated collagen matrices. Maximum shrinkage temperature and wet tensile strength of collagen felts prepared in the presence of 1×10^{-3} M DOPA were significantly higher than control felts. The shrinkage temperature was, in fact, comparable to that of rat tail tendons. These changes in stability were not associated with a change in the collagen fibrillar structure. D-banding appeared normal at the E.M. level.

The stabilizing effect of DOPA was consistently time dependent. Collagen gel stability increased in what appeared to be gradual manner between 1.5 hours and 24 hours of incubation. At least a one hour lag period occurred in which DOPA did not stabilize the collagen gels, which was indicative of a biphasic process in which DOPA bound to collagen and then formed crosslinks. The shrinkage temperature of DOPA collagen gels also increased over a 24 hour period. The tensile strength, on the other hand, increased to a maximum over three days. Finally, DOPA-collagen felt extensibility increased to a maximum value after four days of incubation, followed by a decrease to below control values following ten days of incubation at 37°C. These results were consistent with polymerization model of crosslink formation in which bound *ortho*-quinones derived from DOPA reacted to form dimers and other higher melanin-like polymers. The decrease in the extensibility, we propose, resulted from the increase in the complexity of the crosslinking polymer. As dimer crosslinks became incorporated into the growing polymer, the ability of crosslinked collagen fibrils to achieve a parallel alignment was inhibited, with a resultant decrease in the extensibility.

DOPA bound covalently to what appeared to be specific lysine side chains of collagen molecules. It was possible to demonstrate that DOPA formed irreversible

interactions with collagen fibrils formed in its presence and also with soluble collagen. The products formed were covalently modified collagen molecules stable under denaturing conditions. Lysine was implicated as the amino acid which binds DOPA by demonstrating the ability of poly-L-lysine, and the inability of polypeptides lacking free amino groups, to bind covalently with DOPA. Additional evidence showed a two to three residue per α chain decrease in the amino acid composition of DOPA-collagen hydrolysates. These results agreed with the molar binding value of 2.3 to 3.0 moles of DOPA per mole of collagen α chain after 72 hours of incubation at 4°C. Taken together, these results supported a limited number of reactive lysine residues within the collagen molecule, which bind DOPA. The binding value of 21.4 moles of DOPA bound per collagen α chain obtained when collagen was exposed to excess DOPA for extended periods of time represented melanin-like polymers bound at three specific lysine residues.

Cyanogen bromide peptide mapping also supported the existence of a small population of reactive lysyl binding sites. The $\alpha 1(I)CB6$ peptide which contains one of the two crosslinking residues of the helical region, appeared to have a high affinity for DOPA. On the other hand, the $\alpha 1(I)CB3$ peptide, which has a higher lysine content than does the $\alpha 1(I)CB6$ peptide, appeared to bind DOPA poorly, if at all.

The *ortho*-quinone derived from DOPA, once bound to the collagen molecule, polymerized into a melanin-like crosslink structure. This was the conclusion drawn from the experiments presented in Part III of the experimental section of this thesis. Under the conditions of fibril formation employed throughout this thesis, melanin-like polymer formation occurred readily. It was, therefore, not surprising that this

process would play a role in the DOPA induced collagen gel stabilization phenomenon described in Part I of the experimental section. The DOPA effect was shown to be concentration dependent. Collagen gel stability and solubility declined dramatically at molar binding values below one mole of DOPA per collagen α chain. The reaction of bound DOPA to form melanin-like polymers occurred rapidly whereas the production of melanin occurred over a 7 day time period. These results supported the hypothesis that bound *ortho*-quinones formed melanin-like polymer crosslinks, and that the overall process of gel stabilization was based upon the polymerization of both bound and excess DOPA. Gel stabilization was, therefore, dependent upon the oxygen availability in solution.

The structure of melanin has proven elusive, and is based in large part upon the structure and chemistry of melanin precursors described by Raper⁸⁷ and Mason⁸⁸. The role of catechol polymerization in collagen gel stability could not be studied directly because the putative crosslinks could not be isolated. Thus, an indirect approach was pursued where evidence of the production of the melanin precursors was sought and catechols with differing polymerization potentials were investigated for the ability to stabilize collagen matrices.

Oxygen was shown to be required for gel stabilization to occur. Oxygen provides the oxidation potential necessary for the production of the reactive *ortho*-quinones which are the precursors of melanin-like polymers. Tyrosinase, an enzyme which catalyzes the oxidation of DOPA to dopaquinone, enhanced the rate of stabilization at the surface of collagen gels where oxygen was plentiful. On the other hand, the oxygen in solution had been depleted and polymerization and gel stabilization was diminished. *ortho*-quinones are Lewis acids which react with Lewis

bases of collagen in a derivatization process. As long as oxygen is available, these bound *ortho*-quinones could polymerize and stabilize the matrix.

Spectrophotometric analysis of DOPA-collagen gels demonstrated the production of dopachrome and melanochrome, both precursors of melanin. The timing of synthesis coincided roughly with the gel stabilization data with time presented in Part I of the experimental section. The decarboxylation of DOPA was also measurable in DOPA-collagen gels and indicated the synthesis of another of the precursors of melanin-like polymers.

In general, collagen fibrillar matrices exposed to 4-*tert*-butylcatechol, a catechol capable of binding to collagen and forming less complex polymeric crosslinks, were stabilized to the same degree as matrices exposed to DOPA. Only the solubility was increased due to the decreased complexity of the polymer formed.

Blocking groups which inhibit polymer formation appeared to eliminate the effect of the catechol derivative, 3,5-ditert-butylcatechol (diTBC) on the wet tensile strength of exposed collagen felts, after ten days of incubation at 37°C. DOPA-collagen gels, prepared at the same concentration, did cause an increase in the wet tensile strength. DOPA can, of course, self polymerize following binding to collagen. Taken together, these results give support to a polymerization model of crosslink formation.

The gel stability and solubility of diTBC-collagen gels, following one day of incubation at 37°C, were comparable with that of unblocked analogues. This result may be more indicative of binding, than of crosslink formation. Vincent and Hillerton ⁷⁷ proposed that quinone-protein tanning was caused by a matrix dehydration mechanism. Interaction of *ortho*-quinones with hydrophilic protein side

chains, which normally interact with water, would expel water causing a dehydration of the protein matrix. The matrix would be forced to collapse inward, forming a more stable matrix. diTBC is capable of binding through a single unblocked, but slightly hindered reactive site. The binding of diTBC, as well as DOPA, to collagen lysine side chains could, in this manner, dehydrate and stabilize the matrix. Crosslink formation, if possible, would further stabilize the matrix. This enhanced stability would be evident in dramatic increases in gel insolubility, and increases in tensile strength.

In conclusion, DOPA and other unblocked catechols are proposed to stabilize collagen fibrillar matrices by first being oxidized to the *ortho*-quinone form and then binding to collagen reactive groups. Binding of a high enough level results in dehydration and stabilization of the matrix. Once bound, the *ortho*-quinones react to form melanin-like crosslinks. It is in this final form that the extreme characteristics of collagen gel stability, which have been described, are exhibited. These include insolubility in boiling acid, high tensile strength and thermal stability, and decreased extensibility of the matrix. In Figure 51, the simplest form of a DOPA-collagen crosslink is shown. This melanochrome dimer crosslink of two indole-5,6-quinone subunits could be replaced by much larger polymers comprised of at least three types of *ortho*-quinone subunits derived from DOPA. Catechols other than DOPA form polymeric crosslinks with differing degrees of complexity. Changes in complexity alter the properties of the exposed matrix. The complexity and resultant stability of the crosslinks formed make their isolation difficult. Attempts have been made, though have to this point proven uninformative. Future

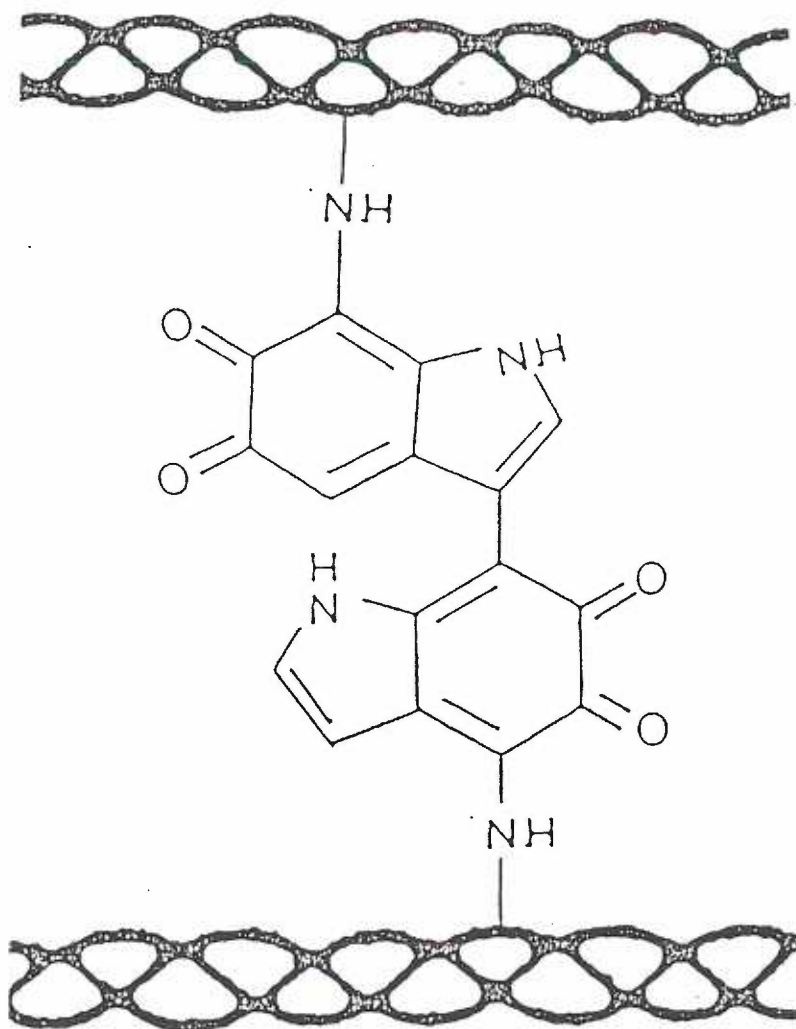


Figure 51. The proposed structure of the simplest (dimer) DOPA crosslink between collagen molecules. Higher polymeric structures, though not shown, are possible.

studies will attempt to derivatize collagen with DOPA at much lower molar concentration and again to isolate the crosslinks with a limited number of subunits.

How might the conclusions drawn from this thesis be practically applied? DOPA may be used as a crosslinking agent in the development of stable biological prostheses such as heart valves and artificial skin. Crosslinking agents currently used, such as glutaraldehyde, create problems due to toxicity. DOPA, on the other hand, is a natural metabolic compound which has been applied in high doses to Parkinson's patients with only limited side effects, and melanin is a non-antigenic macromolecule. Both of the attributes would make the DOPA crosslinking model a favorable one for physiological use.

Another possibility which is currently being investigated in this lab is the efficacy of DOPA as an *in vivo* crosslinking agent. DOPA stabilized intact collagen fibrils though the effect was not as pronounced as when fibrils were formed in the presence of DOPA. DOPA-exposed collagen felts had elevated thermal stability and were insoluble in dilute acid at 4°C. These results suggest that DOPA could have much the same effect *in vivo*.

We are currently determining the effect that high doses of DOPA have on poorly crosslinked collagen. A β -aminopropionitrile induced lathyrism in rats is being treated with DOPA. Changes in collagen solubility of the treated tissue is being determined. Depending upon the outcome of these types of studies, we could envision DOPA being used to crosslink abnormal collagen produced in various disease states such as Ehlers Danlos type VI ^{29,30} and VII ^{32,36} and cutis laxa ³⁴.

VI. REFERENCES.

1. Buxman MM, Wuepper KD. Keratin cross-linking and epidermal transglutaminase. A review with observations on the histochemical and immunochemical localization of the enzyme. *J Invest Dermatol* 1975; 65:107-112.
2. Kühn K. In: Furthmayr H, ed. *Immunochemistry of the Extracellular Matrix*. Boca Raton, Fla.: CRC Press, 1982:1-29.
3. Bentley JP. Aging of collagen. *J Invest Derm* 1979; 73(1):80-83.
4. Pinnell SR. The cross-linking of collagen and elastin: Enzymatic conversion of lysine in peptide linkage to α -amino adipic- δ -semialdehyde (allysine) by an extract from bone. *Proc Nat Acad Sci USA* 1969; 61:708-714.
5. Tanzer ML. Experimental lathyrism. *Inter Rev Conn Tissue Res* 1965; 3:91-112.
6. Robins SP, Bailey AJ. Age related changes in collagen. The identification of reducible lysine-carbohydrate condensation products. *Biochem Biophys Res Commun* 1972; 48:76-84.
7. Eyre DR, Paz MA, Gallop PM. Cross-Linking in collagen and elastin. In: Richardson CC, Boyer PD, Meister A, eds. *Annual Review of Biochemistry*. Palo Alto, California: Annual Reviews, Inc., 1984:717-748.
8. Tanzer ML. Crosslinking. In: Ramachandram GN, Reddi AH, eds. *Biochemistry of Collagen*. New York: Plenum Press, 1976:137-162.
9. Eyre DR, Glimcher MJ. Analysis of a crosslinked peptide from calf bone collagen - evidence that hydroxylysyl glycoside participates in crosslink. *Biochem Biophys Res Commun* 1973; 52:663-71.
10. Robins SP, Bailey AJ. Relative stabilities of intermediate reducible crosslinks present in collagen fibers. *FEBS Lett* 1973; 33:167-71.
11. Robins SP, Bailey AJ. The chemistry of collagen crosslinks: The mechanism of stabilization of the reducible intermediate crosslinks. *Biochem J* 1975; 149:381-385.
12. Verzar F. The aging of collagen fibers. *Experientia [Suppl]* 1956; 4:35-41.
13. Robins SP, Shimokomaki M, Bailey A. The chemistry of the collagen cross-links. Age related changes in the reducible components of intact bovine collagen fibres. *Biochem J* 1973; 131:771-780.

14. Volpin D, Giro MG, Castellani I, Peserico A. Age related changes in the reducible cross-links of human dermis collagen. *Dermatologica* 1977; 155:335-339.
15. Bailey AJ, Shimokomaki MG. Age related changes in the reducible cross-links of collagen. *FEBS Lett* 1971; 16:86-88.
16. Bailey AJ, Ranta MH, Nicholls AC, Partridge SM, Elsdon DF. Isolation of α -aminoadipic acid from mature dermal collagen and elastin. Evidence for an oxidative pathway in the maturation of collagen and elastin. *Biochem Biophys Res Commun* 1977; 78:1403-1410.
17. Fujimoto D, Akiba K, Nakamura N. Characterization of a fluorescent material in bovine achilles-tendon collagen. *Biochem Biophys Res Commun* 1977; 76:1124-29.
18. Fujimoto D, Moriguchi T. Pyridinoline, a non-reducible crosslink of collagen. Quantitative determination, distribution, and isolation of a crosslinked peptide. *J Biochem (Tokyo)* 1978; 83:863-67.
19. Fujimoto D, Moriguchi T, Ishida T, Hayashi H. Pyridinoline, a non-reducible crosslink of collagen - quantitative determination, distribution, and isolation of a crosslinked peptide. *Biochem Biophys Res Commun* 1978; 84:52-57.
20. Henkel W, Glanville RW, Greifendorf D. Characterization of a type-I collagen trimeric cross-linked peptide from calf aorta and its cross-linked structure. Detection of pyridinoline by time-of-flight secondary ion-mass spectroscopy and evidence for a new cross-link. *Eur J Biochem* 1987; 165:427-436.
21. Robins SP, Duncan A. Cross-linking of collagen. Location of pyridinoline in bovine articular cartilage at two sites of the molecule. *Biochem J* 1983; 215:175-182.
22. Fujimoto D, Moriguchi T. Pyridinoline, a non-reducible crosslink of collagen. Quantitative determination, distribution, and isolation of a crosslinked peptide. *J Biochem (Tokyo)* 1978; 83:863-867.
23. Eyre DR, Koob TJ, Van Ness KP. Quantitation of hydroxypyridinium crosslinks in collagen by high-performance liquid chromatography. *Anal Biochem* 1984; 137:380-388.
24. Sakura S, Fujimoto D, Sakamoto K, Mizuno A, Motegi K. Photolysis of pyridinoline, a cross-linking amino acid of collagen, by ultraviolet light. *Can J Biochem* 1982; 60:525-529.
25. Robins SP, Bailey AJ. Chemistry of collagen crosslinks: Characterization of fraction C, a possible artifact produced during reduction of collagen fibers with borohydride. *Biochem J* 1973; 135:657-65.

26. Bernstein PH, Mechanic GL. A natural histidine-based imminum cross-link in collagen and its location. *J Biol Chem* 1980; 255:414-422.
27. Housley T, Tanzer ML, Henson E, Gallop PM. Collagen crosslinking: Isolation of hydroxyaldol-histidine, a natural occurring crosslink. *Biochem Biophys Res Commun* 1975; 67:824-830.
28. Mechanic GL, Katz EP, Henmi M, Noyes C, Yamauchi M. Locus of a histidine-based, stable trifunctional, helix to helix collagen cross-link: stereospecific collagen structure of type I skin fibrils. *Biochemistry* 1987; 26:3500-3509.
29. Pinnell SR, Krane SM, Kenzora JE, Glimcher MJ. A heritable disorder of connective tissue. Hydroxylysine-deficient collagen disease. *N Engl J Med* 1972; 286:1013-1020.
30. Eyre DR, Glimcher MJ. Reducible crosslinks in hydroxylysine-deficient collagens of a heritable disorder of connective tissue. *Proc Natl Acad Sci (Wash)* 1972; 69:2594-2598.
31. Verzar F. Das Altern des Kollagens. *Helvetica Physiologica et Pharmacologica Acta* 1956; 14:207-220.
32. Bailey AJ, Lapiere CM. Effect of an additional peptide extension of the N-terminus of collagen from dermatosparactic calves on the cross-linking of the collagen fibres. *Eur J Biochem* 1973; 34:91-96.
33. Kuivaniemi H, Peltonen L, Palotie A, Kaitila I, Kivirikko KI. Abnormal copper metabolism and deficient lysyl oxidase activity in a heritable connective tissue disorder. *J Clin Invest* 1982; 69:730-733.
34. Byers PH, Narayanan AS, Bornstein P, Hall JG. An X-linked form of cutis laxa due to deficiency of lysyl oxidase. *Birth Defects* 1976; 12:293-298.
35. Soskel NT, Watanabe S, Hammond E, Sandberg LB, Renzetti AD Jr, Crapo JD. A copper-deficient, zinc-supplemented diet produces emphysema in pigs. *Am Rev Respir Dis* 1982; 126:316-325.
36. Lichtenstein JR, Martin GR, Kohn LD, Byers PH, McKusick VA. Detecting conversion of procollagen to collagen in a form of Ehlers-Danlos Syndrome. *Science* 1973; 182:298-300.
37. McMurray CH. Copper deficiency in ruminants. *Ciba Found Symp* 1980; 79:183-207.
38. Narayanan AS, Siegel RC, Martin GR. On the inhibition of lysyl oxidase by β -amino-propionitrile. *Biochem Biophys Res Commun* 1972; 46:745-748.

39. Levene CI, Gross J. Alteration in state of molecular aggregation of collagen induced in chick embryos by β -amino propio nitrile. *J Exp Med* 1959; 110:771-790.
40. Wirtschafter ZT, Bentley JP. Extractable collagen in the normal and aneurysmal aorta. *Arch Path* 1965; 79:635-640.
41. Peacock EE, Madden JW. Some studies on the effect of beta-aminopropionitrile on collagen in healing wounds. *Surgery* 1966; 60(1):7-12.
42. Wang JH. Chemical modification of active sites in relation to the catalytic mechanism of F1. *J Bioenerg Biomembr* 1988; 20:407-422.
43. Kaiser ET, Lawrence DS, Rokita SE. The chemical modification of enzymatic specificity. *Annu Rev Biochem* 1985; 54:565-595.
44. Coleman JE, Oakley JL. Physical chemical studies of the structure and function of DNA binding (helix-destabilizing) proteins. *CRC Crit Rev Biochem* 1980; 7:247-289.
45. Maeda H. Chemical modification of anticancer agents for improved properties: Towards macromolecular therapeutics and prospects. *Tanpakushitsu Kakusan Koso* 1988; 33:211-216.
46. Sternson LA. The application of chemical derivatization to clinical drug analysis. *Xenobiotica* 1987; 17:385-396.
47. Richardson T. Chemical modifications and genetic engineering of food proteins. *J Dairy Sci* 1985; 68:2753-2762.
48. Glazer AN. The chemical modification of proteins: Group- and site-specific reagents. In: Neurath H, The Proteins. Volume II. New York: Academic Press, Inc., 1975:226-287.
49. Koenig RJ, Cerami A. Synthesis of hemoglobin A1c in normal and diabetic mice: Potential model of basement membrane thickening. *Proc Natl Acad Sci USA* 1975; 72:3687-3691.
50. Perejda AJ, Uitto J. Nonenzymatic glycosylation of collagen and other proteins: relationship to development of diabetic complications. *Coll Relat Res* 1982; 2:81-88.
51. Bienkiewicz K. Physical chemistry of leather making. Malabar, Florida: Robert E. Krieger Publishing Co., 1983: 325-366.
52. Chvapil M, Kronenthal RL, Van Winkle W. Medical and Surgical Applications of Collagen. In: Hall DA, Jackson DS, eds. *International Review of Connective Tissue Reseach*. New York: Academic Press, 1973:1-61.

53. Cheung DT, Nimni ME. Mechanism of cross-linking of proteins by glutaraldehyde. I. Reaction with model compounds. *Connect Tissue Res* 1982; 10:187-189.
54. Cheung DT, Nimni ME. Mechanism of crosslinking of proteins by glutaraldehyde. II. Reaction with monomeric and polymeric collagen. *Connect Tissue Res* 1982; 10:201-216.
55. Cheung DT, Nimni ME. Mechanism of crosslinking of proteins by glutaraldehyde. III. Reaction with collagen in tissue. *Connect Tissue Res* 1984; 13:109-115.
56. Bowes JH, Cater CW. The formal titration for the determination of E-amino groups substituted in modified collagens. *Biochim Biophys Acta* 1968; 168:353-355.
57. Cater CW. Glutaraldehyde tannages. *J Soc Leather Trade Chemists* 1967; 52:236-239.
58. Tomimatsu Y, Jansen EF, Gaffield W, Olsen AC. Physical chemical observations on the -chymotrypsin glutaraldehyde system during formation of an insoluble derivative. *J Colloid Interface Sci* 1971; 36:51-55.
59. Hardy PM, Hughes GJ, Rydon HN. Formation of quarternary pyridinium compounds by the action of glutaraldehyde on proteins. *J C S Chem Comm* 1976; 5:157-158.
60. Richards FM, Knowles JR. Glutaraldehyde as a protein cross-linkage reagent. *J Mol Biol* 1968; 14:37.
61. Monsan P, Puzo G, Mazarquil. Mechanism of glutaraldehyde-protein bond formation. *Biochimie* 1975; 57:1281-1292.
62. Sewell BT, Bouloukos C, von Holt C. Formaldehyde and glutaraldehyde in the fixation of chromatin for electron microscopy. *J Microsc* 1984; 136:103-112.
63. Bell PB, Lindroth M, Freriksson BA. Preparation of cytoskeletons of cells in culture for high resolution scanning and scanning electron microscopy. *Scanning Microsc* 1988; 2(3):1647-1661.
64. Nimni ME, Cheung DT, Strates B, Kodama M, Sheikh K. Bioprothesis derived from cross-linked and chemically modified collagenous tissues. In: *Collagen. Biotechnology*. Boca Raton, Fla: CRC Press, 1988:1-38.
65. Lee TM, Grammer LC, Shaughnessy MA, Patterson R. Modified antigens in the treatment of allergic disease. *Year Immunol* 1986; 2:338-350.

66. Guillochon D, Vijayalakshmi MW, Thiam Sow A, Thomas D. Effect of glutaraldehyde on hemoglobin: functional aspects and Mossbauer parameters. *Biochem Cell Biol* 1986; 64:29-37.
67. Tam JW, Cheng LY. Chemical cross-linking of hemoglobin H. A possible approach to introduce cooperativity and modification of its oxygen transport properties. *Biochim Biophys Acta* 1979; 580:75-84.
68. Bajpai PK, Stull PA. Immunogenicity of glutaraldehyde cross-linked porcine heart valve xenografts. *Int Res Commun Syst Med Sci* 1980; 8:642-643.
69. Fraenkel-Conrat H, Olcott HS. The reaction of formaldehyde with proteins v. cross-linking between amino and primary amide or guanidyl groups. *J Amer Chem Soc* 1948; 70:2673-2684.
70. Gendler E, Gendler S, Nimni ME. Toxic reactions evoked by glutaraldehyde-fixed pericardium and cardiac valve tissue bioprosthesis. *J Biomed Mater Res* 1984; 18:727-736.
71. Gustavson KH. The Vegetable Tannage. In: Gustavson KH, ed. *The Chemistry of Tanning Processes*. New York: Academic Press, Inc., 1956:142-201.
72. Mason HS. Reactions between quinones and proteins. *Nature* 1955; 771-772.
73. Sugumaran M, Henzel WJ, Mulligan K, Lipke H. Chitin-bound protein of sarcophagid larvae: Metabolism of covalently linked aromatic constituents. *Biochemistry* 1982; 27:6509-6515.
74. Sugumaran M, Lipke H. Crosslink precursors for the dipteran puparium. *Proc Natl Acad Sci USA* 1982; 79:2480-2484.
75. Lipke H, Strout K, Henzel W, Sugumaran M. Structural proteins of sarcophagid larval exoskeleton: Composition and distribution of radioactivity derived from [7-14 C] dopamine. *J Biol Chem* 1981; 256(9):4241-4246.
76. Sugumaran M, Semensi V. Sclerotization of mosquito cuticle. *Experientia* 1987; 43:172-174.
77. Vincent JFV, Hillerton JE. The tanning of insect cuticle -- a critical review and a revised mechanism. *J Insect Physiol* 1979; 25:653-658.
78. Fogal W, Fraenkel G. Melanin in the puparium and adult integument of the flesh fly. *J Insect Physiol* 1969; 15:1437-1447.
79. Anderson SO. Sclerotisation of the insect cuticle. *Proc First European Congr Entomol* 1978;

80. Pryor MGM. On the hardening of ootheca of *Blatta Orientalis*. *Proc R Soc* 1940; 128:378-393.
81. Fraenkel G, Rudall KM. The structure of insect cuticles. *Proc R Soc* 1947; 134:111-143.
82. Fietzek PP, Kühn K. The Primary Structure of Collagen. In: Hall DA, Jackson DS, eds. *International Review of Connective Tissue Research*. New York: Academic Press, Inc., 1976:1-60.
83. Grant NH, Alburn HE. Enhancement of collagen aggregation by catecholamines and related polyhydric phenols. *Biochemistry* 1965; 4(7):1271-1276.
84. Dabbous MK. Inter- and intramolecular cross-linking in tyrosinase-treated tropocollagen. *J Biol Chem* 1966; 241(22):5307-5312.
85. Waite JH, Tanzer ML. The bioadhesive of mytilus byssus: A protein containing L-DOPA. *Biochem Biophys Res Commun* 1980; 96(4):1554-1561.
86. Bloch B. Chemische Untersuchungen über das spezifische pigmentbildende Ferment der Haut, die Dopaoxydase. *Z Physiol Chem* 1916; 98:227-254.
87. Raper HS. The aerobic oxidases. *Physiol Revs* 1928; 8:245-282.
88. Mason HS. The chemistry of melanin: Mechanism of the oxidation of dihydroxyphenylalanine by tyrosinase. *J Biol Chem* 1948; 172:183-192.
89. Prota G. Some new aspects of eumelanin chemistry. *Prog Clin Biol Res* 1988; 256:101-124.
90. Swan GA. Structure, Chemistry, and Biosynthesis of the Melanins. In: Herz W, Griseback H, Kirby GW, eds. *Fortschritte der Chemie Organischer Naturstoffe*. New York: Springer Verlag, 1974:522-528.
91. Ito S. A reexamination of the structure of eumelanin. *Biochim Biophys Acta* 1986; 883:155-161.
92. Gruhn WB, Pomeroy JS, Maurer LH. An oligomeric hydroxyphenylalanine in malignant melanoma: A new type of melanogen. *Biochem Biophys Res Commun* 1974; 61(2):704-709.
93. Palumbo A, d'Ischia M, Misuraca G, Prota G, Schultz TM. Structural modifications in biosynthetic melanins induced by metal ions. *Biochim Biophys Acta* 1988; 964(2):193-199.

94. Kato T, Ito S, Fujita K. Tyrosinase-catalyzed binding of 3,4-dihydroxyphenylalanine with proteins through the sulfhydryl group. *Biochim Biophys Acta* 1986; 881:415-421.
95. Ito S, Kato T, Shinpo K, Fujita K. Oxidation of tyrosine residues in proteins by tyrosinase. Formation of protein-bonded 3,4-dihydroxyphenylalanine and 5-S-cysteinyl-3,4-dihydroxyphenylalanine. *Biochem J* 1984; 222:407-411.
96. Rorsman H. The melanocyte illuminated. *Trans St Johns Hosp Derm Soc* 1974; 60:135-141.
97. Riley PA. The mechanism of melanogenesis. *Symp zool Soc Lond* 1977; 39:77-95.
98. Bu'Lock JD, Harley-Mason J. Melanin and its precursors: Model experiments on the reactions between quinones and indoles, and consideration for a possible structure for the melanin polymer. *J Chem Soc* 1951; 703-721.
99. Fattorusso E, Cimino G. Sul Processo di Polimerizzazione dei 5,6-diossindoli. *Rend Acc Sc Fis Mat (Napoli)* 1971; 38:173-182.
100. Scannon PJ. Molecular modifications of hemoglobin. *Crit Care Med* 1982; 10:261-265.
101. Avakian OV, Gillespie JS. Uptake of noradrenaline by adrenergic nerves, smooth muscle and connective tissue in isolated perfused arteries and its correlation with the vasoconstrictor response. *Br J Pharmacol Chemother* 1968; 32:168-184.
102. Gross J. Studies on the formation of collagen: III. Time-dependent solubility changes of collagen in vitro. *J Exp Med* 1958; 108:215-225.
103. Williams BR, Gelman RA, Poppke DC, Piez KA. Collagen fibril formation: Optimal in vitro conditions and preliminary kinetic results. *The Journal of Biological Chemistry* 1978; 253(18):6578-6585.
104. Drake MP, Davidson PF, Bumps S, Schmitt FO. Action of proteolytic enzymes on tropocollagen and insoluble collagen. *Biochemistry* 1966; 5:301-312.
105. Bello J, Bello HR. Spontaneous cross-linking of collagen: evidence for metal-catalyzed and oxidative reactions. *Biochim Biophys Acta* 1967; 147:272-279.
106. Fraenkel-Conrat H, Olcott HS. Reaction of formaldehyde with proteins v.i. cross-linking of amino groups with phenol, imidazole or indole groups. *J Biol Chem* 1948; 174:827-843.
107. Jackson DS, Bentley JP. On the significance of the extractable collagen. *J Biophys Biochem Cytol* 1960; 7(1):37-42.

108. Miller EJ, Rhodes RK. Preparation and Characterization of the Different Types of Collagen. In: *Methods in Enzymology*. New York: Academic Press, Inc., 1982:33-64.
109. Gustavson KH. The Thermal Shrinkage of Collagen. In: Gustavson KH, ed. *The Chemistry and Reactivity of Collagen*. New York: Academic Press, Inc., 1956:211-220.
110. Jeffrey JJ. The Biological Regulation of Collagenase Activity. In: Mecham RP, ed. *Regulation of Matrix Accumulation*. New York: Academic Press, Inc., 1986:53-98.
111. Gross E, Witkop B. Nonenzymatic cleavage of peptide bonds: The methionine residues in bovine pancreatic ribonuclease. *J Biol Chem* 1962; 237:1856-1860.
112. Hanson AN, Bentley JP. Quantitation of type I to type III collagen ratios in small samples of human tendon, blood vessels, and atherosclerotic plaque. *Anal Biochem* 1983; 130(1):32-40.
113. Fairbanks G, Steck TL, Wallach DF. Electrophoretic analysis of the major polypeptides of the human erythrocyte membrane. *Biochemistry* 1971; 10:2606-2617.
114. Yamasaki RB, Osuga DT, Feeney RE. Periodate oxidation of methionine in proteins. *Anal Biochem* 1982; 126:183-189.
115. Joppich KR, Corkill JA, Giese RW. Oxidation of methionine to methionine sulfoxide as a side reaction of cyanogen bromide cleavage. *Anal Biochem* 1982; 119:73-77.
116. Laurent GJ, Cockerill P, McAnulty RJ, Hastings JR. A simplified method for quantitation of the relative amounts of type I and type III collagen in small tissue samples. *Anal Biochem* 1981; 113:301-312.
117. Cohen SA, Bidlingmeyer BA, Tarvin TL. PITC derivatives in amino acid analysis. *Nature* 1986; 320:769-770.
118. Rollet A. In: Stricker, ed. *Handbuch der Lehre von den Geweben*, Vol.1.: 1871:35-50.
119. Danielsen CC. Thermal stability of reconstituted collagen fibrils. Shrinkage characteristics upon in vitro maturation. *Mechanisms of Ageing and Development* 1981; 15:269-278.
120. Snowden JM. The effects of polymers on the shrinkage temperature of tendon. *Biochim Biophys Acta* 1982; 707:142-146.

121. Verzar F. Veränderungen der thermoelastischen Kontraktion von Sehnenfasern im Alter. *Helvetica Physiologica et Pharmacologica Acta* 1955; 13:C64-C67.
122. Doillon CJ. Porous collagen sponge wound dressings: in vivo and in vitro studies. *J Biomater Appl* 1988; 2:562-578.
123. Doillon CJ, Whyne CF, Brandwein S, Silver FH. Collagen-based wound dressings: control of the pore structure and morphology. *J Biomed Mater Res* 1986; 20:1219-1228.
124. Viidik A. Functional Properties of Collagenous Tissues. In: Hall DA, Jackson DS, eds. *International Review of Connective Tissue Research*. New York: Academic Press, Inc., 1973:127-215.
125. Simpson RL. Collagen as a biomaterial. In: Rubin LR, ed. *Biomaterials in reconstructive surgery*. St. Louis: C.V. Mosby, 1983:1-29.
126. Elliot DH. The biochemical properties of tendon in relation to muscular strength. *Ann Phys Med* 1967; 9:1-7.
127. Bear RS. Long x-ray diffraction spacings of collagen. *J Am Chem Soc* 1942; 64:727-733.
128. Petruska JA, Hodge AJ. Recent Studies with the Electron Microscope on Ordered Aggregates of the Tropocollagen Molecule. In: Ramachandran N, ed. *Aspects of Protein Structure*. New York: Academic Press, Inc., 1963:289.
129. Leibovich SJ, Weiss JB. Electron microscope studies of the effects of endo- and exopeptidase digestion on tropocollagen. *Biochim Biophys Acta* 1970; 214:445-454.
130. Kühn K, Kühn J, Schuppler G. Kollagenfibrillen mit anormalem Querstreifungsmuster. *Naturwissenschaften* 1964; 51:337.
131. Meek KM, Chapman JA. Glutaraldehyde-induced changes in the axially projected fine structure of collagen fibrils. *J Mol Biol* 1985; 185:359-370.
132. Veis A, Payne K. Collagen Fibrillogenesis. In: Nimmi ME, ed. *Collagen: Biochemistry*. Boca Rotan, Florida: CRC Press, 1988:113-137.
133. Powis G. Binding of catecholamines to connective tissue and the effect upon the responses of blood vessels to noradrenaline and to nerve stimulation. *J Physiol* 1973; 234:145-162.
134. Nelson JC, Tomei RT. Direct determination of free thyroxin in undiluted serum by equilibrium dialysis/radioimmunoassay. *Clin Chem* 1988; 34:1737-1744.

135. Ha HR, Vozeh S, Follath F. Evaluation of a rapid ultrafiltration technique for determination of quinidine protein binding and comparison with equilibrium dialysis. *Ther Drug Monit* 1986; 8:331-335.
136. Desoye G. Error analysis in equilibrium dialysis: evaluation of absorption phenomena. *J Biochem Biophys Methods* 1988; 17:3-16.
137. Page RC, Benditt EP. Collagen has a discrete family of reactive hydroxylysyl and lysyl side-chain amino groups. *Science* 1969; 163:578-579.
138. Page RC, Benditt EP, Kirkwood CR. Schiff base formation by the lysyl and hydroxylysyl side chains of collagen. *Biochem Biophys Res Commun* 1968; 33:752-757.
139. Hackman RH, Todd AR. Some observations on the reaction of catechol derivatives with amines and amino acids in presence of oxidizing agents. *J Insect Physiol* 1953; 55:631-637.
140. Gustavson KH. The quinone and oil tannages. In: Gustavson KH, ed. *The Chemistry of Tanning Processes*. New York: Academic Press Inc., 1956:283-307.
141. Mason HS. Comparative biochemistry of the phenolase complex. *Adv Enzymology* 1955; 13:104-185.
142. Bio-Rad Price List L. Richmond, CA: Bio-Rad Laboratories, 1986: 110-114.
143. Ansari AA, Kidwai SA, Salahuddin A. Acetylation of amino groups and its effect on the conformation and immunological activity of ovalbumin. *J Biol Chem* 1975; 250:1625-1632.
144. Rauterberg J, Timpl R, Furthmayr H. Structural characterization of n-terminal antigenic determinants in calf and human collagen. *Eur J Biochem* 1972; 27:231-237.
145. Glanville RW, Breitreutz D, Meitinger M, Ma PP. Completion of the amino acid sequence of the $\alpha 1$ chain from type I calf skin collagen. *Biochem J* 1983; 215:183-189.
146. Fietzek PP, Kuhn K. The covalent structure of collagen: Amino-acid sequence of the cyanogen-bromide peptides $\alpha 1$ -CB2, $\alpha 1$ -CB4 and $\alpha 1$ -CB5 from calf-skin collagen. *Eur J Biochem* 1975; 52:77-82.
147. Fietzek PP, Rexrodt FW, Hopper KE, Kuhn K. The covalent structure of collagen: 2. The amino-acid sequence of $\alpha 1$ -CB7 from calf-skin collagen. *Eur J Biochem* 1973; 38:396-400.

148. Fietzek PP, Wendt P, Kell I, Kuhn K. The covalent structure of collagen: Amino acid sequence of $\alpha 1$ -CB3 from calf skin collagen. FEBS Letters 1972; 26:74-76.
149. Rauterberg J, Fietzek P, Rexrodt F, Becker U. The amino acid sequence of the carboxyterminal nonhelical cross link region of the $\alpha 1$ chain of calf skin collagen. FEBS Letters 1972; 21:75-79.
150. Fietzek PP, Rexrodt FW, Wendt P, Stark M, Kuhn K. The covalent structure of collagen: Amino-acid sequence of peptide $\alpha 1$ -CB6-C2. Eur J Biochem 1972; 30:163-168.
151. Click E, Bornstein P. Isolation and characterization of the cyanogen bromide peptides from the $\alpha 1$ and $\alpha 2$ chains of human skin collagen. Biochemistry 1970; 9:4699-4706.
152. Epstein F. $\alpha 1$ (III) human skin collagen. Release by pepsin digestion and preponderance in fetal life. J Biol Chem 1974; 249:3225-3231.
153. Miller EJ, Rhodes RK, Furuto DK. Identification of collagen chains as a function of cyanogen bromide peptide patterns using gel permeation high-performance liquid chromatography. Coll Relat Res 1983; 3:79-87.
154. Menter JM, Willis I. Interaction of several mono- and dihydroxybenzene derivatives of various depigmenting potencies with L-3,4-dihydroxyphenylalanine-melanin 1,2R. Arch of Biochem and Biophys 1986; 244(2):846-856.
155. Menter JM, Willis I. The interaction of L-DOPA melanin with p-tert-butylcatechol. J Invest Derm 1980; 75:257-260.
156. Bentley JP, Fellman JH. Collagen cross links, natural and unnatural. Cosmetic Derm 1986; 1:89-96.
157. Grant RA. Technical methods: Estimation of hydroxproline by the Auto Analyser. J Clin Path 1964; 17:685-686.
158. Sykes B, Puddle B, Francis M, Smith R. The estimation of two collagens from human dermis by interrupted gel electrophoresis. Biochem Biophys Res Commun 1976; 72:1472-1480.
159. Laemli I. Cleavage of structural proteins during the assembly of the head of the bacteriophage. Nature 1970; 227:680-685.

VII. APPENDIX: GENERAL EXPERIMENTAL METHODS.

Detailed descriptions of the general experimental methods referred to repeatedly throughout the Experimental section of this thesis are presented here.

A. Type I collagen extraction and purification.

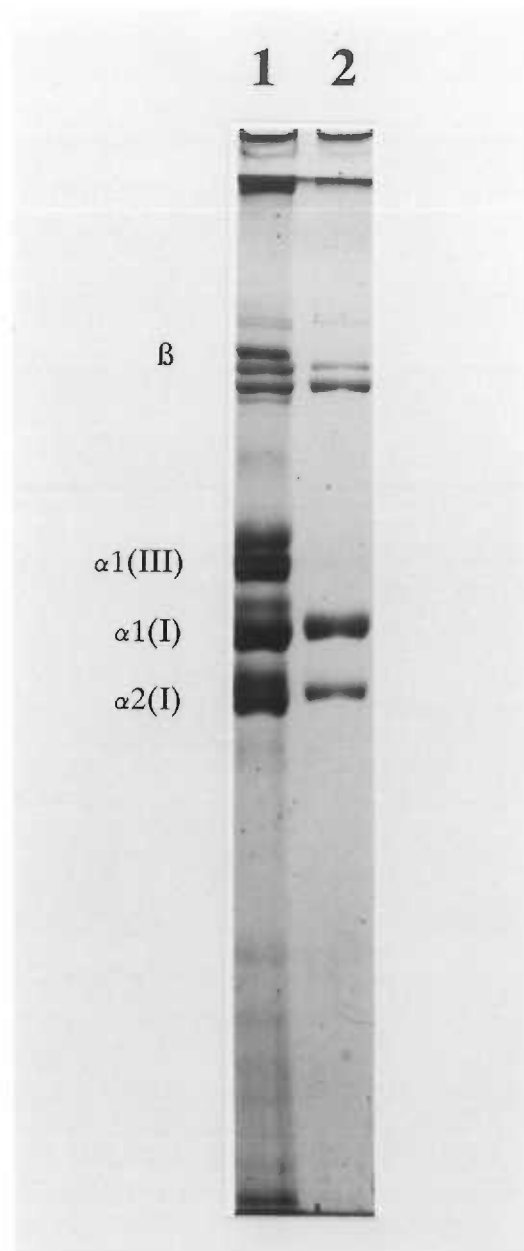
Type I collagen was extracted and purified by the method of Miller and Rhodes¹⁰⁸ with certain modifications to ensure complete removal of type III collagen contaminants. The collagen source was either 4 month fetal calf skin or adult bull scrotum. The tissues were defatted by scraping and homogenized in phosphate buffered saline containing the enzyme inhibitors N-ethylmaleimide (1.23 g/l), phenyl methyl sulfonyl fluoride (0.174 g/l), and (ethylenedinitrilo)-tetraacetic acid (5.84 g/l).

The pellet was collected by centrifugation (2500 x g) in a Sorval RC-3 centrifuge, and washed two additional times in the same manner. The pellet was resuspended in 0.5 M acetic acid for 1 hour with shaking, centrifuged at 2500 x g to collect and discard the wash, and resuspended in either 0.5M acetic acid or in 0.5M acetic acid containing pepsin (E.C. NO. 3.4.4.1) at an approximate concentration of 2 g/l. The pepsin (Sigma Chemical Co.) was from porcine stomach mucosa and had been purified 60,000 fold. The media were allowed to shake overnight and then centrifuged at 2500 x g.

The fibrous collagens salt out at different salt concentrations when the pH of the medium is changed. Types I and III collagen are insoluble at 0.7M NaCl under acid conditions, whereas as at neutral pH, type III collagen becomes insoluble at a much lower concentration (1.5M to 1.8M) than does type I collagen (2.5M). Thus, both type III and type I collagen were precipitated from the extraction supernatants at 0.7 M NaCl, and the precipitate collected by centrifugation at 5650 x g in a Beckman J-21 High Speed Centrifuge, and resuspended in 1.0 M NaCl, 50 mM tris-HCL (pH 7.5). The resulting solution containing both types I and III collagen was adjusted to a concentration of 2.0 M NaCl to precipitate all type III collagen which could be removed by centrifugation at 3900 x g. The supernatant was adjusted to a final concentration of 2.5 M NaCl, and the type I collagen precipitate was collected by centrifugation at 2950 x g. The type III collagen precipitation step was repeated and the pellet resuspended in dilute acetic acid. Excess salt was removed by exhaustive dialysis against 5.0mM acetic acid. The collagen concentration was measured by hydroxyproline assay using the auto analyzer method ¹⁵⁷, and the relative purity was analyzed by interrupted SDS-polyacrylamide gel electrophoresis ¹⁵⁸. Collagen solutions were stored in 5.0mM acetic acid, at an approximate concentration of 3.0mg/ml under liquid nitrogen. Figure 52 shows the crude preparation of collagen containing the α chains of types I and III collagen (lane 1) and the final stock solution containing purified type I collagen (lane 2) separated by interrupted SDS-PAGE (described below).

Figure 52. Interrupted SDS-PAGE separation of α -chains of type I and type III collagen. In lane 1, a non purified bovine skin extract containing both types of collagen are shown. In lane 2, following two salt precipitations, no type III collagen is found. The purification procedure also removes other contaminants.

* β notation indicates aldol crosslinked collagen α chains.



at concentrations of 1.0, 2.0, 4.0, 6.0 and 8.0 $\mu\text{mole/ml}$, and were used to prepare a standard curve. Hydroxyproline content was measured by the Technicon autoanalyzer method. In this procedure each hydrolyzed sample is mixed with an excess of citrate acetate buffered (pH 6.0) chloramine-T-hydrate (2.82g/l) and incubated at room temperature for 18 minutes. The product of this reaction was then mixed with 3.0M perchloric acid which deactivates excess chloramine T over a six minute room temperature incubation period. Finally, the reaction was completed by mixing with 5% *para*-dimethylaminobenzaldehyde, and incubating at 60° C for 24 minutes. The production of a chromophore was measured at 550nm using a Technicon 15 mm cell Colorimeter. The hydroxyproline content of the test samples are from the standard curve.

E. Interrupted SDS-Polyacrylamide Gel Electrophoresis ¹⁵⁸.

A 14 X 12 cm 6.5% running gel slab with a 4% stacking gel was prepared from a 30% acrylamide (0.7% bis) stock solution in a bio-rad SE500 Vertical Slab Gel Unit. The conditions of the running gel were as described by Laemli ¹⁵⁹, with modifications. In short, the running gel consisted of 0.375M Tris (pH 8.8), 0.1% SDS and 0.5M urea. The stacking gel differed from the running gel in the Tris concentration (0.125M) and pH (6.8). 15 μg loads of purified collagens in 0.03M Tris-HCl, 0.1% SDS, .0025% Bromphenol Blue, and 20% Glycerol, were layered in 1cm sample wells. The gel slab unit was immersed in a running buffer consisting of 0.025M Tris-HCl (pH 8.8), 0.195M glycine, and 0.1% SDS. The pulse rate was raised from 100 to 200 pps over 30 minutes using a Ortec 4100 Constant Pulsed

Power Supply. The pulse rate was maintained at 200pps for an additional 10 minutes. The electrical current was then interrupted, buffer removed from the sample wells, and 10 μ l of 10% β -mercaptoethanol (BME) in running buffer layered in the wells. The BME was allowed to penetrate the gel for 1 hour, after which time the electrical current was re-applied and maintained throughout the remainder of the run at 200pps. The gel slab was stained with Coomassie Brilliant Blue R-250 stain ¹¹³.

F. Radioassay by liquid scintillation counting.

Samples were radioassayed by liquid scintillation counting using a Beckman L-250 Liquid Scintillation Counter. Samples were prepared in high efficiency, low quench scintillation cocktails including Instagel (Packard Instruments Co.), Opti-Fluor, and Hionic Fluor. The latter was used when tissue solubilizers had been used in sample preparation. All cocktails were purchased from Packard Instruments Co.. Samples were counted for time periods which allowed for the collection of at least 1000 counts. Background values were subtracted, and DPM values were determined from a channels ratio correlation curve.

G. Collagen gel solubility assay.

Reconstituted collagen fibrillar matrices in the form of either gels or felts were treated using up to three sequential solubility protocols. In treatment 1, the sample was homogenized in 4.0ml of 0.5M acetic acid, and rotated on a Boekel

Orbitron Rotator and allowed to extract for 12 hours at 4°C. In treatment 2, the sample was homogenized in 4.0ml of 0.01M acetic acid, and boiled for two hours. In treatment 3, the samples were homogenized in 4.0ml of 0.01M acetic acid and autoclaved at a pressure of 15 lbs for 20 minutes. At the end of each extraction, the samples were centrifuged at 39,000 x g using a Beckman J-21 high speed centrifuge. The supernatant and pellet were separate and assayed for collagen content by the hydroxyproline Autoanalyzer method ¹⁵⁷.

H. The preparation of collagen felts.

Multiple 6.0ml aliquots of buffered collagen solutions were transferred to Pyrex covered petri dishes (60mm x 15mm), preheated to 37°C, and incubated at 37°C for varying time periods in a humidified Hova-Bator Still Air Incubator. At the end of the incubation periods, the samples were flash frozen in liquid nitrogen, and lyophilized.

I. Shrinkage temperature measurements.

Shrinkage temperature apparatus used is shown in Figure 54. One end of the sample was place between the jaws of a hemostat and the other end was attached to a 0.65g mass. The end attached to the mass was immersed in phosphate buffered saline equilibrated at 37°C in a water jacketed column. The PBS was heated at a uniform rate (2.5°C/min) using a Tecam TE1 Tempette circulating water bath. The shrinkage temperature was the first observed contraction of the sample.

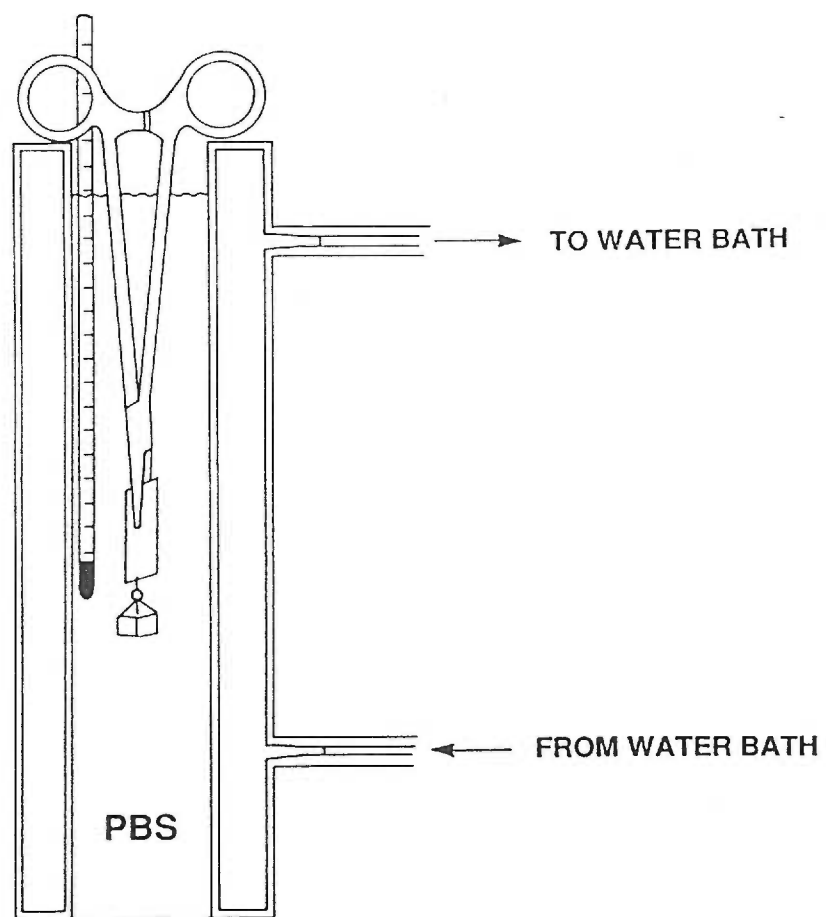


Figure 54. Schematic of the apparatus used to measure the shrinkage temperature of collagen felts.

J. Gel filtration HPLC elution of labeled DOPA-collagen adducts.

A Beckman 110B Solvent Delivery Module was primed with a 2.0 M low U.V. absorbance guanidine-HCL (U.S. Biochemical Corp.), 50 mM tris-HCl (pH 7.5) run buffer ¹⁵³. An isocratic system with a 0.6 ml/min flow rate was maintained. Lyophilized incubation samples were dissolved in the run buffer to a concentration of 2 mg/ml, and from this, a 50 μ l aliquot was eluted on a Bio-Sil TSK-250 (10 x 300 mm) gel filtration HPLC column fitted with the appropriate guard column. The eluent was monitored at 220 nm with a Beckman Model ISS Variable Wavelength Detector. 0.3ml elution fractions were collected beginning 5 minutes post injection with a Pharmacia Frac-100 fraction collector, and 200 μ l aliquots of the fractions were radioassayed by liquid scintillation counting. Figure 55 shows the elution of 3-¹⁴C-DOPA labeled collagen and free labeled DOPA using this technique.

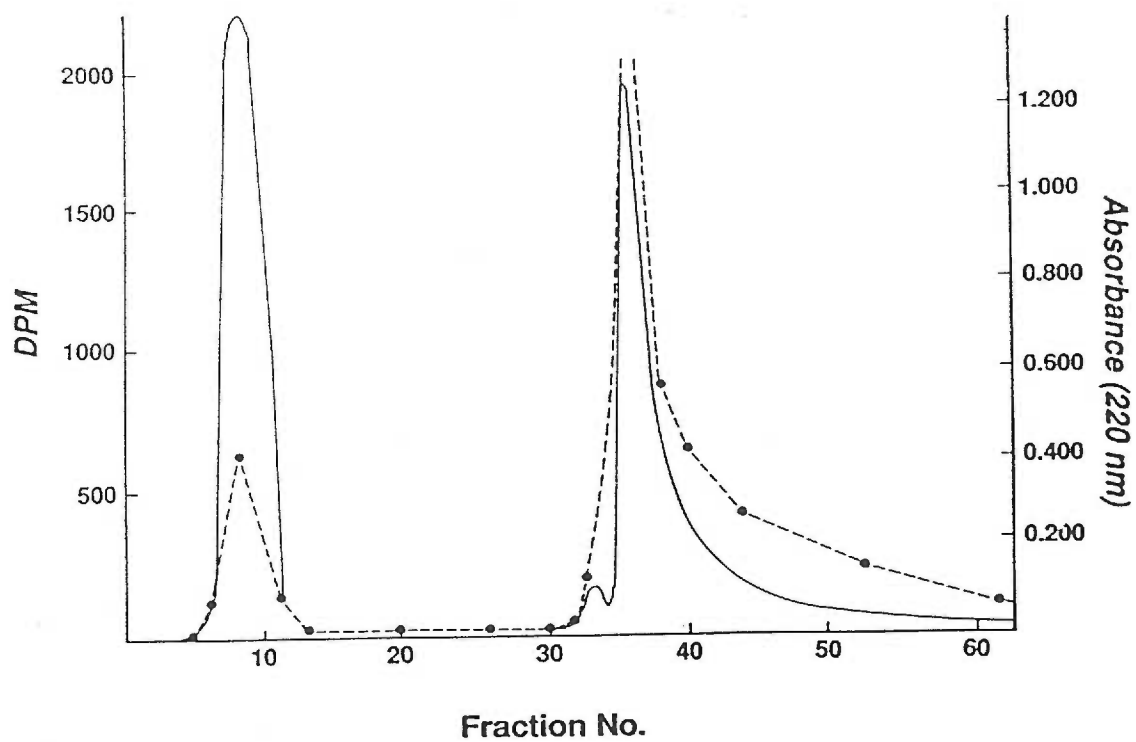


Figure 55. Gel filtration separation of labelled DOPA-collagen adducts at the v_0 and unbound labelled DOPA at the v_1 .

(—): 220nm absorbance of eluant.
(-·-): DPM in elution fractions.